S
uiS

FACULTY OF SCIENCE AND TECHNOLOGY

MASTER THESIS

Study programme / specialisation: Marine and Offshore Technology

The spring semester, 2020

Open / ~~Confidential~~

Author: Pawel Janusz Klis

Klis Pawel
(signature author)

Course coordinator: Prof. Yihan Xing

Supervisor(s): Prof. Yihan Xing

Thesis title: Technical and Economic Feasibility Analysis of a Conceptual Subsea Freight Glider for CO2 Transportation

Credits (ECTS): 30

Keywords: subsea freight glider, subsea technology, economic analysis, cargo vessel, CO_2 transporting

Pages: 60

+ appendix: 48

Stavanger, June 15, 2022
date/year

Technical and Economic Feasiblity Analysis of a Conceptual Subsea Freight Glider for CO$_2$ transportation

Author:
Pawel Janusz Klis

Supervisor:
Prof. Yihan Xing
University of Stavanger

University of Stavanger
Faculty of Science and Technology
Department of Mechanical and Structural Engineering and Materials Science

Abstract

The aim of this thesis is to analyze the technical and economic aspects of a conceptual Subsea Friegit Glider (SFG). The SFG is an ideal alternative to tanker ships and offshore pipelines for transporting liquefied CO_2. Moreover, it can also be used to transport any type of cargo. The SFG travels below the sea surface, which makes it weather independent. Firstly, the technical feasibility study is carried out by developing a baseline design with a length of 56.5 m, a beam of 5.5 m, and a cargo volume of 1194 m^3. The design for the SFG is developed following the standard originally created for military vessels DNV GL-RU-NAVAL-Pt4Ch1 and ASME Boiler and Pressure Vessel Code. Additionally, two more submarines are designed and included in the analysis: the half-scaled 469 m^3 and double-scaled 2430 m^3 models of the SFG baseline design. The technical feasibility analysis shows that the models meet the requirements and they are able to perform the mission. Secondly, the economic feasibility analysis is performed using publicly open MUNIN D9.3 and ZEP cost models. The cost analysis presents a case study with a CO_2 transport of 180 km to 1500 km and a capacity of 0.5 to 2.5 mtpa (million tons per annum). The results of cost analysis are compared with the SFG, crewed and autonomous ship tanker, offshore pipelines and conceptual Subsea Shuttle Tanker. The results of the study indicate that the various types of the SFG (469 m3, 1194 m3, and 2430 m3) are technically feasible. They are also competitive with the smaller CO2 capacities of around 0.5 and 1 mtpa and distances of 180 to 500 km.

Acknowledgements

This thesis is the final project of a master's degree in the Marine and Offshore Technology programme at the University of Stavanger.

I would like to express my special thanks of gratitude to my supervisor Prof. Yihan Xing for giving me the possibility to work under his supervision. Moreover, I would like to thank him for his guidance and encouragement and for providing the opportunity to develop my interest in subsea technology.

I would also like to thank my fellow co-student and friends for their support, motivation, and shared adventures during the study period.

I owe my deepest gratitude to my father Janusz Klis, for his continuous support and encouragement during my studies.

Stavanger, June 2022
Pawel Klis

Contents

List of Figures

List of Tables

1. Introduction

1.1. Global Warming Problem

Global warming is one of the most significant problems in today's world. This problem is caused by the concentration of carbon dioxide in the atmosphere. Scientific research shows that CO_2 in the atmosphere is continuously increasing. According to (Wigley, 1983), the concentration of CO_2 before the industrial revolution was equal to 260 ppm. However, a new study (Letcher, 2019) has shown that in 2022 concentration of carbon dioxide will reach 420 ppm. The Keeling Curve (**Figure 1.1**) displays the annual changes in CO_2 accumulation in the atmosphere from 1958 to 2022. The data show a systematic increase of carbon dioxide in the atmosphere. The average growth until 2021 was equal to 415 ppmv.
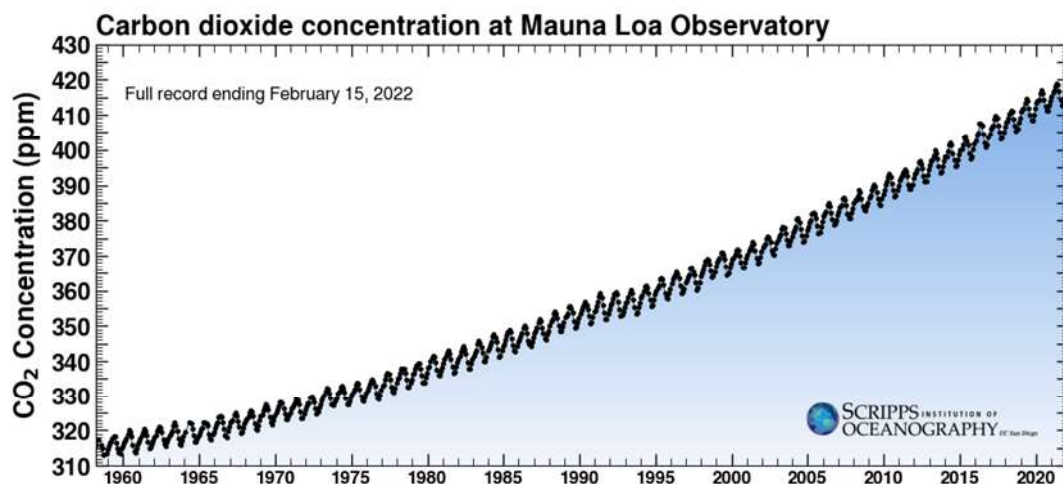
Figure 1.1 *Keeling Curve. Atmospheric CO_2 concentration from 1958 to 2020. Reproduced from* (SIO, 2022)

The consequences of the large concentration of carbon dioxide in the atmosphere can increase the Earth's average temperature. Hence, the warmer condition will warm the ocean and melt the ice sheet and glaciers. Moreover, ocean water will also expand if it warms, contributing to sea-level rise (NASA, 2008). What is more, climate extremes can appear, such as floods or droughts. These factors can cause crop losses and threaten the livelihoods of agricultural producers and the food security of communities worldwide (US EPA, 2017).

1.2. Paris Agreement

On 12 December 2015, during COP21, the Paris Agreement was established (UN FCCC, 2015). It is a legally binding international treaty on climate change. The Agreement stipulates that all counties which have signed the Agreement commit to limit global warming

to well under 2, preferably to 1.5 degrees Celsius, compared to the pre-industrial level. The Paris Agreement works on a 5-year cycle of increasingly ambitious climate action performed by countries. By 2020 all countries had to submit their climate action plans, known as Nationally Determined Contributions (NDCs).

This decision has encouraged many countries and production companies to reduce their absolute emissions to near zero by 2050 (International Energy Agency, 2021). Therefore, many production enterprises are looking for a new solution to reduce or eliminate carbon dioxide from the production cycle.

1.3. Capturing the CO_2

The carbon dioxide is emitted into the atmosphere by burning fossil fuels. CO_2 can be released by large combustion units such as electric power generators and smaller sources like engines in motor vehicles and furnaces used in apartment and commercial buildings. A Carbon Capture and Storage system would most likely be applied to large sources of CO_2 (Metz et al., 2005).

CCS is a technology that consists of three main steps:

- Capturing and separating carbon dioxide from other gases,
- Transporting the captured CO_2 to the storage place,
- Storing carbon dioxide safely under the seabed.

Many claims that CCS is carbon recycling because the plan is to return CO_2 to where it came from – underground (Benjaminsen, 2019). This technology has been implemented in a few Norwegian fields. One of the most famous fields where the CCS was implemented is Sleipner, where more than 23 million tonnes of CO_2 have been safely stored (Ronca & Mancimi, 2021).
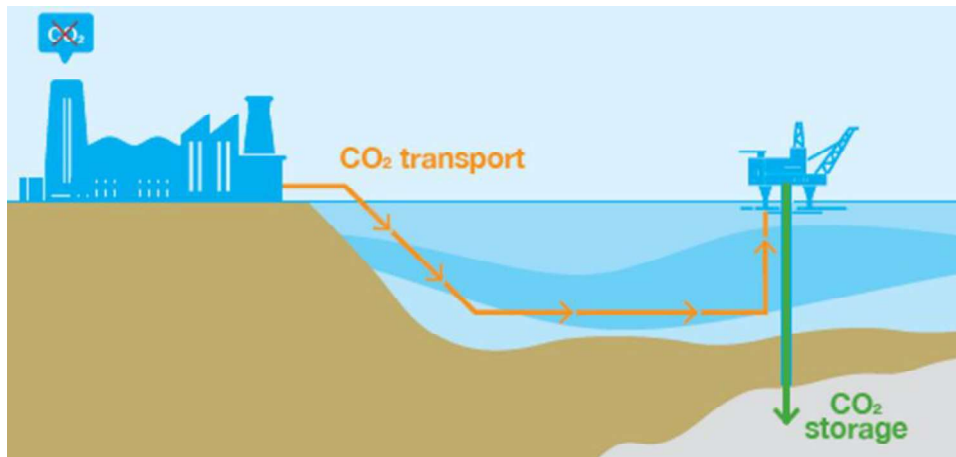
Figure 1.2 *Diagram showing Carbon Capture and Storage technology. Reproduced from* (Pollard, 2022).

1.4. Transport of CO_2

The Carbon Capture and Storage system requires the development of transportation infrastructure. The capture system should be interconnected with a storage system. Very often, these systems are hundreds of kilometres apart. Additionally, depending on the method of transmission, transport of carbon dioxide takes place under appropriate pressure conditions. The transport of CO_2 via the pipeline will take place at a different temperature and pressure than the transport by vessels.
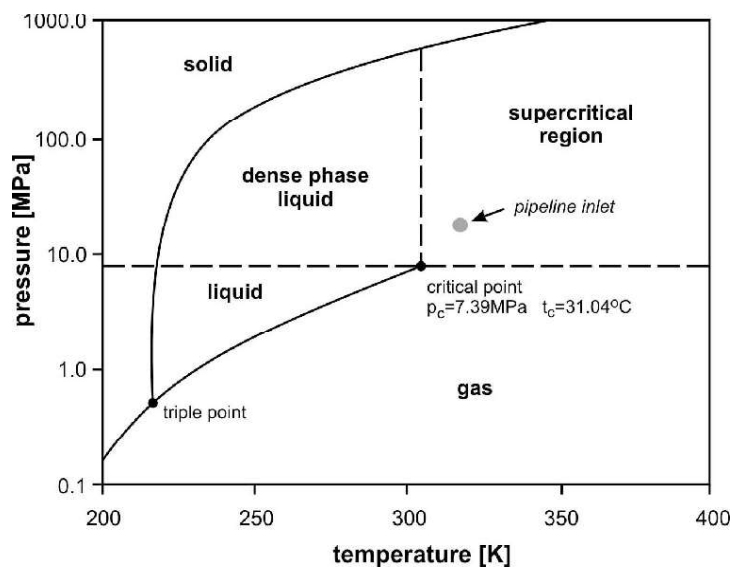
Figure 1.3 *Phase diagram of the CO_2. Reproduced from* (Witkowski et al., 2014).

The most common carbon dioxide transport method is transferred by underwater pipelines (Witkowski et al., 2014). By implementing this method, products are transported

continuously, making this solution one of the most efficient ways of transportation. Additionally, pipelines can transport carbon dioxide in three states: liquid, gaseous and solid. They can also take shortcuts and be installed anywhere, including underwater or underground. What is more, it is a closed type of transportation, which is why there is no loss, and it is safe and reliable with no pollution. However, this solution has some limitations. Impurities like water or hydrogen sulfide in the CO_2 stream can cause corrosion in the pipelines. In the case of pipe cracks in a populated area, the unexpected release of carbon dioxide can lead to severe environmental and human threats. The installation and maintenance of a subsea system to transport gases can furthermore be very expensive. Steel prices are increasing every year (Trading Economics, 2022), which means the design and construction is a costly solution, often unprofitable in the case of small reservoirs.

Liquefied hydrocarbon gases are transported in very large LNG or LPG tanks. However, it was proven that these carries could also be used for CO_2 transportation. The largest LNG carriers have a capacity of 266,000 m^3, which means that they could carry 230,000 t of CO_2. The efficiency of the transport is maximized when the density of liquid CO_2 is as high as possible. The density increases sharply with the decreasing pressure in the triple point region, reaching 1200 kg/m^3 (Rackley, 2017), however, it is essential to avoid the formation of dry ice. The optimal conditions for transportation of the CO_2 are at a temperature of 218.15 K and a pressure of 7 bar.

Transporting CO_2 by vessel tanks allows carrying massive quantities of goods over long distances. Yet sometimes, it is impossible to perform a marine operation due to inclement weather conditions. Factors such as wind or rain may prevent or delay the performance of maritime operations.

Pipelines seem to be a perfect solution if continuous transport for a relatively short distance of CO_2 is needed (Odland, 2018). Vessel tanks should be utilized when the transportation distance is long. On the other hand, there is a gap between these two solutions. Currently, there is no transportation method that can transfer carbon dioxide for medium distances without continuous delivery. Pipelines and marine transportation leave a carbon footprint that negatively impacts the environment. Many countries and oil & gas companies have decided to reduce their absolute emissions to near zero by 2050 (Equinor ASA, 2020). Therefore, looking for alternative CO_2 transportation methods are needed.

1.5. Previous Work

In 2019, Equinor ASA proposed the concept of an underwater drone to transport CO_2 (Equinor ASA, 2019). The Subsea shuttle is an autonomous 135-meter vehicle that could transport carbon dioxide back to the reservoirs, replacing the pipeline carrying CO_2. Even though the concept has been presented, there were very limited studies. In (Xing, Ong, et al., 2021) performed a detailed description of the baseline design and conducted a finite element analysis of ring-stiffened cylinders of the design. In (Xing, Santoso, et al., 2021) presented and compared three different models of the Subsea Shuttle Tanker and proved that they are technically feasible. Also, an economic analysis was performed.

In the study of (Xing, 2021), a new type of underwater vehicle for CO_2 transportation was proposed. The concept is an autonomous Subsea Freight Glider, which is a novel cargo submarine equipped with large hydrodynamic wings that allow gliding underneath the sea surface. This solution covers the gap with the previous studies and enables transporting vast amounts of cargo autonomously over long distances. The gilder does not have a propeller, and the only driving force is buoyancy force. In the study of Ahmad (U. N. Ahmad & Xing, 2021), a control methodology was proposed based on feedback from the developed glider model and obtained the glide path.

These studies show that the concept of Subsea Freight Glider can compete with different methods of CO_2 transportation. However, performed analyses are insufficient, and some limitations exist. Previous studies concerned that large submarines that can transport an enormous amount of CO_2. On the other hand, there are some small offshore facilities close to land where CO_2 can be stored, and the conventional way of transporting CO_2 is too expensive. This thesis presents the methodology of designing the small-size underwater gliding vehicle and compares it with traditional ways of CO_2 transportation. The research will cover the gap in shipping small amounts of carbon dioxide for small distances.
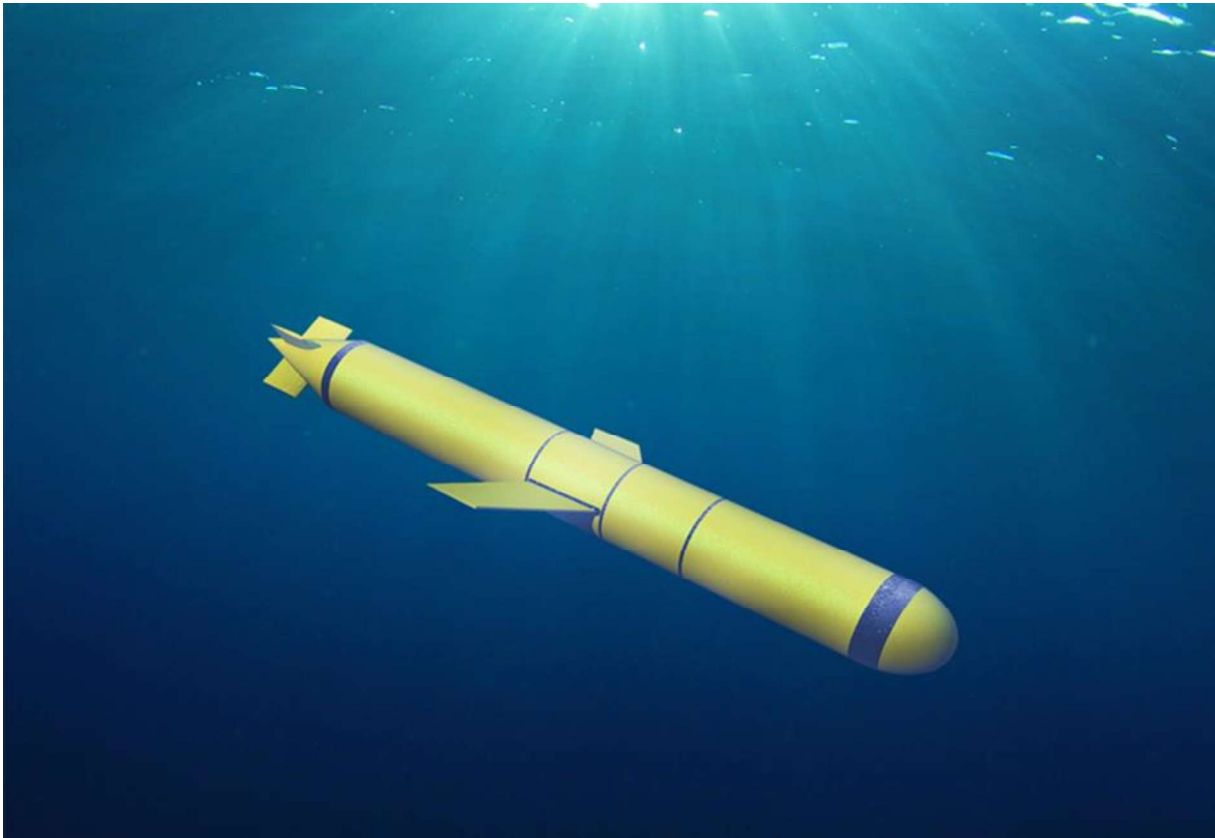
Figure 1.4 *Subsea Freight Glider.*

1.6. Outline of the Thesis

This thesis contains descriptions and calculations that are needed to design Subsea Freight-Glider. This work also includes an economic feasibility analysis.

The structure of the thesis was divided into chapters in the following way:

- **Chapter 2: Methodology of Subsea Freight Glider Design**
- **Chapter 3: Technical Feasibility Analysis**
- **Chapter 4: Economical Feasibility Analysis**
- **Chapter 5: Results**
- **Chapter 6: Conclusions and recommendations**
- **Appendix A**
- **Appendix B**
- **Paper**

2. Methodology of Subsea Freight Glider Design

This chapter presents the literature and concept study for the design of the Subsea Freight Glider. The scope of this chapter covers the various aspects of the SFG's mission requirements, the internal and external hull design, power consumption, and hydrostatic load case.

The SFG baseline design is a 1224-ton autonomous submarine that can carry over 1194 m^3 carbon dioxide. The length of the SFG is 56.5 m, and the beam is 5.5 m long. The distance that the SFG can reach with the speed of 1 m/s (2 knots) is 400 km. The methodology for the SFG design is displayed in **Figure 2.1**.

The design process for the SFG begins with establishing the mission requirements such as operation range, cargo capacity, operating depth and environmental data and operational conditions like speed, depth demotions or design loads. Next, the external hull arrangement is developed, including stiffeners dimensions determination and pressure design. Then, the internal hull arrangement includes the layout of the vessel's main cargo, auxiliary cargo, compensation, trim, and buoyancy tanks. Moreover, the wing is added to enable the submarine to glide. Finally, the stability check is performed. If the vessel is unstable, dimensions need to be adjusted. The design loop is repeated as all criteria are fulfilled. Once the design is finished, the power consumption is determined (Ma et al., 2021).
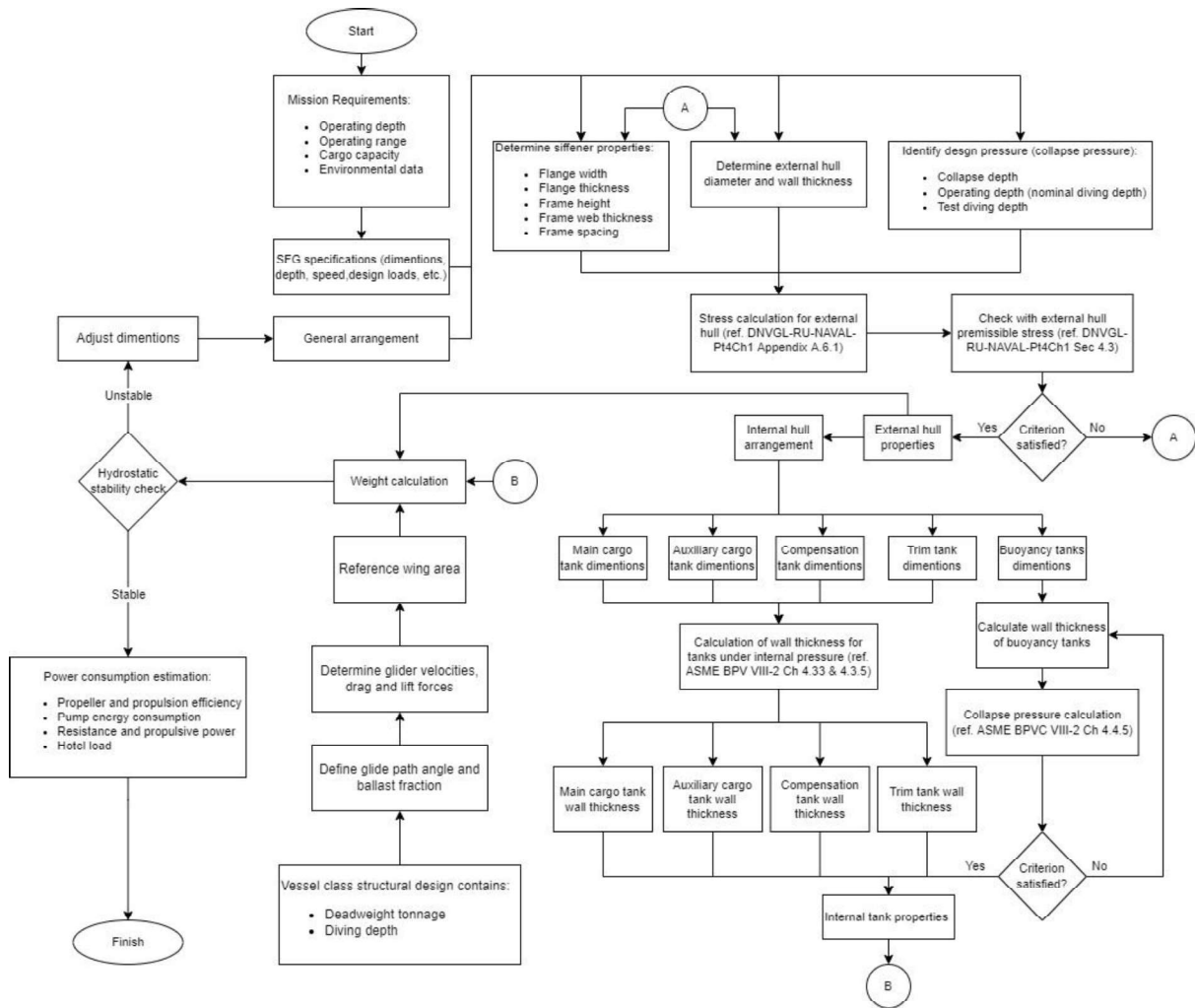
Figure 2.1 *Methodology for SFG technical design.*

2.1. Mission Requirements and SFG Operating Specifications

The SFG operating specifications provide a detailed description of the submarine's capabilities and are used to determine operational conditions. The SFG specifications are defined based on the mission requirements, such as range, depth, cargo capacity and other environmental data. Subsequently, these factors determine the SFG specifications that affect the vessel's performance, such as required velocity, maximum range expected load case or CO_2 properties.

The SFG specifications and requirements of a mission provide the basis for the whole design process. **Table 2.1** presents the baseline SFG operating parameters.

Table 2.1 SFG Operating Specifications.

Parameter	Value	Unit
Operating depth (nominal diving depth)	200	[m]
Collapse depth	400	[m]
Safety depth	40	[m]
Operating velocity	1	[m/s]
Maximum range	400	[km]
Cargo pressure	35 – 55	[bar]
Cargo temperature	0 – 20	[ºC]
Current velocity	1	[km]

2.1.1. Operating Depth Range

The safety depth of the SFG is defined as 40 meters to prevent a collision or any impact from floating structures. This level ensures that the submarine can operate safely and independently from the weather conditions. In addition, this feature helps to minimise the effects of the waves' dynamic loads on the vessel.

The nominal diving depth of the SFG, while it is carrying CO_2, is 200 meters. The nominal diving depth is the working depth for the SFG. This value is also used to determine the minimal recoverable depth from a loss of control.

Following the DNVGL Rules for Classification for Naval Vessels, Part 4 Sub-surface ship, Chapter 1 Submarine DNVGL-RU-NAVAL-Pt4Ch1 (DNV GL AS, 2018), the test diving depth equals 1.25 times the nominal diving depth. On the other hand, the collapse depth of the ship is two times greater than its nominal diving depth. Hence:

- The safety depth is 40 m,
- The operating depth is 200 m,
- The test diving depth is 250 m,
- The collapse depth is 400 m.

Figure 2.2 shows the depths at which SFG performs a mission and the depth of the CCS facilities where the SFG transfers CO_2.
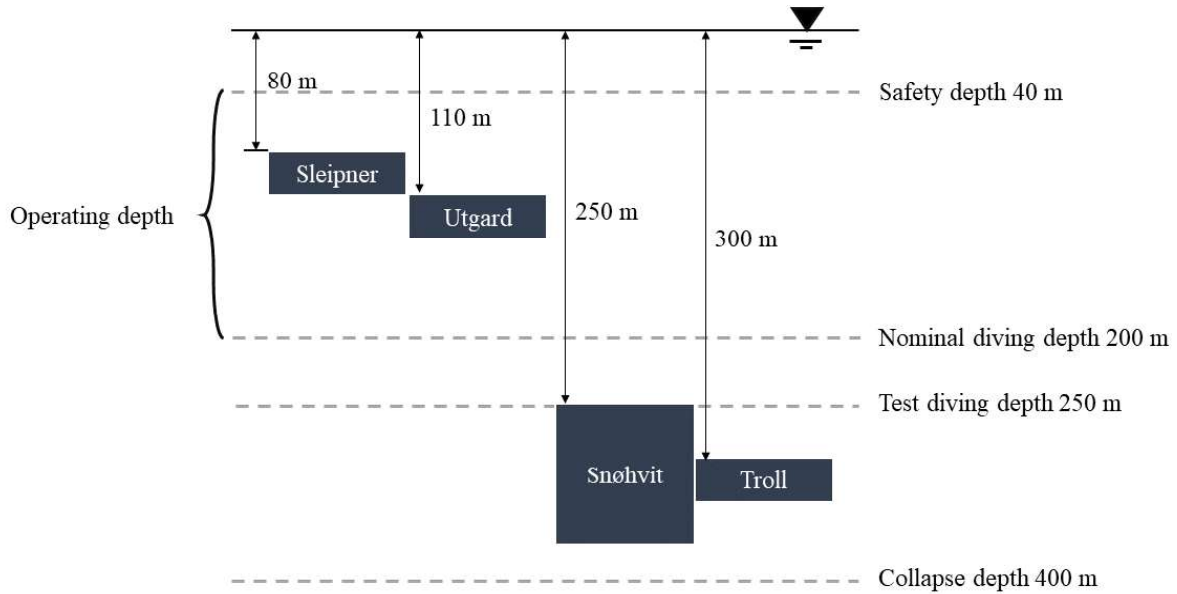
Figure 2.2 Operational depth of SFG. Reproduced from (Ma et al., 2021).

2.1.2. Operating range

The operating depth range identifies the transportation distance of the SFG. The SFG's baseline maximum range is 400 kilometres. This range allows it to transport CO_2 between the Snøhvit and Troll fields. Moreover, the SFG can also travel one way between Utgard and Sleipner. All gliders have a maximum range of 400 km. Therefore, the results are correlated.

2.1.3. Cargo Capacity

The baseline design of SFG has a cargo capacity of 1224 tons, which allows for 510 tons of CO_2 transportation.

2.1.4. Environmental and Weather Conditions

The environmental information is specified to understand the working condition and fulfil the requirements of transporting CO_2 in a specific location. The SFG is designed to transport carbon dioxide in the Norwegian Sea (0ºE − 10ºE, 60ºN − 70ºN). The expected temperature range of the seawater in that region is in the range of 0 and 20 degrees Celsius (NCEI, 2022.). The density of the seawater is 1025 kg/m3. The design current's velocity is 1 m/s, characterising the largest average current speed for the North Atlantic and Norwegian

coastal areas. Nonetheless, the noted mean current velocity in the Norwegian Sea is about 0.2 m/s (Ersdal, 2001).

2.2. Layout of SFG

The layout of the SFG specifies the placement of all structural elements. The submarine is divided into two main parts: internal hull and external hull. The general arrangement is presented in **Figure 2.3**.
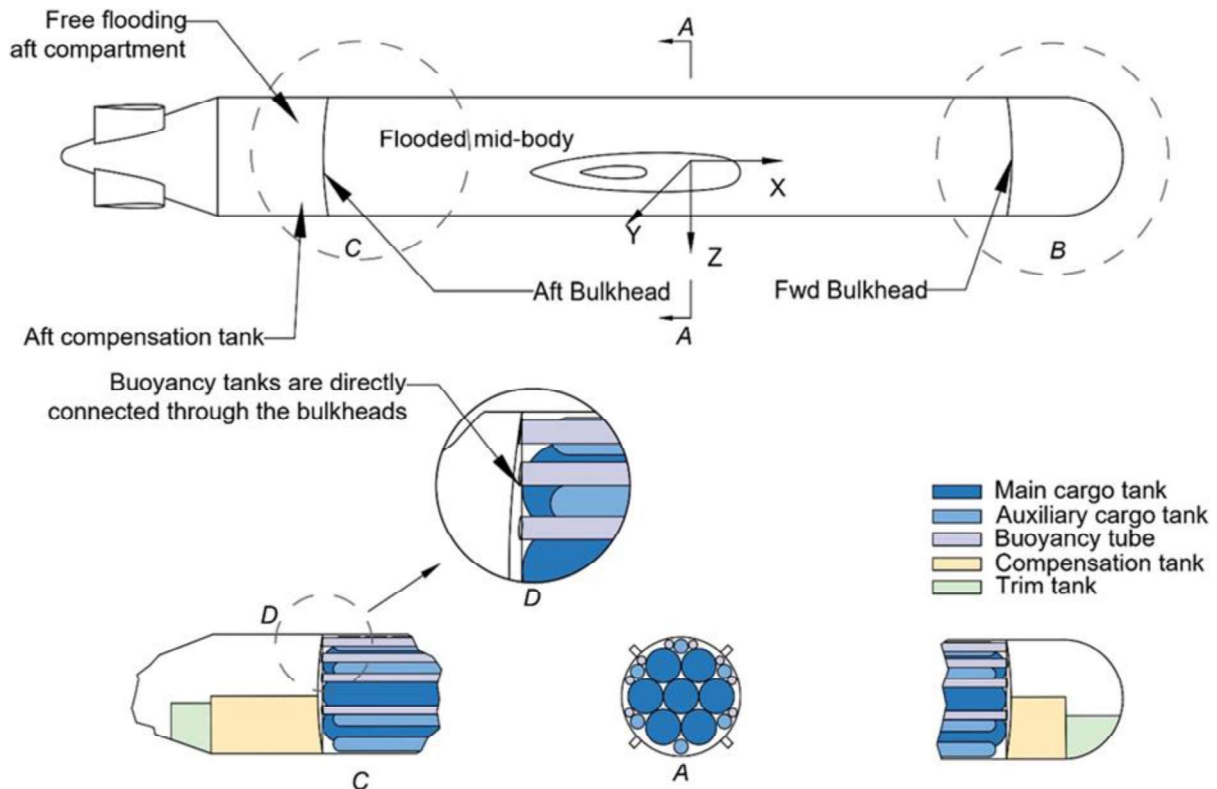
Figure 2.3 *General arrangement of SFG. Created based on the* (Xing, Santoso, et al., 2021).

2.2.1. External Hull

The external hull of the SFG is one of the most critical components of the vessel. It defines the shape and the characteristics of the underwater vehicle, as well as affects the vessel's hydrodynamic performance, and specifies the necessary power to move through the water. To achieve low drag resistance, the SFG has a torpedo shape.

The external hull of the SFG consists of free main different sections:

- **a flooded mid-body compartment** which houses cargo tanks, buoyancy tanks and piping. This section is placed in the centre of the SFG, and it is the largest part of the vessel;
- **a free-flooding bow compartment** which houses the front trim tanks, front compensation tank, sonar, load/offload pipes, radio, and control station;
- **a free-flooding aft compartment** holds sensitive apparatus, i.e., rear compensation tank, driving controls, gearbox, rear trim tanks, and batteries.

A double hull structure is adopted for the cylindrically shaped mid-body to avoid the design requirements for collapse pressure. By implementing this solution, the external hull of the mid-body is not exposed to any differential loading, i.e., hydrostatic pressure. The cargo and buoyancy tanks are designed to resist collapse and burst pressure. The SFG is also equipped with four bulkheads that support internal cargo and buoyancy tanks and isolate the free-flooding compartment from the flooded mid-body compartment. The aft and bow modules' mass is around 22% of the external hull's overall weight. The SFG is also equipped with four bulkheads separate the flooded mid-body from its supporting tanks and flooding compartments.

2.2.2. Internal Hull

The main task of the internal hull is to hold all tanks and equipment necessary for operations. The SFG's internal hull is composed of three main components. The bow section houses various equipment such as the control station, sonar, sensors, pumps, radio, trim and compensation tanks. The mid-body section contains pipes and cargo, auxiliary, and buoyancy tanks. The aft section houses sensitive equipment such as the battery, motor, gearbox, aft compensation tank, aft trim tan, and rudder control.

The internal compartment of SFG contains five different internal pressure modules is the SFG, that are:

- **Main cargo tanks**. The main cargo tank of the SFG is composed of seven large tanks. These tanks are circularly distributed in the mid-body and have hemispherical ends. The purpose of this component is to hold CO_2 or seawater.
- **Buoyancy tanks**. Eight buoyancy tanks are distributed in the upper part of the mid-body to make the SFG neutrally buoyant. All tubes are the same volume. They have the same length as the main cargo and auxiliary tanks. These tanks

are attached to the front and back bulkhead and are empty to the reach neutral buoyancy.

- **Auxiliary cargo tanks**. There are six auxiliary cargo tanks. Analogous to main cargo tanks, they are also circularly distributed in the mid-body but have a smaller diameter. These tanks hold CO_2 or seawater.

- **Compensation tanks**. This compartment comprises two compensation tanks that give the weight and trimming moment required to make the SFG neutral buoyancy under different hydrostatic loads. One of the compensation tanks is placed in the front of the vessel, and the second in the back.

- **Trim tanks**. There are two trim tanks inside the SFG. These tanks make the vessel neutrally trim by placing the centre of gravity under the centre of buoyancy. The trim tank is located in the front and back of the SFG. Both tanks are in free-flooding compartments and do not interact with the open sea, so they are free from external hydrostatic pressure and have to deal with the internal hydrostatic pressure.

2.3. Hydrostatic Load Cases

Hydrostatic load cases are several different scenarios to check if the SFG is stable for all conditions. The hydrostatic stability is studied with the requirements provided in the DNVGL-RU-NAVAL-Pt4Ch standard (DNV GL AS, 2018). For the submarine with a displacement of 1000-2000 tons, the distance between the centre of gravity G and the centre of buoyancy B must be greater than 0.32. Moreover, the location of metacentric height GM must exceed 0.20 (Gudmestad, 2015).

- **Submerged (CO_2 filled)**: seven main tanks and six auxiliary tanks are fully submerged with liquified CO_2. In this case, SFG is fully loaded.

- **Surfaced (CO_2 filled)**: seven main tanks and six auxiliary tanks are fully submerged with liquified CO_2. In this case, SFG is floating on the surface of the Sea and ready to dive to the nominal operating depth.

- **Submerged (seawater filled)**: seven main tanks and six auxiliary tanks are fully inundated with seawater. This case occurs after the SFG offloads the CO_2 at a well.

- **Surfaced (seawater filled)**: five primary and three auxiliary submarine tanks at the bottom side are filled with seawater. This case occurs when the vessel starts or finishes its mission.

2.4. External Hull Methodology Design

In this section, the methodology of the external hull design is presented. The external hull is constructed with three different components. Bow and aft are free-flooding compartments, and mid-body is the flooded part. Pressure hulls in the free-floating compartments are subjected to hydrostatic pressure. The sections' stresses at the collapse depth − 40 bar, nominal diving depth − 20 bar, and test diving depth − 25 bar are computed and compared with the permissive stresses available in the DNVGL-RU-NAVAL-Pt4Ch1 standard (DNV GL AS, 2018). The design of the flooded mid-body module uses the same procedure as for the free-flooded compartments. Nonetheless, the flooded mid-body does not handle the hydrostatic pressure. Therefore, this section uses 20 bar (200 m) for collapse pressure to avoid mechanical failure in unintentional load cases.

The external hull of the SFG is reinforced by stiffeners, which prevents the external hull from having a buckling effect. The dimensions of the stiffener are in **Table 2.2**. The stiffeners are designed following the procedures provided in DNVGL-RU-NAVAL-Pt4CH1 (DNV GL AS, 2018).

Table 2.2 Stiffener dimensions.

Component	Symbol	Free-flooding compartment	Flooded compartment	Units
Frame web thickness	s_w	30	30	[mm]
Frame web height	h_w	165	165	[mm]
Inner radius to the flange of the frame	R_f	2532	2532	[mm]
Flange width	b_f	80	80	[mm]
Frame spacing	L_f	1000	1500	[mm]
Flange thickness	s_f	30	30	[mm]
Frame cross-sectional area	A_f	73500	73500	[mm^2]

The various inputs used in the design process of the SFG include the hull thickness, design pressure, hull radius, stiffener dimensions, young modulus, and Poisson ratio. The scheme of the stiffener used for external hull design is displayed in **Figure 2.4**. For simplicity, all designs of the SFG presented in this work use stiffener with the exact dimensions. For ferritic steel, the Young modulus equals 206 GPa and the Poisson ratio 0.3.
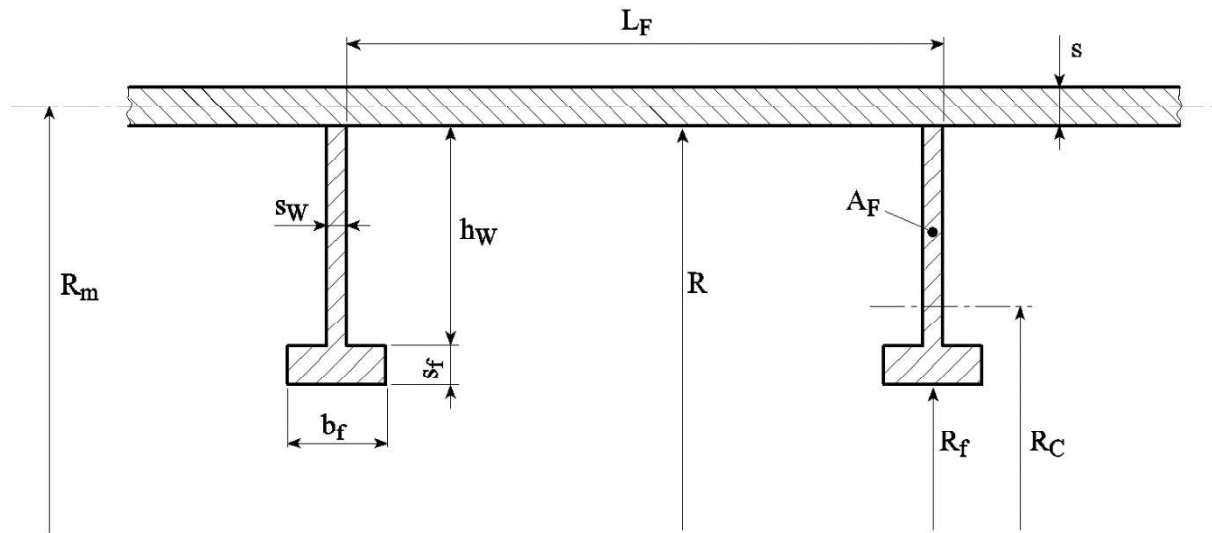
Figure 2.4 *Geometrical situation of frames stiffening the pressure hull. Reproduced from* (DNV GL AS, 2018).

The various materials used for the flooding compartment and the supporting tanks of the SFG are shown in **Table 2.3**. These materials are selected using DNVGL-RU-NAVAL-Pt4CH1 (DNV GL AS, 2018).

Table 2.3 *Material selection for the SFG design.*

Properties	Material	Yield Strength	Tensile Strength
Bulkhead	VL D37	360 MPa	276 MPa
External hull – bow compartment	VL D47	460 MPa	550 MPa
External hull – aft compartment	VL D47	460 MPa	550 MPa
External hull – mid-body	VL D47	460 MPa	550 MPa
Internal hull – main cargo tank	SA-738 Grade B	414 MPa	550 MPa
Internal hull – compensation tank	SA-738 Grade B	414 MPa	586 MPa
Internal hull – auxiliary cargo tank	SA-738 Grade B	414 MPa	586 MPa

The wall thickness of the SFG is obtained by repeating the calculation process with different pressure variables to assure that its external hull properties can endure the design pressure. The computations follow DNVGL-RU-NAVAL-Pt4Ch1 Appendix A, Section 6 (DNV GL AS, 2018). Next, the stresses are computed and evaluated to determine the collapse pressure of the SFG. The values of the design pressure are shown in **Table 2.4**. After the stress is calculated, the collapse pressure of the SFG is evaluated.

Table 2.4 Permissible and equivalent stress in the external hull of the SFG baseline design.

Case	Permissible stress calculation	Permissible Stress (Ref. Sec. 4.3 in DNVGL-RU-Pt4Ch1	Maximum Equivalent Stress
Nominal diving depth	$\min\left\{\dfrac{460\ MPa}{1.7}; \dfrac{550\ MPa}{2.7}\right\}$	203 MPa	196 MPa
Test diving depth	$\dfrac{460\ MPa}{1.1}$	418 MPa	247 MPa
Collapse depth	$\dfrac{460\ MPa}{1.0}$	460 MPa	402 MPa
Flooded compartment	$\dfrac{460\ MPa}{1.0}$	460 MPa	432 MPa

The procedure for stress calculations provided in DNVGL-RU-NAVAL-Pt4Ch1 (DNV GL AS, 2018) follows:

1. Calculation of basic equations and factors (formulas given in **Equation 2.1** and **Equation 2.2**).
2. Calculation of radial displacement between the frames in the middle w_M (**Equation 2.3**) and at the frames w_F (**Equation 2.4**).
3. Calculation of the circumferential stress in the unstiffened cylindrical pressure hull as reference stress (σ_0) and average membrane stress in the longitudinal direction (σ_x^m) (**Equation 2.5**).
4. Calculation of the membrane stress in the circumferential direction between frames in the middle and at the frames ($\sigma_{\varphi,M}^m$ and $\sigma_{\varphi,F}^m$) (**Equation 2.6**), bending stresses in the longitudinal direction between the frames in the middle and at the frames ($\sigma_{x,M}^b$ and $\sigma_{x,F}^b$) (**Equation 2.7**), also the bending stresses in the circumferential direction between the frames in the middle and at the frames ($\sigma_{\varphi,M}^b$ and $\sigma_{\varphi,F}^b$).

5. Calculation of the equivalent stresses formed by the single stresses in the longitudinal and circumferential directions (σ_v) (**Equation 2.8**).

The summery of stress in a stiffened cylindrical shell is presented in **Table 2.5**.

$$p^* = \frac{2E \cdot s^2}{R_m^2 \sqrt{3(1-v^2)}}$$ $$\eta_1 = \frac{1}{2}\sqrt{1-\gamma}$$ $$L = L_F - S_w$$ $$A_{eff} = A_F \frac{R_m}{R_c}$$	$$\gamma = \frac{p}{p^*}$$ $$\eta_2 = \frac{1}{2}\sqrt{1+\gamma}$$ $$L_{eff} = \frac{2}{\sqrt[4]{3(1-v^2)}}\sqrt{R_m \cdot s}$$ $$\theta = \frac{2L}{L_{eff}}$$	**Equation 2.1**

$$F_1 = \frac{4}{\theta}\left(\frac{\cosh^2 \eta_1\theta - \cos^2 \eta_2\theta}{\frac{\cosh \eta_1\theta \cdot \sinh \eta_1\theta}{\eta_1} + \frac{\cosh \eta_2\theta \cdot \sinh \eta_2\theta}{\eta_2}}\right)$$ $$F_2 = \left(\frac{\frac{\cosh \eta_1\theta \cdot \sin \eta_2\theta}{\eta_2} + \frac{\sinh \eta_1\theta \cdot \cos \eta_1\theta}{\eta_1}}{\frac{\cosh \eta_1\theta \cdot \sinh \eta_1\theta}{\eta_1} + \frac{\cos \eta_2\theta \cdot \sin \eta_2\theta}{\eta_2}}\right)$$ $$F_3 = \sqrt{\frac{3}{1-v^2}}\left(\frac{-\frac{\cosh \eta_1\theta \cdot \sin \eta_1\theta}{\eta_1} + \frac{\cos \eta_2\theta \cdot \sin \eta_2\theta}{\eta_2}}{\frac{\cosh \eta_1\theta \cdot \sinh \eta_1\theta}{\eta_1} + \frac{\cos \eta_2\theta \cdot \sin \eta_2\theta}{\eta_2}}\right)$$ $$F_4 = \sqrt{\frac{3}{1-v^2}}\left(\frac{\frac{\cosh \eta_1\theta \cdot \sin \eta_2\theta}{\eta_1} + \frac{\sinh \eta_2\theta \cdot \cos \eta_2\theta}{\eta_2}}{\frac{\cosh \eta_1\theta \cdot \sinh \eta_1\theta}{\eta_1} + \frac{\cos \eta_2\theta \cdot \sin \eta_2\theta}{\eta_2}}\right)$$	**Equation 2.2**

$$w_M = -\frac{p \cdot R_m^2}{E \cdot s}\left(1 - \frac{v}{2}\right)\left(1 - \frac{A_{eff} \cdot F_2}{A_{eff} + s_w \cdot s + L \cdot s \cdot F_1}\right)$$	**Equation 2.3**

$$F_{WF} = \cosh \eta_1 \theta \cdot \cos \eta_2 \theta + \frac{\sqrt{\frac{1-v^2}{3} \frac{F_4}{F_3} + \gamma}}{4\eta_1 \eta_2} \sinh \eta_1 \theta \cdot \sin \eta_2 \theta$$ $$w_F = -\frac{p \cdot R_m^2}{E \cdot s}\left(1 - \frac{v}{2}\right)\left(1 - \frac{A_{eff} \cdot F_2}{A_{eff} + s_W \cdot sL \cdot s \cdot F_1} \cdot F_{WF}\right)$$	**Equation 2.4**

$$\sigma_0 = -\frac{p \cdot R_m}{s}$$ $$\sigma_x^m = -\frac{p \cdot R_m}{2s}$$	**Equation 2.5**

$$\sigma_{\varphi,M}^m = E\frac{w_M}{R_m} + v \cdot \sigma_x^m$$ $$\sigma_{\varphi,F}^m = E\frac{w_F}{R_m} + v \cdot \sigma_x^m$$	**Equation 2.6**

$$\sigma_{x,M}^b = \pm\sigma_0\left(1 - \frac{v}{2}\right) \cdot F_4 \frac{A_{eff}}{A_{eff} + s_w \cdot s + L \cdot s \cdot F_1}$$ $$\sigma_{x,F}^b = \pm\left(\sigma_0 - \sigma_{\varphi,F}^m\right)F_3$$ $$\sigma_{\varphi,M}^b = v \cdot \sigma_{x,M}^b$$ $$\sigma_{\varphi,F}^b = v \cdot \sigma_{x,F}^b$$	**Equation 2.7**

$$\sigma_v = \sqrt{\sigma_x^2 + \sigma_\varphi^2 - \sigma_x \cdot \sigma_\varphi}$$	**Equation 2.8**

Table 2.5 *Summary of stress in the stiffened cylindrical shell.*

Types of stresses	At the frame			In the middle of the field		
	Circum-ferential	Equivalent	Axial	Circum-ferential	Equivalent	Axial
Membrane stress	$\sigma_{\varphi,F}^m$		$\sigma_{x,F}^m$	$\sigma_{\varphi,M}^m$		$\sigma_{x,M}^m$
Membrane equivalent stress		$\sigma_{v,F}^m$			$\sigma_{v,M}^m$	
Bending stress	$\sigma_{\varphi,F}^b$		$\sigma_{x,F}^b$	$\sigma_{\varphi,M}^b$		$\sigma_{x,M}^b$
Normal stress outside	$\sigma_{\varphi,F}^m + \sigma_{\varphi,F}^b$		$\sigma_{x,F}^m + \sigma_{x,F}^b$	$\sigma_{\varphi,M}^m + \sigma_{\varphi,F}^b$		$\sigma_{x,M}^m + \sigma_{x,M}^b$
Equivalent normal stress outside		$\sigma_{v,F,o}^{m+b}$			$\sigma_{v,M,o}^{m+b}$	
Normal stresses inside	$\sigma_{\varphi,F}^m - \sigma_{\varphi,F}^b$		$\sigma_{x,F}^m - \sigma_{x,F}^b$	$\sigma_{\varphi,M}^m - \sigma_{\varphi,M}^b$		$\sigma_{x,M}^m - \sigma_{x,M}^b$
Equivalent normal stress inside		$\sigma_{v,F,i}^{m+b}$			$\sigma_{v,M,i}^{m+b}$	

The procedure for calculating the collapse pressure for the SFG provided in (DNV GL AS, 2018):

1. Calculation of the function of the elastic-plastic buckling pressure (E_t and E_s) and the elastic-plastic Poisson's ratio (v_p) (**Equation 2.9**).
2. Calculation of factors provided in **Equation 2.10**.
3. Calculation of the elastic buckling pressure and the theoretical elastic-plastic buckling pressure (p_{cr}^{el} and p_{cr}^i) (**Equation 2.11**).
4. Calculation of the reduction factor (r). The collapse pressure in the theoretical elastic-plastic buckling pressure multiplied by the reduction factor (p_{cr}^*) (**Equation 2.12**).

$$E_t = E \cdot \left(1 - \left(\frac{\sigma_v - z \cdot \sigma_{0.2}}{(1-z) \cdot \sigma_{0.2}}\right)^2\right)$$

$$E_s = E \cdot \frac{\sigma_v}{\sigma_{0.2}\left(z + (1-z) \cdot \tanh^{-1}\frac{\sigma_v - z \cdot \sigma_{0.2}}{(1-z) \cdot \sigma_{0.2}}\right)}$$

$$v_p = \frac{1}{2} - \frac{E_s}{E}\left(\frac{1}{2} - v\right)$$

Equation 2.9

$$k = \frac{\sigma_{\varphi,M}^m}{\sigma_x^m} \qquad K = \sqrt{|1 - k + k^2|}$$

$$a_1 = \left((2 - v_p) - (1 - 2v_p)k\right)^2 \qquad a_2 = \left((1 - 2v_p) - (2 - v_p)k\right)^2$$

$$H = 1 + \frac{1 - \dfrac{E_t}{E_s}}{4(1 - v_p^2)K^2}\left(a_1 - 3(1 - v_p^2)\right)$$

$$A_1 = 1 - \frac{1 - \dfrac{E_t}{E_s}}{4(1 - v_p^2)K^2 H}a_1$$

$$A_2 = 1 - \frac{1 - \dfrac{E_t}{E_s}}{4(1 - v_p^2)K^2 H}a_2$$

$$A_{12} = 1 + \frac{1 - \dfrac{E_t}{E_s}}{4(1 - v_p^2)K^2 H}\sqrt{a_1}\cdot\sqrt{a_2}$$

$$C = \sqrt{\frac{A_1 \cdot A_2 - v_p^2 \cdot A_{12}^2}{1 - v_p^2}} \qquad \alpha = \sqrt[4]{\frac{3\left(\dfrac{A_2}{A_1} - v_p^2 \cdot \dfrac{A_{12}^2}{A_1^2}\right)}{R_m^2 \cdot s^2}}$$

Equation 2.10

$$p_{cr}^{el} = \frac{2}{\sqrt{3(1 - v^2)}} \cdot E \cdot \frac{s^2}{R_m^2}\left(\left(\frac{2L}{\pi \cdot L_{eff}}\right)^2 + \frac{1}{4}\left(\frac{\pi \cdot L_{eff}}{2L}\right)^2\right)$$

$$p_{cr}^{i} = \frac{2}{\sqrt{3(1 - v^2)}} \cdot E \cdot \frac{s^2}{R_m^2} \cdot C \cdot \left(\left(\frac{\alpha \cdot L}{\pi}\right)^2 + \frac{1}{4}\left(\frac{\pi}{\alpha \cdot L}\right)^2\right)$$

Equation 2.11

$$r = 1 - 0.25 \cdot e^{-\frac{1}{2}\left(\frac{p_{cr}^{el}}{p_{cr}^{i}} - 1\right)}$$

$$p_{cr}^* = p_{cr}^i \cdot r$$

Equation 2.12

2.5. Internal Design for Internal Pressure

This section presents the calculation procedure of the SFG internal tank design. All the internal tanks are designed following the guidelines of the American Society of Mechanical Engineers ASME BPVC Section VIII, Division 2, Chapter 4 (ASME, 2017). All internal tanks – main cargo, auxiliary, compensation, and trim tanks are designed to resist the burst pressure (internal pressure). On the other hand, buoyancy tubes are mainly used against collapse pressure (external pressure).

All internal tanks except buoyancy tanks are designed to take burst pressure. **Equation 2.13** and **Equation 2.14** calculate the minimum wall thickness that the hemispherical heads and cylindrical shells have to fulfil the requirements. The minimum thickness that a tank has to have to resist internal pressure is described by the **Equation 2.13**:

$$t_{shell} = \frac{D_t}{2}\left(\exp\left[\frac{p_i}{S_a \cdot E_w}\right] - 1\right)$$ | **Equation 2.13**

Correspondingly, the minimum thickness that a hemisphere head has to have to resist internal pressure is described by the **Equation 2.14**:

$$t_{shell} = \frac{D_t}{2}\left(\exp\left[\frac{0.5 \cdot p_i}{S_a \cdot E_w}\right] - 1\right)$$ | **Equation 2.14**

Where: t_{shell} is wall thickness; D_t is the diameter of the tank; p_i is a design pressure (it is assumed to be 55 bar for main, auxiliary, compensation, and trim tanks); S_a is the permissible material stress; E_w is an efficiency of the weld joint (it is assumed to be 1.0 for longitudinal and circumferential joints).

The calculation procedure for external pressure provided in ASME BPVC Section VIII, Division 2, Chapter 4 (ASME, 2017) follows:

1. Calculation of the predicted elastic buckling (F_{he}) (**Equation 2.15**)
2. Calculation of the predicted buckling stress (F_{ic}) (**Equation 2.16**)
3. Calculation of the design factor value (FS) (**Equation 2.17**)
4. Calculation of the allowable pressure (P_a) (**Equation 2.18**

If the external pressure is less than P_a the tank's thickness should be increased. This step should be repeated until the external pressure equals to or exceeds the external design pressure.

$$M_X = \frac{L}{\sqrt{R_0 t}}$$

$$F_{he} = \frac{1.6 \cdot C_h \cdot E_y \cdot t}{D_0}$$

$$C_h = 0.55 \left(\frac{t}{D_0}\right) \qquad for \ M_X \geq 2\left(\frac{D_0}{t}\right)^{0.94}$$

$$C_h = 1.12 M_X^{-1.058} \qquad for \ 13 < M_X < 2\left(\frac{D_0}{t}\right)^{0.94}$$

$$C_h = \frac{0.92}{M_X - 0.579} \qquad for \ 1.5 < M_X < 13$$

$$C_h = 1.0 \qquad for \ M_X \leq 1.5$$

Equation 2.15

$$F_{ic} = S_y \qquad for \ \frac{F_{he}}{S_y} \geq 2.439$$

$$F_{ic} = 0.7 \cdot S_y \left(\frac{F_{he}}{S_y}\right)^{0.4} \qquad for \ 0.552 < \frac{F_{he}}{S_y} < 2.439$$

$$F_{ic} = F_{he} \qquad for \ \frac{F_{he}}{S_y} < 0.552$$

Equation 2.16

$$FS = 2 \qquad for \ F_{ic} \leq 0.55 S_y$$

$$FS = 2.407 - 0.741 \left(\frac{F_{ic}}{S_y}\right) \qquad for \ 0.55 S_y < F_{ic} < S_y$$

$$FS = 1.667 \qquad for \ F_{ic} = S_y$$

Equation 2.17

$$F_{ha} = \frac{F_{ic}}{FS}$$

$$P_a = 2 F_{ha} \left(\frac{t}{D_0}\right)$$

Equation 2.18

2.6. Wing Design

The procedure of the design for the wings is illustrated in **Figure 2.5**. The nominal operating depth of the SFG defines the vessel class, which provides the foundations for selecting an actual angle of the glide path (Rudnick et al., 2004). It is possible to compute SFG velocities, lift and yield drag forces based on the gliding angle. Next, the reference area of the hydrofoil and lift/drag ratio can be estimated. The parameters of the glider are shown in **Figure 2.6**, where W is the weight of the SFG; Fb is the buoyancy force (Wood & Stephen, 2009).
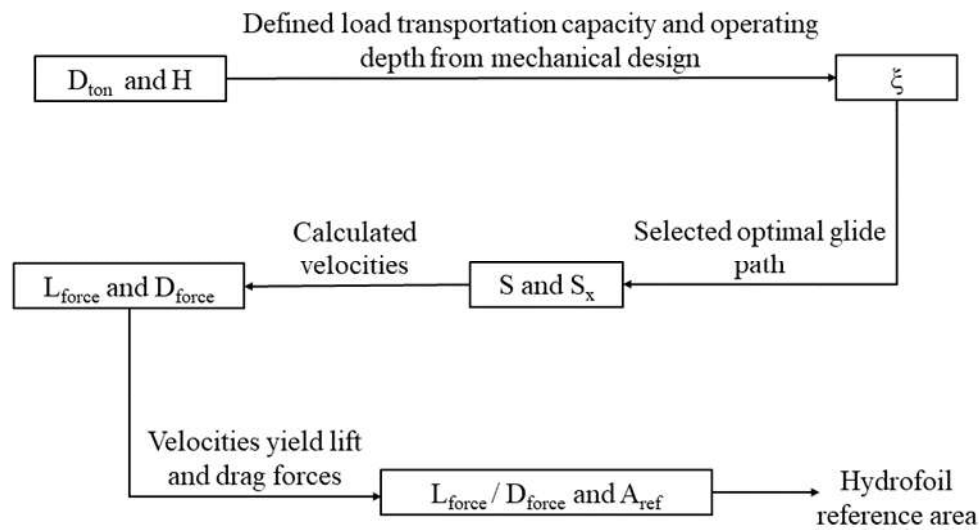
Figure 2.5 Global parameters of the SFG. Reproduced from (U. Ahmad et al., 2022)

The area of the hydrofoil is calculated using the following equations. The calculations follow the procedure given in (Graver, 2005).

$$BF = \frac{m_o}{D_{ton} \cdot 1000}$$ **Equation 2.19**

Where: m_o is the mass of the SFG.

$$S = \sqrt[2]{\left(\frac{m_o \cdot g \cdot \sin \xi}{\frac{1}{2} \cdot \rho_w \cdot C_{DVol} \cdot Vol^{\frac{2}{3}}}\right)}$$ **Equation 2.20**

Where: S is the glider velocity; ρ_w is the water density; g is the gravitational constant.

$$S_x = S \cdot \cos \xi$$

$$D_{force} = \frac{1}{2} \cdot S^2 \cdot \rho_w \cdot C_{DVol} \cdot V^{\frac{2}{3}}$$

Equation 2.21

where: C_{DVol} is the SFG volumetric drag coefficient; C_L is the SFG volumetric lift coefficient; V is the total SFG volume.

$$L_{force} = \frac{D_{force}}{\tan \xi}$$

Equation 2.22

where: L_{force} is the lift force and D_{force} is the drag force.

$$A_{reference} = \frac{L}{\frac{1}{2} \cdot S^2 \cdot \rho_w \cdot C_L}$$

Equation 2.23
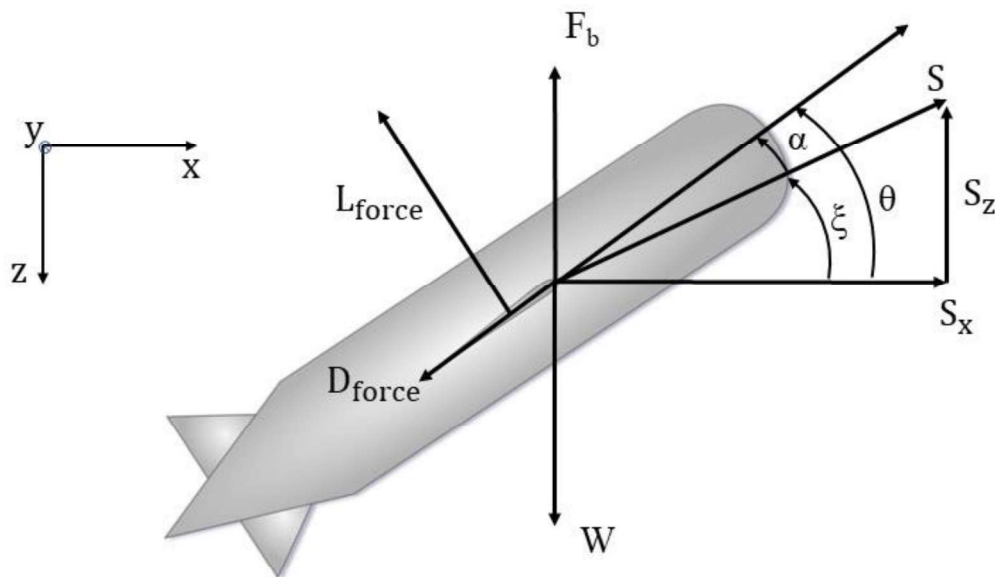
Figure 2.6 Scheme of the SFG parameters. Based on (Tsang et al., 2018).

2.7. Power Calculations

The total energy consumption of the SFG is computed by taking into account the various energy costs associated with its operation, hotel load and pump energy consumption.

2.7.1. Resistance force

The resistance force of SFG is determined by its speed and vessel dimensions. To minimise the resistance and maximise the energy efficiency of the submarine, the vehicle should travel at a slow speed. The resistance force is more significant if the vessel has a higher

speed. The underwater vehicle transports the CO_2 with a velocity of 1 m/s, as it is defined in **Table 2.1**. The SFG's slenderness ratio is also considered to determine the drag resistance. For all SFG designs, the slenderness ratio is set at 9.7, which is near the theoretical minimum.

Two types of friction occur when the SFG moves forward: body drag and skin friction. The former is caused by the differential pressure between the aft and bow of the ship, while the latter is caused by the friction between the SFG's surface area and seawater. For slender structures, the wet surface area/volume ratio is high. It implies that the skin friction is higher than the body drag. The resistance components are calculated by computing the Reynold number (**Equation 2.24**), which is used to calculate the resistance coefficient (**Equation 2.25**). The factor k is defined by the formula from (Cheeseman, 1976). The factor k is described as beam D and length L (**Equation 2.26**).

The drag load is estimated analytically from Hoerner's scheme (Cheeseman, 1976). Furthermore, the correlation line established at the International Towing Tank Conference (ITTC, 2002) estimates the resistance power of the skin friction.

$$Re = \frac{L \cdot u}{v}$$	**Equation 2.24**

$$C_{sf} = \frac{0.075}{(\log_{10} Re - 2)^2}$$ $$C_{vs} = (1 + k_s) \cdot C_{sf}$$ $$D_{vs} = \frac{1}{2} \rho A_w C_{vs} u^2$$	**Equation 2.25**

$$k = 1.5 \left(\frac{D}{L}\right)^{1.5} + 7 \left(\frac{D}{L}\right)^3$$	**Equation 2.26**

2.7.2. Hotel Load Estimation

The hotel load of the SFG is the total power utilized by its various systems except for the pumps. This is computed by considering the control units, sensors, and navigation systems. The power consumption of the SFG is estimated using the power ratios in the MUNIN (MUNIN, 2015) and Wartsila LR2 product tankers (Wärtsilä, 2017). For SFG, the reduction in the power consumption by 40% is equivalent to the ship's hotel load since the SFG is autonomous and can be operated without a crew.

2.7.3. Pump Energy Consumption

The power of the pump is approximated based on the flow of the pump duration to load and unload the freight. It takes 4 hours to load and reload the cargo since the pumps give 3 bars of differential pressure. Every SFG design has different volumetric flow rates to guarantee the same loading and offloading intervals. The efficiency of the pumps is assumed to be not lower than 75% (Hall, 2018).

The energy consumption of cargo pumps and ballast pumps utilised during the unloading and loading process is calculated by taking into account the two load cycles in a trip. The first cycle involves unloading at the port, and the second cycle consists of loading at the well. Each time the SFG takes four hours to load and offload, the energy consumption of each process is equal. In accordance with (Hall, 2018) and (Elsey, 2020), the efficiency of the pumps is estimated to be 75%. That value equals the efficiency of centrifugal compressor and large centrifugal pumps. The energy consumption is computed using **Equation 2.27**.

$$P_{pump} = n_l \cdot t_l \cdot \frac{Q_{cargo} \cdot \Delta p_{cargo} + Q_{ballast} \cdot \Delta p_{ballast}}{3.6 \cdot 10^6 \cdot \eta_{pump}}$$	**Equation 2.27**

Where: n_l is the offload or load time; t_l is a number of the load cycle; Q_{cargo} is the flow rate of the cargo pump; $Q_{ballast}$ is the flow rate of the ballast pump; Δp_{cargo} is the pressure differential of the cargo pump; $\Delta p_{ballast}$ is pressure differential of the ballast pump; η_{pump} is the pump efficiency.

3. Technical Feasibility Analysis

This chapter provides the technical feasibility study of SFG. This process involves creating different sizes for the SFG tank to meet the mission requirements. The goal of the technical feasibility analysis is to identify the technical limitations that can be encountered when the baseline cargo capacity of the tank decreases or increases. The design process follows the procedure shown in **Figure 2.1**.

The external hull of the SFG baseline design is 56.5 m long, with a diameter of 5.5 m and a total volume of 1194 m^3. Up-scale and down-scale models are designed with about ±50% of the SFG baseline design volume. The up-scale design is 71.5 m long, with a diameter of 7 m and a volume of 2430 m^3. In contrast, the down-scale design has a volume of 469 m^3 with a length of 42.25 m and a diameter of 4 m. In addition, the baseline design is recalculated and included in the study with other designs. One assumed condition is that the payload should be around 45% of the displacement and the mission requirements are the same.

3.1. The Baseline Design of SFG

3.1.1. External Hull Design

In this section, the external hull design is performed. The inputs and results used in the design process are displayed in **Table 3.1**. The table's symbols and equation numbers are the same as the notation used in (DNV GL AS, 2018)**.** The stresses at nominal, test diving and collapse for free-flooding and flooded compartments of SFG are shown in **Table 3.2**, **Table 3.3**, **Table 3.4**, and **Table 3.5**.

This analysis indicates that the wall thickness of the flooding compartments is equal to 0.03 m, while the wall thickness for the free-flooding section is 0.013. The weight of the external hull is also calculated by considering the steel material and the external hull dimensions. The outline of the external hull design for the SFG baseline design is displayed in **Table 3.7**.

Table 3.1 Calculation for the external hull of SFG baseline design.

Parameter	Symbol	Free flooding compartment			Flooded compartment	Units	Equation number (DNV GL RU Pt4C1 Appendix A)
		Nominal diving depth	Test diving depth	Collapse depth	Collapse		
Design pressure	p	20	25	40	20	[bar]	User input
Hull thickness	s	0.03	0.03	0.03	0.013	[m]	User input
Hull radius	R_m	2.75	2.75	2.75	2.75	[m]	User input
Frame web height	h_w	0.165	0.165	0.165	0.165	[m]	User input
Frame web thickness	s_w	0.003	0.003	0.003	0.003	[m]	User input
Flange width	b_f	0.08	0.08	0.08	0.08	[m]	User input
Flange thickness	s_f	0.03	0.03	0.03	0.03	[m]	User input
Frame spacing	L_f	1.0	1.0	1.0	1.5	[m]	User input
Frame cross-sectional area	A_f	0.0074	0.0074	0.0074	0.0074	[m^2]	User input
Inner radius to the flange of the frame	R_f	2.53	2.53	2.53	2.53	[m]	User input
Youngs modulus	E	206	206	206	206	[GPa]	User input
Poisson Ratio	v	0.3	0.3	0.3	0.3	-	User input
Poisson ratio in elastic-plastic range	v_p	0.44	0.44	0.44	0.44	-	(A48)
Frame distance without thickness	L	0.97	0.97	0.97	0.97	[m]	(A9)
Effective length	L_{eff}	0.447	0.447	0.447	0.294	[m]	(A10)
Effective area	A_{eff}	0.0076	0.0076	0.0076	0.0077	[m^2]	(A11)
The radial displacement in the middle between the frames	w_M	-0.002	-0.0025	-0.0042	-0.0047	[m]	(A15)
The radial displacement at the frames	w_F	-0.0021	-0.0027	-0.0041	-0.0032	[m]	(A16)
The reference stress is the circumferential stress in the unstiffened cylindrical pressure hull	σ_0	183	229	367	423	[MPa]	(A13)
The equivalent stresses are composed of the single stresses in a longitudinal and circumferential direction in the middle between frames	$\sigma^m_{v,m}$	156	196	318	360	[MPa]	(A14)
The equivalent stresses are composed of the single stresses in a longitudinal and circumferential direction at the frames	$\sigma^m_{v,f}$	164	203	317	268	[MP]	(A14)
Average membrane stress in longitudinal direction	σ^m_x	91	115	183	212	[MPa]	(A17)
Membrane stress in circumferential the direction in the middle between the frames	$\sigma^m_{\varphi,M}$	181	227	367	416	[MPa]	(A18)
Membrane stress in circumferential direction at the frames	$\sigma^m_{\varphi,F}$	189	235	366	301	[MPa]	(A19)
Bending stresses in longitudinal direction in the middle between the frames	$\sigma^x_{\varphi,M}$	52	67	117	27	[MPa]	(A20)
Bending stresses in longitudinal direction at the frames	$\sigma^b_{x,F}$	11	11	16	221	[MPa]	(A21)
Bending stresses in circumferential the direction in the middle between the frames	$\sigma^b_{\varphi,M}$	16	20	32	8	[MPa]	(A22)
Bending stresses in circumferential direction at the frames	$\sigma^b_{\varphi,M}$	3	3	5	66	[MPa]	(A23)
Tangential module	E_t	206	206	206	206	[MPa]	(A38)
Secant module	E_s	204	204	204	204	[GPa]	(A39)
Elastic buckling pressure	p^{el}_{cr}	82	82	82	62	[GPa]	(A28)
Theoretical elastic-plastic buckling pressure	p^i_{cr}	93	93	93	70	[bar]	(A29)
Reduction factor	R	0.75	0.75	0.75	0.75	[bar]	(A43)

Table 3.2 *Stresses at nominal diving depth for SFG baseline design in the free-flooding compartment.*

Type of stresses	As the frame			In the middle of the field		
	Circumferential	Equivalent	Axial	Circumferential	Equivalent	Axial
Membrane stress	189 MPa	-	92 MPa	181 MPa	-	92 MPa
Membrane equivalent stress	-	156 MPa	-	-	164 MPa	-
Bending stress	3 MPa	-	11 MPa	16 MPa	-	52 MPa
Normal stress outside	192 MPa	-	102 MPa	196 MPa	-	144 MPa
Equivalent stress outside	-	166 MPa	-	-	176 MPa	-
Normal stress inside	192 MPa	-	102 MPa	196 MPa	-	144 MPa
Equivalent normal stress inside	-	166 MPa	-	-	176 MPa	-

Table 3.3 *Stresses at test diving depth for SFG baseline design in the free-flooding compartment.*

Type of stresses	As the frame			In the middle of the field		
	Circumferential	Equivalent	Axial	Circumferential	Equivalent	Axial
Membrane stress	235 MPa	-	115 MPa	227 MPa	-	115 MPa
Membrane equivalent stress	-	196 MPa	-	-	203 MPa	-
Bending stress	3 MPa	-	11 MPa	20 MPa	-	67 MPa
Normal stress outside	238 MPa	-	126 MPa	247 MPa	-	182 MPa
Equivalent stress outside	-	206 MPa	-	-	221 MPa	-
Normal stress inside	238 MPa	-	126 MPa	247 MPa	-	182 MPa
Equivalent normal stress inside	-	206 MPa	-	-	221 MPa	-

Table 3.4 *Stresses at collapse diving depth for SFG baseline design in the free-flooding compartment.*

Type of stresses	As the frame			In the middle of the field		
	Circumferential	Equivalent	Axial	Circumferential	Equivalent	Axial
Membrane stress	366 MPa	-	183 MPa	367 MPa	-	183 MPa
Membrane equivalent stress	-	318 MPa	-	-	317 MPa	-
Bending stress	1 MPa	-	2 MPa	35 MPa	-	117 MPa
Normal stress outside	366 MPa	-	185 MPa	402 MPa	-	301 MPa
Equivalent stress outside	-	317 MPa	-	-	362 MPa	-
Normal stress inside	366 MPa	-	185 MPa	402 MPa	-	301 MPa
Equivalent normal stress inside	-	317 MPa	-	-	362 MPa	-

Table 3.5 *Stresses at collapse diving depth for SFG baseline design in the flooded compartment.*

Type of stresses	As the frame			In the middle of the field		
	Circumferential	Equivalent	Axial	Circumferential	Equivalent	Axial
Membrane stress	301 MPa	-	212 MPa	416 MPa	-	212 MPa
Membrane equivalent stress	-	360 MPa	-	-	268 MPa	-
Bending stress	66 MPa	-	221 MPa	8 MPa	-	27 MPa
Normal stress outside	368 MPa	-	433 MPa	424 MPa	-	238 MPa
Equivalent stress outside	-	404 MPa	-	-	368 MPa	-
Normal stress inside	368 MPa	-	433 MPa	424 MPa	-	238 MPa
Equivalent normal stress inside	-	404 MPa	-	-	368 MPa	-

Table 3.6 *Permissible and equivalent stresses in the external hull of SFG baseline design.*

Case	Depth	Maximum equivalent stress	Permissible stress (DNVGL RU P4C1 Sec. 4.3)	Citation fulfilled?
Nominal diving depth	200 m	196 MPa	203 MPa	Yes
Testing diving depth	250 m	247 MPa	418 MPa	Yes
Collapse depth	400 m	402 MPa	460 MPa	Yes
Flooded compartment	-	432 MPa	460 MPa	Yes

Table 3.7 *SFG Baseline design of the external hull.*

Parameter		SFG 1194 m³	Units
Free-floating bow compartment	Thickness	0.030	[m]
	Length	8.750	[m]
	Steel weight	43.877	[ton]
	Material	VL D47	-
	Design collapse pressure	40	[bar]
Flooded mid-body	Thickness	0.013	[m]
	Length	33.75	[m]
	Steel weight	80.850	[ton]
	Material	VL D47	-
	Design collapse pressure	20	[bar]
Free-floating aft compartment	Thickness	0.030	[m]
	Length	14.00	[m]
	Steel weight	54.581	[ton]
	Material	VL D47	-
	Design collapse pressure	40	[bar]

3.1.2. Internal Tanks Design

The internal tanks on the mid-body are adjusted to optimise their internal hull volume. The arrangement of the internal tanks inside the mid-body is shown in **Figure 3.1**, which was created using the software Autodesk Inventor 2022. The external hull diameter is 5.5 meters, which results in the main cargo tanks having a diameter of 1.62 meters, the auxiliary tanks having a diameter of 0.7 meters, and the buoyancy tubes having a diameter of 0.35 meters. The design of the various internal tanks is shown in Table 8. This analysis indicates that the main cargo tanks have a thickness of 0.018 m. In comparison, the auxiliary tanks have a thickness of 0.008 m, and the buoyancy tubes are 0.004 meters thick. The weight of these tanks is also calculated by considering the steel density, thickness of the tanks and steel volume.
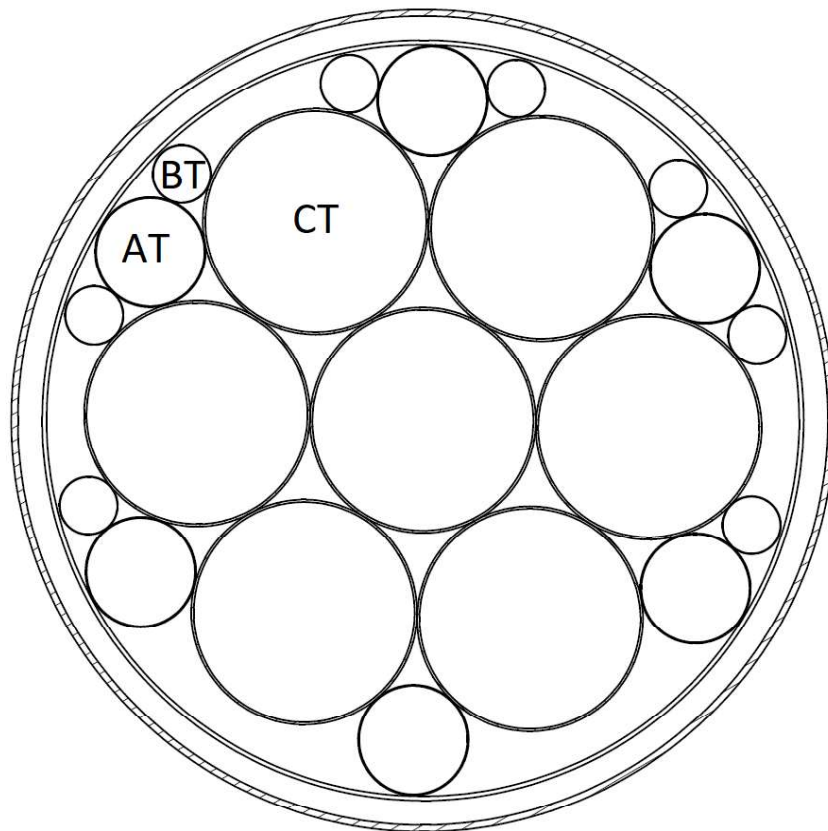
Figure 3.1 *Cross-section of the SFG. CT – Main Cargo Tank; AT – Auxiliary Tank; BT – Buoyancy Tube.*

Table 3.8 SFG Internal tank properties.

Parmeter		SFG 1194 m^3	Units
Main Cargo Tank (Total No. = 7)	Diameter	1.62	[m]
	Length	33.75	[m]
	Thickness	0.018	[m]
	Hemisphere head wall thickness	0.009	[m]
	Steel weight	168.998	[ton]
	Total volume	468.395	[m^2]
	Allowable burst pressure	55.0	[bar]
	Material	SA-738 Grade B	
Auxiliary Cargo Tank (Total No. = 6)	Diameter	0.70	[m]
	Length	32.83	[m]
	Thickness	0.008	[m]
	Hemisphere head wall thickness	0.004	[m]
	Steel weight	26.670	[ton]
	Total volume	73.568	[m^2]
	Allowable burst pressure	55.0	[bar]
	Material	SA-738 Grade B	
Compensation Tank (Total No. = 2)	Diameter	3.5	[m]
	Length	2.5	[m]
	Thickness	0.02	[m]
	Steel weight	72.063	[ton]
	Total volume	61.25	[m^2]
	Allowable burst pressure	8.0	[bar]
	Material	SA-738 Grade B	
Trim Tank (Total No. = 2)	Diameter	1.8	[m]
	Length	2.50	[m]
	Thickness	0.008	[m]
	Steel weight	14.702	[ton]
	Total volume	45.00	[m2]
	Allowable burst pressure	10.0	[bar]
	Material	SA-738 Grade B	
Buoyancy Tube (Total No. = 8)	Diameter	0.35	[m]
	Length	32.5	[m]
	Thickness	0.004	[m]
	Hemisphere head wall thickness	0.002	[m]
	Steel weight	8.845	[ton]
	Total volume	24.910	[m^2]
	Allowable burst pressure	20.0	[bar]
	Material	SA-738 Grade B	

3.2. Weight Estimation

The weight of the SFG structure is calculated for stability check following the various hydrodynamic loading conditions mentioned in **Chapter 2.3**. At operating conditions, the structure's weight is divided into the following parts: machinery, permanent ballast (to ensure stability), structure, mid-body seawater, compensation ballast (compensation tanks), payload, and trim tank weight. The mass of the SFG structure is composed of the external hull and the internal hull weight. The cargo weight is CO_2 liquid or seawater. The payload is aimed at around 40% displacement. The permanent ballast and machinery are designed to be 2% displacement, while the trim ballast is 0.7% of displacement. The weight composition of the SFG baseline design is presented in **Table 3.9**. The results are used to estimate the stability of the vessel.

Table 3.9 Weight distribution of SFG baseline design.

Component	SFG 1194 m³	
	Weight (tons)	**Percentage**
Machinery	24.474	2.00%
Permanent ballast	24.274	2.00%
Structure	476.361	38.93%
Mid-body seawater	179.381	14.66%
Compensation ballast	0.999	0.08%
Payload	509.446	41.63%
Trim tank	8.566	0.70%
Sum	**1223.700**	**100%**

3.3. Hydrostatic Stability

The weight of the SFG structure is checked following the hydrodynamic loading conditions explained in **Chapter 2.3**. The centre of gravity CoG, the centre of buoyancy CoB, and the metacentre M are considered to determine the structure's stability under different conditions. These factors have an impact on parameters that describe the stability – BM and GM. For the submarine with a 1000-2000 tons displacement, the distance between the CoG and CoB must be greater than 0.32 (Berg, 2007). Moreover, the location of metacentric height GM must exceed 0.20. The stability results are presented in **Table 3.10**.

Table 3.10 SFG Baseline design hydrostatic stability.

SFG 1194 m³				
Parameters	**Submerged (CO₂ filled)**	**Submerged (SW filled)**	**Surfaced (CO₂ filled)**	**Surface (SW filled)**
CoG(x,y,z)	[-0.60, 0.00, 0.35]	[-0,54 0.00, 0.36]	[-0.70, 0.00, 0,37]	[-0.66, 0.00, 0.36]
CoB(x,y,z)	[-0.83, 0.00, 0.00]	[-0.84, 0.00, 0.00]	[-0.84, 0.00, 5.50]	[-0.84, 0.00, 4.20]
M(x,y,z)	[0.00, 0.00, 0.00]	[0.00, 0.00, 0.00]	[0.00, 0.00, 0.00]	[0.00, 0.00, 0.00]
BG	0.347	0.361	5.126	3.844
GM	0.347	0.361	0.374	0.356
Result	BG > 0.32 == OK	BG > 0.32 == OK	GM > 0.2 == OK	GM > 0.2 == OK

The stability results show that the submarine fulfils the requirements defined in DNVGL_RU-NAVAL-Pt4Ch1 (DNV GL AS, 2018).

3.4. Power Consumption Estimation

The procedure for calculating power consumption is presented in chapter 2. The calculation of the hotel load is performed after taking into account the power and resistance force. The results are shown in **Figure 3.2**. The analysis of the hotel load can be performed after adjusting the compensation ballast properties and considering the duration of the load and offload.

The pomp power is estimated based on the flow of the pump duration to load and unload the freight. It takes 4 hours to load and reload the cargo owing to the fact that the pumps give 3 bars of differential pressure. Every SFG design has different volumetric flow rates to guarantee the same loading and offloading intervals. The efficiency of the pumps is assumed to be not lower than 75% (Kretschmann et al., 2017).
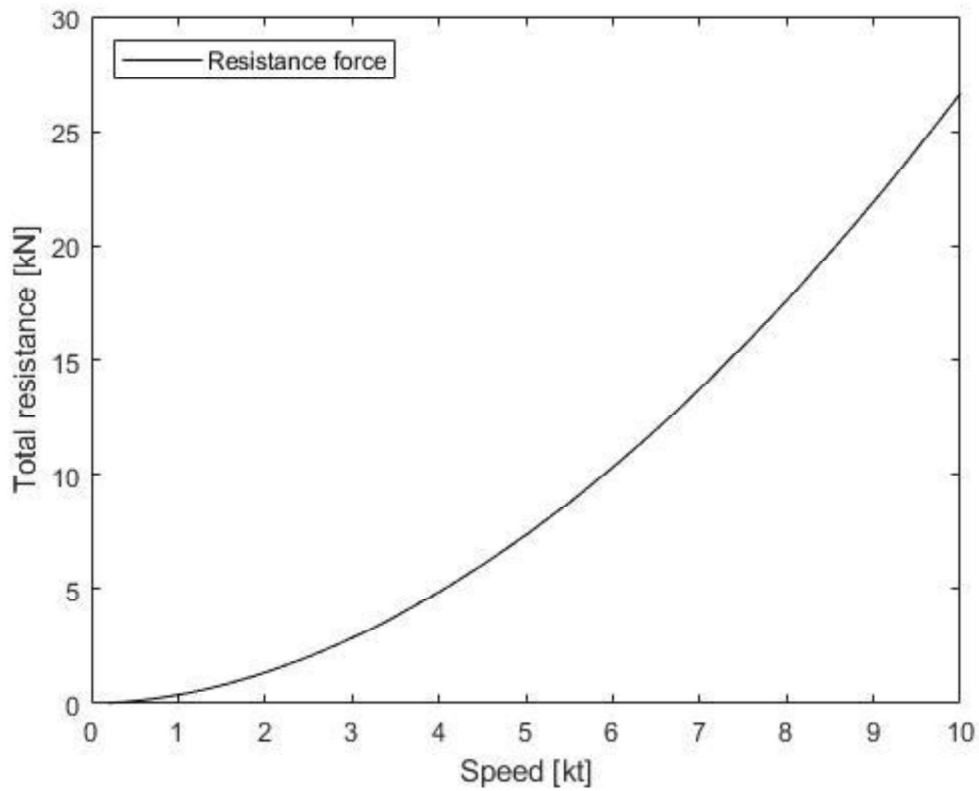
Figure 3.2 *Resistance force of SFG baseline design.*
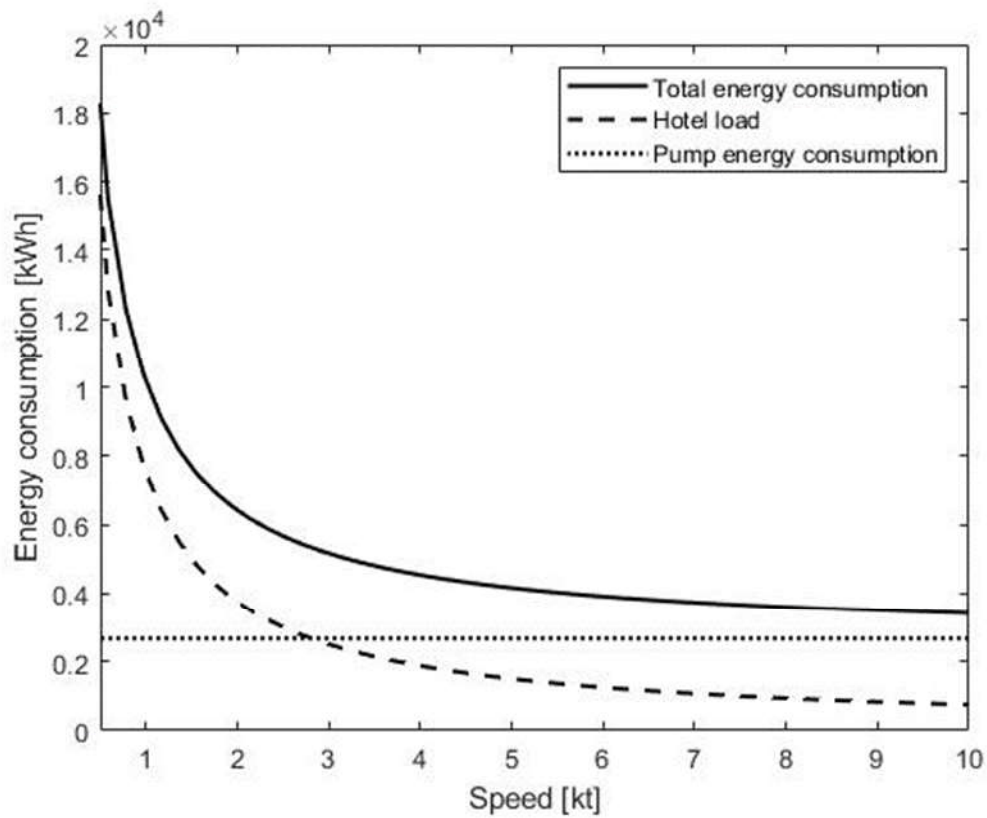
Figure 3.3 *Total energy consumption of the SFG baseline design.*

As an energy source, the Li-ion battery is chosen for the SFG. The batteries are dedicated to the baseline and half-scaled design of SFG weight 20 tons and 10,000 kWh, while the 40-ton batteries with 20,000 kWh are used for double-scaled design.

3.5. Design Overview

The design results for scale-up and scale-down of the SFG baseline design are presented in **Appendix A**, and they follow the procedure given in **Chapter 2**. The external hull analysis for all considered SFG variants is presented in **Table 3.11**. The internal tank properties for three SFG designs are shown in **Table 3.12**. Finally, the weight composition of all derived SFG designs is displayed in **Table 3.13**.

Table 3.11 SFG design of the external hull.

Parameters		SFG 469 m³	SFG 1194 m³	SFG 2430 m³	Units
Free-floating bow compartment	Thickness	0.025	0.030	0.036	[m]
	Length	6.625	8.750	11.50	[m]
	Steel weight	21.899	43.877	87.510	[ton]
	Material	VL D47	VL D47	VL D47	-
	Design collapse pressure	40	40	40	[bar]
Flooded mid-body	Thickness	0.009	0.013	0,026	[m]
	Length	25.00	33.75	42.00	[m]
	Steel weight	34.049	80.850	222.749	[ton]
	Material	VL D47	VL D47	VL D47	-
	Design collapse pressure	20	20	20	[bar]
Free-floating aft compartment	Thickness	0.025	0.030	0.036	[m]
	Length	10.625	14.00	18.00	[m]
	Steel weight	27.412	54.581	105.942	[ton]
	Material	VL D47	VL D47	VL D47	-
	Design collapse pressure	40	40	40	[bar]

Table 3.12 *Internal tank properties for all SFG designs.*

Parameter		SFG 469 m³	SFG 1194 m³	SFG 2430 m³	Units
Main Cargo Tank (Total No. = 7)	Diameter	1.20	1.62	2.20	[m]
	Length	25.00	33.75	42.00	[m]
	Thickness	0.014	0.018	0.025	[m]
	Hemisphere head wall thickness	0.007	0.009	0.012	[m]
	Steel weight	68.688	168.998		[ton]
	Total volume	190.376	468.395	1073.411	[m2]
	Allowable burst pressure	55.0	55.0	55.0	[bar]
	Material	SA-738 Grade B	SA-738 Grade B	SA-738 Grade B	-
Auxiliary Cargo Tank (Total No. = 6)	Diameter	0.45	0.70	0.80	[m]
	Length	24.25	32.83	40.60	[m]
	Thickness	0.005	0.008	0.009	[m]
	Hemisphere head wall thickness	0.003	0.004	0.005	[m]
	Steel weight	8.153	26.670	43.115	[ton]
	Total volume	22,478	73.568	118.894	[m2]
	Allowable burst pressure	55.0	55.0	55.0	[bar]
	Material	SA-738 Grade B	SA-738 Grade B	SA-738 Grade B	-
Compensation Tank (Total No. = 2)	Diameter	3.0	3.5	5.5	[m]
	Length	1.7	2.5	5.0	[m]
	Thickness	0.006	0.010	0.014	[m]
	Steel weight	20.224	72.063	96.214	[ton]
	Total volume	17.34	61.25	75	[m2]
	Allowable burst pressure	8.0	8.0	8.0	[bar]
	Material	SA-738 Grade B	SA-738 Grade B	SA-738 Grade B	-
Trim Tank (Total No. = 2)	Diameter	1.6	1.8	3.00	[m]
	Length	2.24	2.50	6.3	[m]
	Thickness	0.006	0.008	0.022	[m]
	Steel weight	12.479	14.702	78.728	[ton]
	Total volume	10.0	45.00	60.0	[m2]
	Allowable burst pressure	10.0	10.0	10.0	[bar]
	Material	SA-738 Grade B	SA-738 Grade B	SA-738 Grade B	-
Buoyancy Tube (Total No. = 8)	Diameter	0.30	0.35	0.40	[m]
	Length	24.1	32.5	40.2	[m]
	Thickness	0.003	0.004	0.005	[m]
	Hemisphere head wall thickness	0.002	0.002	0.002	[m]
	Steel weight	4.816	8.845	14.300	[ton]
	Total volume	13.572	24.910	40.279	[m2]
	Allowable burst pressure	20.0	20.0	20.0	[bar]
	Material	SA-738 Grade B	SA-738 Grade B	SA-738 Grade B	-

Table 3.13 *Weight composition for individual SFG design (CO_2-filled submerged condition).*

Component	Weight					
	SFG 469 m³		SFG 1194 m³		SFG 2430 m³	
Machinery	9.610	2.00%	24.474	2.00%	49.798	2.00%
Permanent ballast	9.610	2.00%	24.274	2.00%	49.798	2.00%
Structure	187.999	39.12%	476.361	38.93%	962.768	38.67%
Mid-body seawater	69.051	14.37%	179.381	14.66%	277.306	11.14%
Compensation ballast	0.804	0.17%	0.999	0.08%	11.994	0.48%
Payload	200.082	41.64%	509.446	41.63%	1120.768	45.01%
Trim tank	3.364	0.70%	8.566	0.70%	17.429	0.70%
Sum	**480.520**	**100%**	**1223,700**	**100%**	**2489.914**	**100%**

The final derived design of the SFG structure is shown in **Table 3.14**. It shows that the different variants (scale-down SFG 469 m3, baseline SFG 1194 m3, and scale-up SFG 2430 m3) of the SFG structure fulfil the mission requirements. Therefore, the SFG design in this study is considered technically feasible.

Table 3.14 *Main parameters of final derived SFG baseline design.*

Parameter	Value		
	SFG 469 m³	SFG 1194 m³	SFG 2430 m³
Lightweight	197.609	500.835	962.819
Lightweight	192.789	488.619	939.336
Deadweight	282.911	722.866	1527.094
Deadweight	276.011	705,235	1489.848
Length	42.25	56.50	71.50
Beam	4.00	5.50	7.00
Displacement	480.520	1223.701	2489.914
Displacement	468.800	1193.854	2429.184
Total power consumption	6450	9545	14533
Power consumptions	1381	2044	3112
Speed	2.00	2.00	2.00
Speed	1.00	1.00	1.00
Travel distance	400.00	400.00	400.00

4. Economic Feasibility Analysis

In this chapter, the economic study of the SFG is performed. This analysis compares the SFG concepts described in previous chapters with other existing CO_2 transportation solutions. The research consists of different scenarios of capital and operational expenditure analysis of the SFG, offshore pipelines, and crewed/autonomous tanker.

4.1. State of CO_2 Transportation

The ship transporting CO_2 has semi-refrigerated Liquefied Petroleum Gas (LPG) tanks. The liquefied gas is transported at a temperature of -50ºC. During the transportation, the tanker ship requires refrigeration and liquefied gas, which is transported at 7-9 bar and around -55ºC to avoid the risk of the formation of dry ice. While transporting, the temperature of CO_2 will increase, initiating a boil-off and rising internal pressure of the ship. This condition can typically be expected to occur. Therefore, the cargo pressure at the end of the loaded journey will normally be around 8-9 bar.

- The offshore pipelines transport CO_2 in a supercritical state, which requires high-pressure pumps to increase the pressure in the pipeline.
- The SFG vessels are used to transport CO_2 in a saturated liquid form. The surrounding environment controls the temperature of CO_2, which is 0-20 degrees Celsius. This solution requires freezing the cargo. On the other hand, it simplifies the transportation process because buffer storage and onshore liquefaction are unnecessary.
- Refrigerated or Semi-refrigerated vessels are used as tankers ships to transport CO_2 and carry it at a pressure of around 7 bar and a temperature of -55 degrees Celsius to avoid the formation of dry ice. CO_2 requires refrigeration during the voyage.

4.2. Data and Assumption

The cost of a project for developing a subsea project is generally referred to as the CAPEX – capital expenditures and OPEX – operational expenditures. Capital expenditure is the total investment that is required to put a project into operation. It includes the initial design, engineering, and construction of the facility. The term OPEX refers to the expenses that a facility or component incurs during its operation. These expenses include labour, materials, and utilities. Aside from these, other costs such as testing and maintenance are also included in the OPEX (Bai & Bai, 2018).

The economic analysis was performed based on two publicly available cost models from Marine Unmanned Navigation through the Intelligence in Network (MUNIN, 2015) and Zero-Emission Platform ZEP (ZEP, 2011) reports. The MUNIN D9.3 (MUNIN, 2015) report presents a complete study of autonomous ship development, economic effects, security and safety effects, and relevant areas of law. In this study, the data from the MUNIN report related to autonomous ships are used for economic impact assessment cost analysis. The ZEP (ZEP, 2011) report shows the breakdown of CO_2 transportation on the deployment of Carbon Capture and Storage (CCS) and Carbon Capture and Utilisation (CCU). The ZEP (ZEP, 2011) report provides data from members of maritime organisations, including stakeholders and essential players in marine transportation, such as Teekay Shipping, Open Grid Europe, and Gassco. The analysis is very detailed and covers all components. For instance, the cost of actual coating is specified and considered for the offshore pipeline. The research uses cost models from the ZEP report for cost estimation, including OPEX and CAPEX, ship capacities, electricity price, etc., for offshore pipelines. The outline of the MUNIN D9.3 (MUNIN, 2015) and ZEP (ZEP, 2011) reports is presented in **Table 4.1**.

Table 4.1 *Summary of the cost models in MUNIN D9.3 and ZEP reports.*

The cost model shown in MUNIN D9.3	The cost model presented in ZEP
Autonomous ship capital expenditure	Offshore pipelines' capital expenditure
Fuel price	Offshore pipeline operating expenditure
Ship fuel consumption	Electricity price
Discount rate	Discount rate
	Ship capacity
	Vessel loading and offloading durations
	Vessel transport velocity
	Ship capital expenditure
	Ship operating expenditure
	Transport distance cases
	Transport volume cases
	Liquefaction price
	Project lifetime

Based on these two reports, it is assumed that the currency exchange rate is 0.87 EUR/USD, the discount rate is equal to 8%, and the project lifetime is 40 years.

4.2.1. Transport Scenarios

This analysis considers transport distances of 180, 500, 750, and 1500 km with CO_2 shipping capacities of 0.5, 1, and 2.5 million tons per annum (mtpa). The CO_2 is carried from a capture plant at an ambient temperature and pressure of 110 bar. The following assumption of CO_2 transportation are used:

- During the studies, time spent docking in a remote charging station is not considered.
- For some scenario cases, there is more than one vessel needed in case of transporting CO_2 via SFG or tanker.
- The cost of subsea well-head is not considered in the following research.
- The SFG and tankers discharge CO_2 directly to the subsea well without using an intermediate buffer.

The case scenarios presented in this study are different from the technical design specifications of the SFG. For instance, the vessel aims to transport CO_2 at a 400-kilometre distance. It means that the amount of batteries or their capacity needs to be increased. To accommodate the increased weight of the battery, the payload will be reduced. However, this reduction is not significant since the total weight of the battery is only 40 tons and is a small part of the total mass of the whole vehicle.

4.2.2. Crew & Autonomous Ship and SFG

Tanker ships in this analysis have a capacity of 22000 m3. This size is chosen based on the data provided in the ZEP report (ZEP, 2011). The ships are assumed modern and equipped with submerged turret offloading buoy capabilities and dynamic positioning. The properties of the crew tanker ship are shown in **Table 4.2**.

Table 4.2 *Tanker ships properties.*

Parameters	Value	Units
Liquification 2.5 mtpa	5.31	€/ton
Loading/Offloading time	12.00	Hours
Speed	14.00	Knots
Fuel consumption	9.13	Ton/day
Payload	80.00	%

The cost of building a crewed tanker ship is computed by considering the various factors that affect its structure and technical characteristics. The total cost of the vessel is calculated by taking into account the steel price and the ship's volume. Based on the theoretical payload, the ship's weight is expected to be 80%.

The capital expenditure (CAPEX) is calculated based on the price per ton of structural steel weight. According to the ZEP report (ZEP, 2011), the maximum and minimum cost for a ton of steel is 11,63-28,888 € per ton. As presented in **Figure 4.1**, it is assumed that a tanker ship has a CAPEX of 110% of the crew tanker ship. The vessels should be modern and equipped with submerged turret offloading buoy capabilities and dynamic positioning.

Table 4.3 *CAPEX inputs for crew and autonomous tanker ship.*

Inputs to CAPEX of Crew and Autonomous Tanker Ship		
Steel price (max) in ZEP report	28,888.50	€/ton
Steel price (min) in ZEP report	11,631.45	€/ton
Steel price (average) in the ZEP report	18,896.04	€/ton
Residual value	0	€
Autonomous ship price	110% crew ship price	

The CAPEX values of the SFGs and the tanker ships have been calculated using **Equation 4.1**.

$$CAPEX = \text{Steel price} \cdot \text{Vessel structure volume}$$	**Equation 4.1**

The discount rate is estimated to be 8% and the lifetime to be 40 years. Based on these assumed parameters, the annuity is calculated using the **Equation 4.2**:

$$\text{Annuity} = \frac{CAPEX \times \text{discount rate}}{1 - (1 + \text{discount rate})^{-\text{lifetime}}}$$	**Equation 4.2**

Table 4.4 *CAPEX results for tanker ships.*

Parameter	Tanker Ship	Units
Structural volume	5170.00	ton
Price of a ton of the steel for a vessel	18896.00	€/ton
CAPEX	97.69	m€
Annuity	8.19	m€
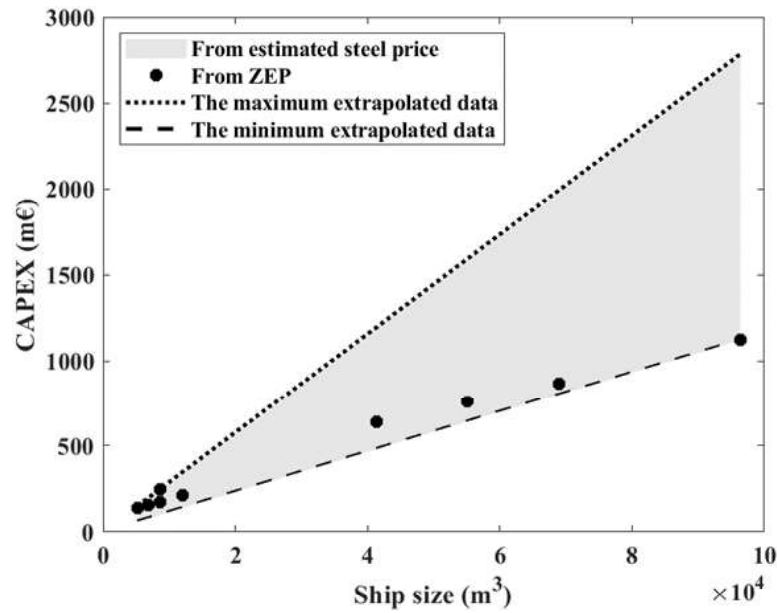
Figure 4.1 *CAPEX of craw tanker in comparison results from the ZEP reports.*

The operation expenditure OPEX refers to the expenses incurred by a facility or component during its operation. These expenses include labour, materials, and utilities. Aside from these, other costs such as testing and maintenance are also included in the OPEX.

$\text{OPEX}_{CS} = \text{Maintenance} + \text{Crew} + \text{Fuel} + \text{Liquefaction}$	**Equation 4.3**

Table 4.5 *OPEX inputs for crew and autonomous tanker ship.*

Parameter	Tanker Ship	Units
Fuel price	573.33	€/ton
Crew price	0.64	m€/year (20 craws)
Maintenance	2.00	% of CAPEX
Liqufication 2.5 mtpa	13.28	m€/year

4.2.3. Autonomous Tanker Ship

One of the main advantages of an autonomous vessel is that it does not require a marine crew. However, it is equipped with other technologies that allow it to operate without a crew. The MUNIN D9.3 report (MUNIN, 2015) estimated that the CAPEX for an autonomous vessel is around 110% of a crew tanker ship. On the other hand, the OPEX of an autonomous vessel is around the same as a crewed tanker ship (**Equation 4.4**). Other expenses for the autonomous vessel are assumed to be the same as for the crew tanker ship.

$\text{OPEX}_{AS} = \text{Maintenance} + \text{Fuel} + \text{Liquefaction}$	**Equation 4.4**

4.2.4. Cost Estimation of SFG

The SFG CAPEX is computed by considering the factors that affect its construction, such as the steel price and the technical maturity. It is assumed that once the SFG reaches the same level of maturity as a tanker ship, the steel price and the economy of scale will be the same. Since the cost of steel is the same for a tanker ship and an autonomous vessel, both OPEX is assumed to be the same.

$OPEX_{SFG} = Maintenace + Electricity$	**Equation 4.5**

Table 4.6 *SFG cost calculations.*

Parameter	SFG 469 m^3	SFG 1194 m^3	SFG 2430 m^3	Units
Electricity price	0.11	0.11	0.11	€/kWh
Maintenance	2.00	2.00	2.00	2% of CAPEX
CAPEX	52.38	56.80	54.53	m€
Annuity	4.39	4.76	4.57	m€
OPEX	1.82	1.63	1.47	m€/year

4.2.5. Offshore Pipelines

Overall, offshore pipeline costs are controlled by CAPEX, and they are proportional to the pipe's length. In the design of offshore pipelines, the essential factors are pipeline diameter, wall thickness, transport capacity, outlet and inlet pressure, and steel quality. Also, factors like corrosion protection, design against trawling, installation method, dropped object protection, and bottom stability should be considered.

In this study, the manifold cost for the well and the injection well drilling are not considered. The capital expenditure is estimated based on the steel market price, pipeline installation cost, trenching, and pipeline coating. CO_2 is sent through pipelines at 55-88 bar in the supercritical phase. In this case, the cost of the pressure boosters and the associated costs are included in the computation of CAPEX. Furthermore, The pressure conditions in the pipeline are considered, and the storage conditions determine it. In this analysis, the cost of pre-transport CO_2 compression is included in the price of the capture facility.

In this study, offshore pipelines' lowest volume case (1 mtpa of CO_2) is not considered. This is because offshore pipelines are too expensive due to their small transportation capacity, and it is not economical to use this transfer method.

Table 4.7 *Properties of the offshore pipelines.*

Properties of the offshore pipelines		
Pressures	250	[bar]
Outlet pressure	60	[bar]
Inlet pressure	200	[bar]
Pipeline internal friction	50	
External coating	3	[mm]
Pipeline material	Carbon steel	
Concrete coating (pipeline above 16")	70 mm; 2600 kg/m3	

Table 4.8 *Pricing of the offshore components.*

Component Pricing of Offshore Pipelines		
Trenching cost	20-40	€/meter
Installation cost	200-300	€/meter
Pipeline OPEX for 2.5 mtpa	2.35	m€/year
Contingency	20%	
Steel price for pipeline 16"	160	€/meter
Steel price for pipeline 40'	700	€/meter
External coating for pipeline 16"	90	€/meter
External coating for pipeline 40"	200	€/meter

The CAPEX values for an offshore pipeline are shown in the ZEP (ZEP, 2011) report. The maximum and minimum values are expected to be 120% and 80%, respectively.

The ZEP (ZEP, 2011) report shows the average OPEX values for an underwater pipeline are shown in the ZEP (ZEP, 2011) report. The pipeline's CO2 volume is expected to be around 2.5 million tons annually. The minimum and maximum OPEX values are approximately 80% and 120%, respectively.

The offshore pipeline annuities are calculated based on the design definitions, and related costs are included in **Table 4.7** and **Table 4.8**, respectively. A 2.5 mtpa transport capacity offshore pipeline will cost about 20.986-126.961 m€. All calculated data is displayed in **Table 4.9**. All operational costs and aspects of maintenance are included in the OPEX. The operating expenditures OPEX are 2.35 m€/year.

Table 4.9 *Offshore Pipeline Annuities.*

CO$_2$ volume	Offshore Pipeline Length			
	180 km	500 km	750 km	1 500 km
2.5 mtpa	20.986 m€	48.688 m€	69.412 m€	126.961 m€

4.3. Cost per CO_2 per Ton

The comparison of SFG, crew ship, autonomous ship, and the offshore pipeline is established on the cost of CO_2 per ton. However, more vessels are often needed to estimate the price due to the long distance. This is the reason the number of vehicles is required to calculate. The minimum number of SFG and tanker ships to fulfil the mission requirements is computed using **Equation 4.6**.

$$N = \text{roundup}\left(\frac{V_{CO_2}}{V_\vartheta \rho_{CO_2} \frac{365}{2L_t U_\vartheta + 2T_L}}\right)$$	**Equation 4.6**

where: N is a number of vessels; V_v is the total capacity for a vessel; U_v is the velocity of the vessel; T_L is the time of loading or offloading; ρ_{CO_2} is the CO_2 density; L_t is the distance of the transportation; V_{CO_2} is the total CO_2 capacity per annum.

$$CO_2\text{cost} = \frac{\text{Annuity} + \text{OPEX}}{\text{Total } CO_2 \text{ per annual}}$$	**Equation 4.7**

Table 4.10 *Average cost of CO_2 per ton for 0.5 mtpa and 180 km.*

Parameter	Crew ship	Autonomous ship	Offshore pipelines	SFG 469 m³	SFG 1194 m³	SFG 2430 m³
Total CO_2 per annual	2.5 million ton	2.5 million ton	2.5 million ton	2.5 million ton	2.5 million ton	2.5 million ton
OPEX	7.18	6.73	-	1.82	1.63	1.47
Annuity	8.19	9.01	-	4.39	4.76	4.57
CO_2 per ton	30.74	31.49	-	12.43	12.78	12.08

5. Results

This chapter provides results for economic calculations. The study focuses on the CAPEX and OPEX analysis, the CO_2 transportation costs, and the number of vessels required to complete the mission. Most of the result is provided in graphical form. The study also includes the economic feasibility of the conceptual submarine Subsea Shuttle Tanker (SST). The results for this large autonomous submarine were performed in (Santoso, 2021) as a master's thesis.

In the graphs with the results, the following abbreviations are used:

- SFG 1 – Subsea Freight Glider with cargo (down-scale design)
- SFG 2 – Subsea Freight Glider with cargo 1194 m^3 (baseline design)
- SFG 3 – Subsea Freight Glider with cargo (up-scale design)
- CS – Crew tanker ship with cargo 22000 m^3
- AS – Autonomous tanker ship with cargo 2200 m^3
- SST – Subsea Shuttle Tanker (down-scale design)

5.1. The Minimum Number of Vessels

The minimum number of vessels is calculated for different scenarios. The presented results consider 180, 500, 750 and 1500 km transportation distances and 0.5, 1.0, 2.5 mtpa amount of CO_2 to transport. The minimum number of vessels required to perform the mission is illustrated in **Figure 5.1**, **Figure 5.2**, **Figure 5.3**, and **Figure 5.4**.
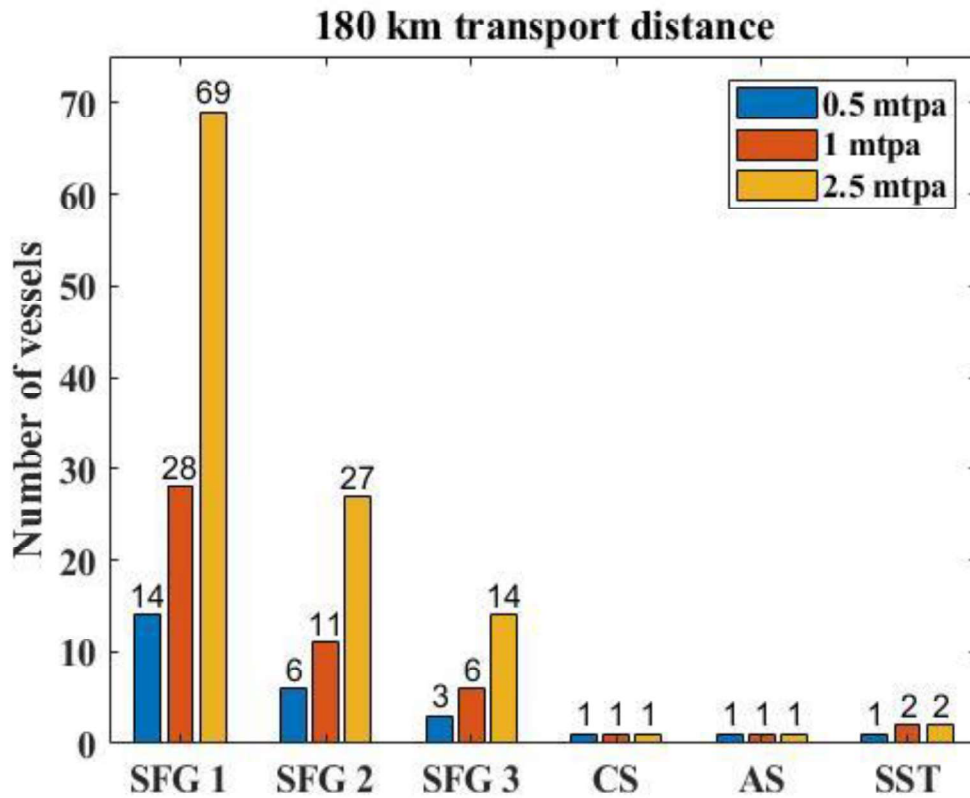
Figure 5.1 *Minimum number of vessels to transport CO_2 for 180 km.*
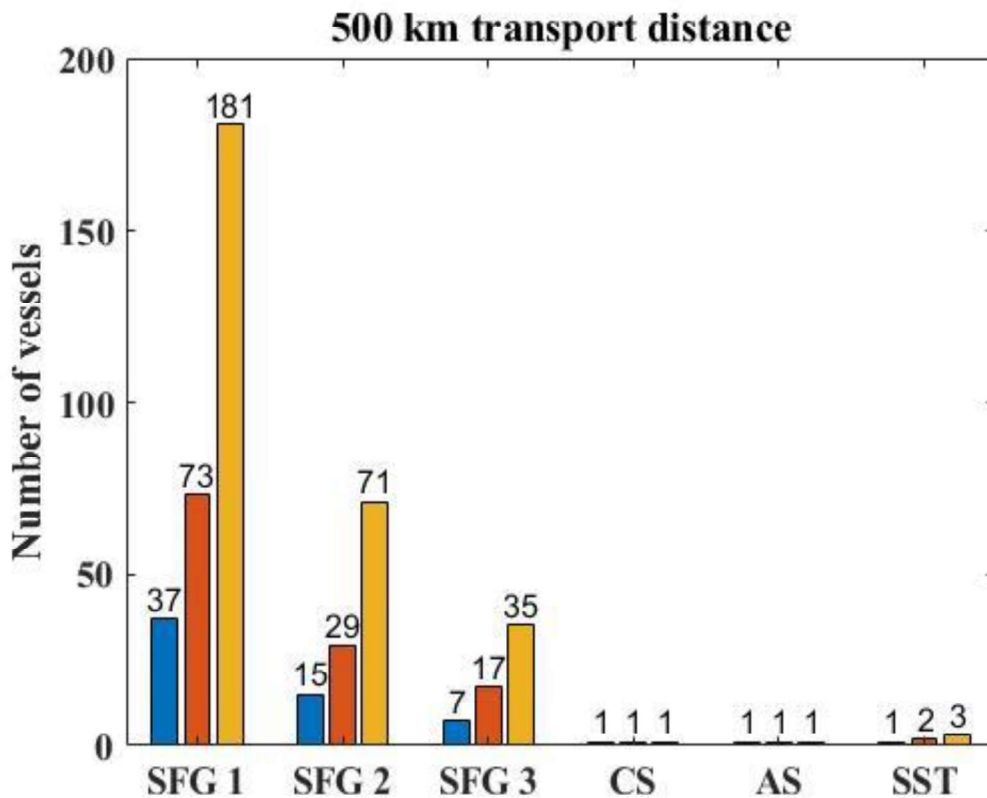
Figure 5.2 *Minimum number of vessels to transport CO2 for 500 km.*
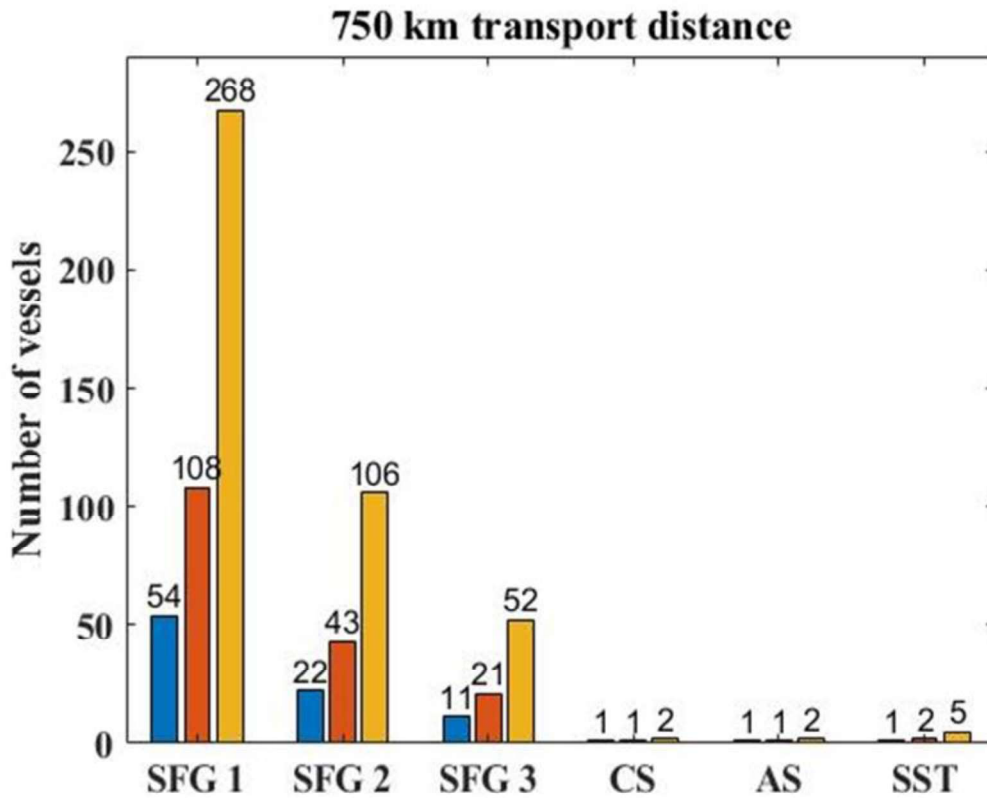
Figure 5.3 *Minimum number of vessels to transport CO₂ for 750 km.*
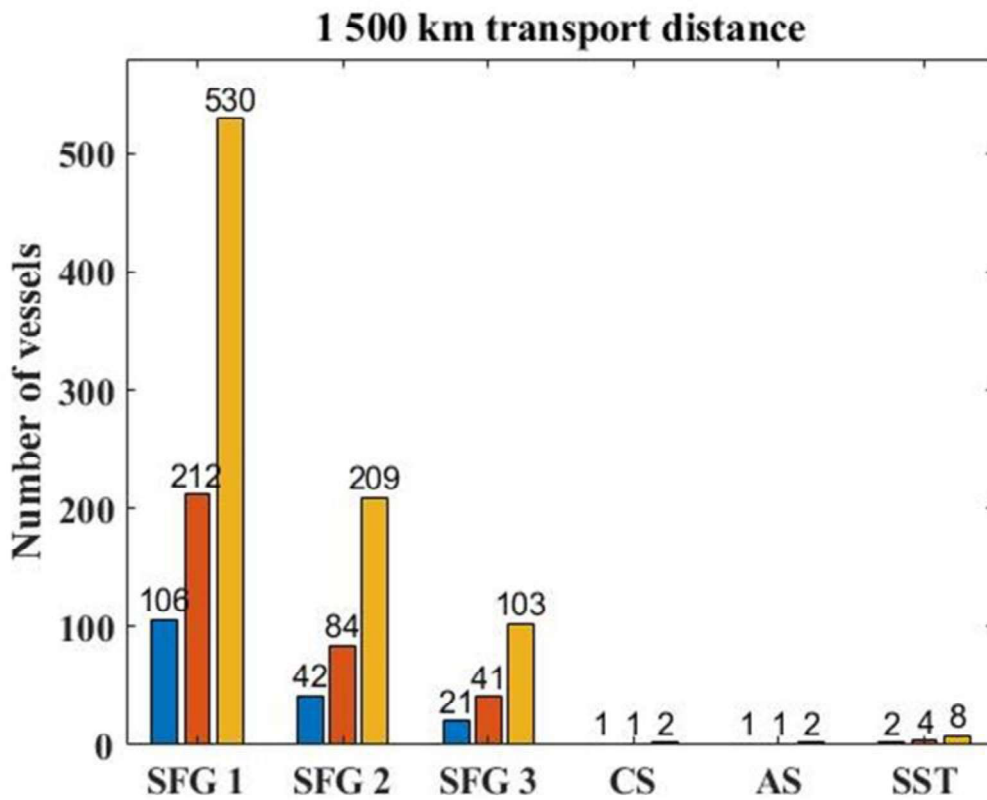
Figure 5.4 *Minimum number of vessels to transport CO₂ for 1500 km.*

The results present that the number of SFGs is the highest for all cases. This is because the size of an SFG is much smaller than the size of a crew/autonomous ship or the SST. In the analysis, offshore pipelines are not included since they transport cargo continuously. The results clearly show that the smallest amount of the SFG is needed for a 180 km distance, and the number of vessels required to fulfil the mission requirements drastically increased with the length of transportation.

5.2. CAPEX and OPEX Studies

Figure 5.8 shows the CAPEX results for various transportation methods. It shows that the SFG's CAPEX increases significantly with the size of its capacity. This indicates the conclusion that SFG is not an economical solution if large transportation capacities are needed.

The SFG is designed based on DNV-RU-NAVAL-Pt4Ch1 (DNV GL AS, 2018), which was initially created for a military submarine design. Due to high safety factor requirements, the SFG has a very high structural weight, making the CAPEX value significantly high. For a specific SFG, a potential solution to reduce the weight and CAPEX is to reduce the design safety factors suggested in the design code for general SFG.
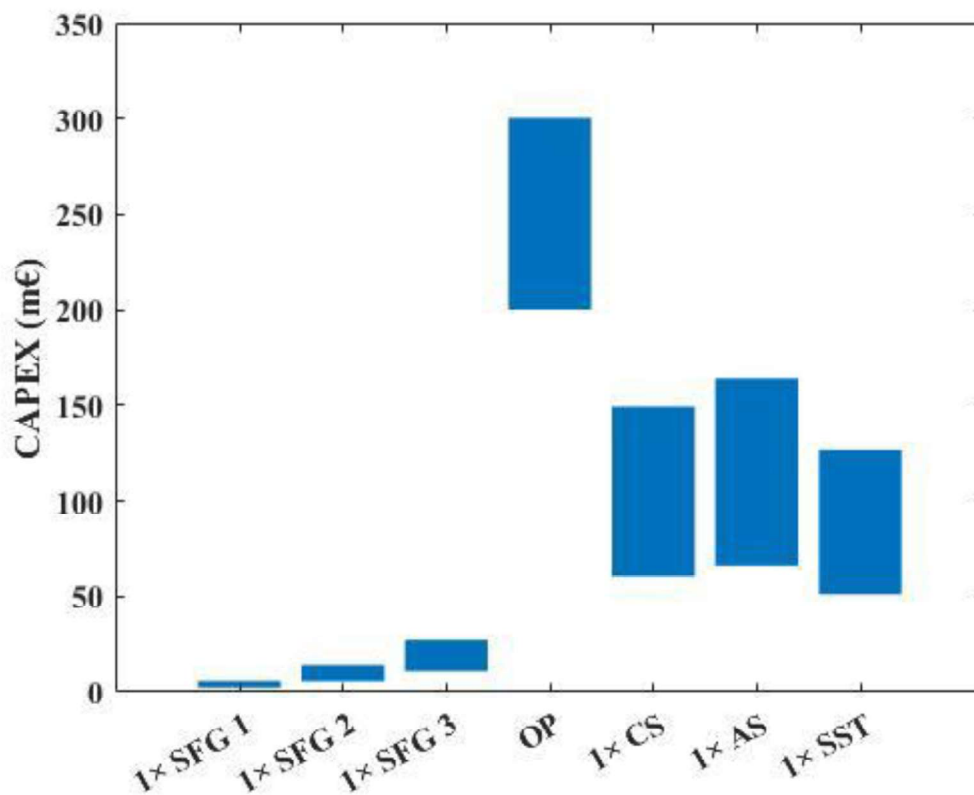
Figure 5.5 Capital expenditure estimation.

The OPEX/CAPEX ratios of analysed vessels are presented in **Figure 5.6**, **Figure 5.7**, **Figure 5.8**, and **Figure 5.9**. It is clearly seen that the OPEX dominates the cost for the crewed and autonomous thanks ships. For these vessels, CAPEX/OPEX ratio ranges between 2.59-7.28. On the other hand, the highest CAPEX and the lowest OPEX results are for offshore pipelines, and the OPEX/CAPEX ratio is 0.06-0.38. For the SFGs, the OPEX is comparable with CAPEX, and their CAPEX/OPEX is 1.07-1.39.
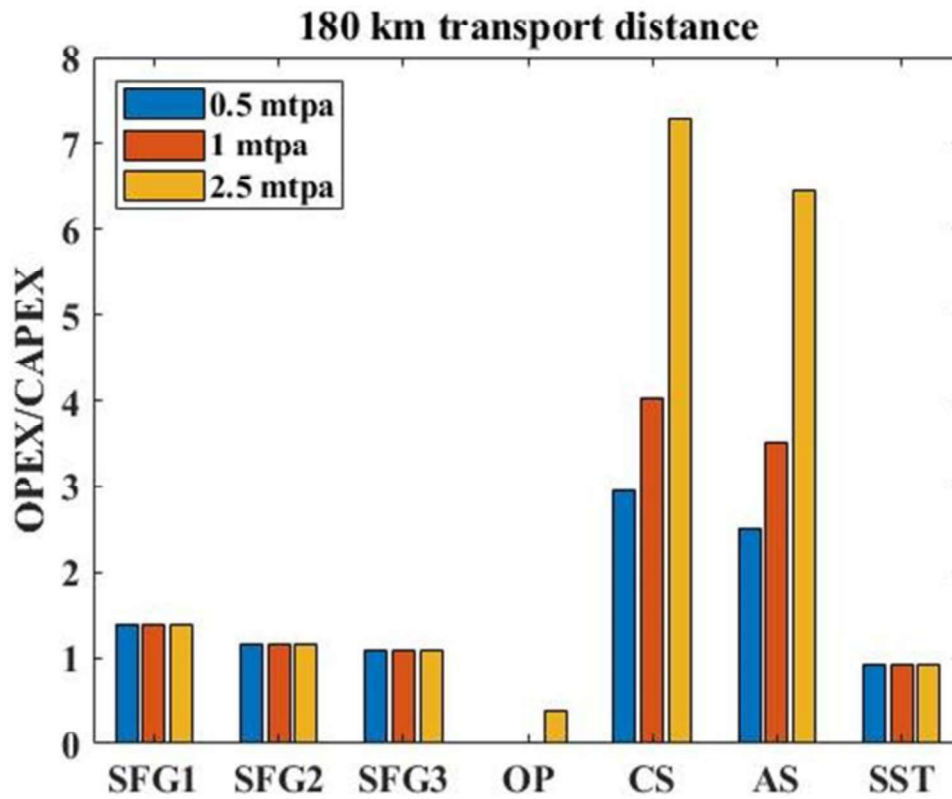
Figure 5.6 *CAPEX/OPEX ratios on different capacities for 180 km distance.*
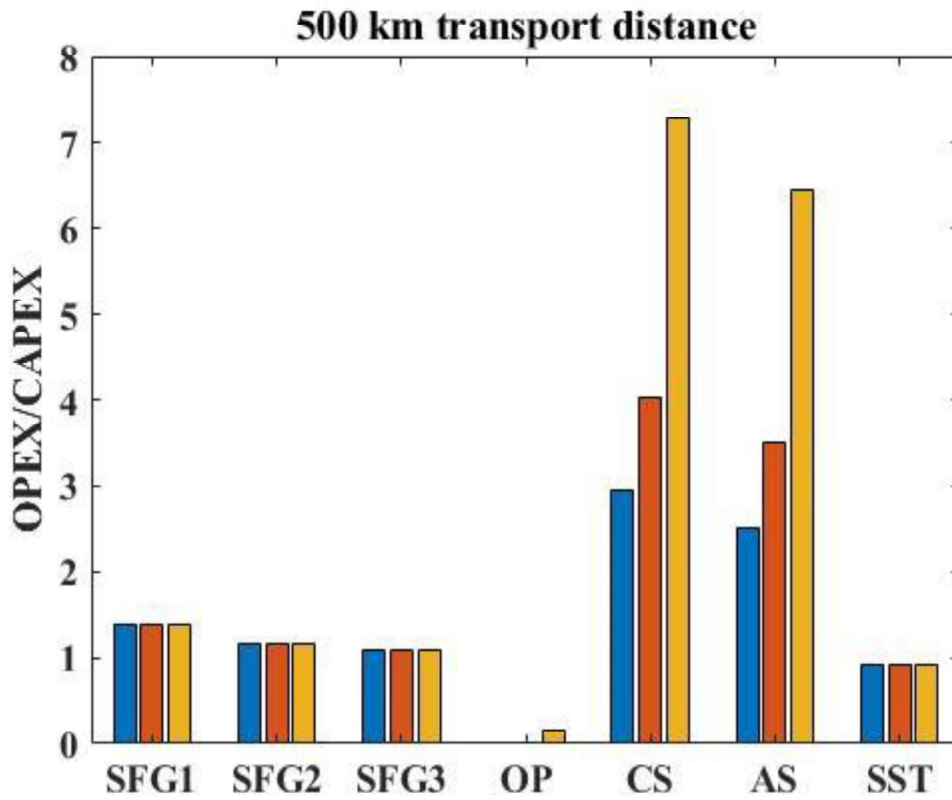
Figure 5.7 *CAPEX/OPEX ratios on different capacities for 500 km distance.*
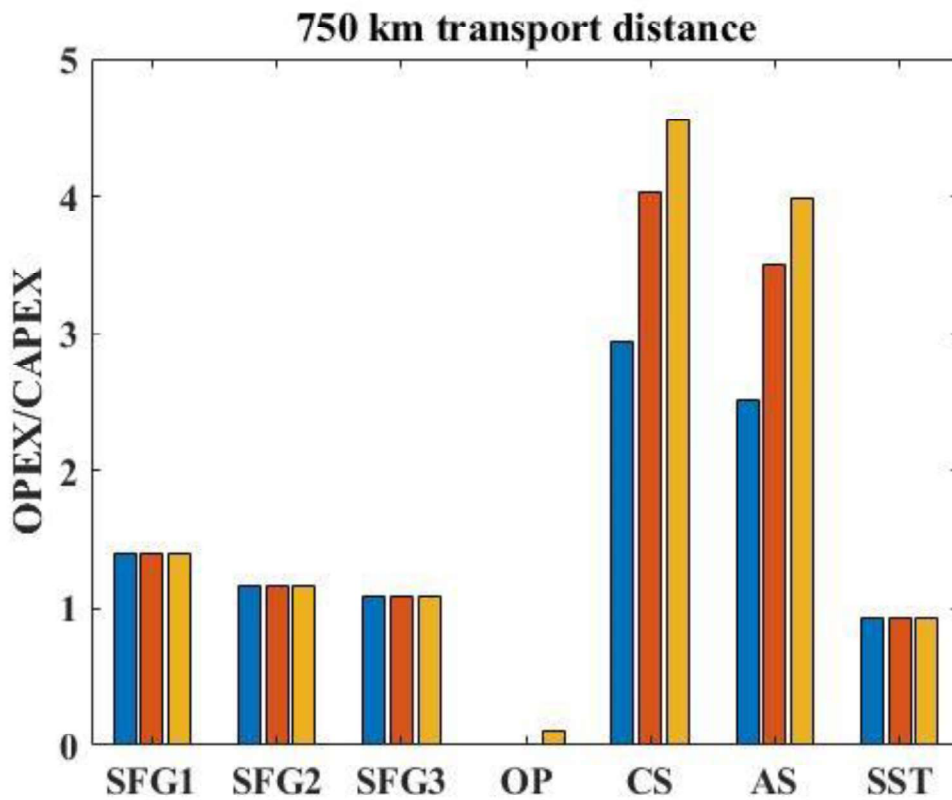
Figure 5.8 *CAPEX/OPEX ratios on different capacities for 750 km distance.*
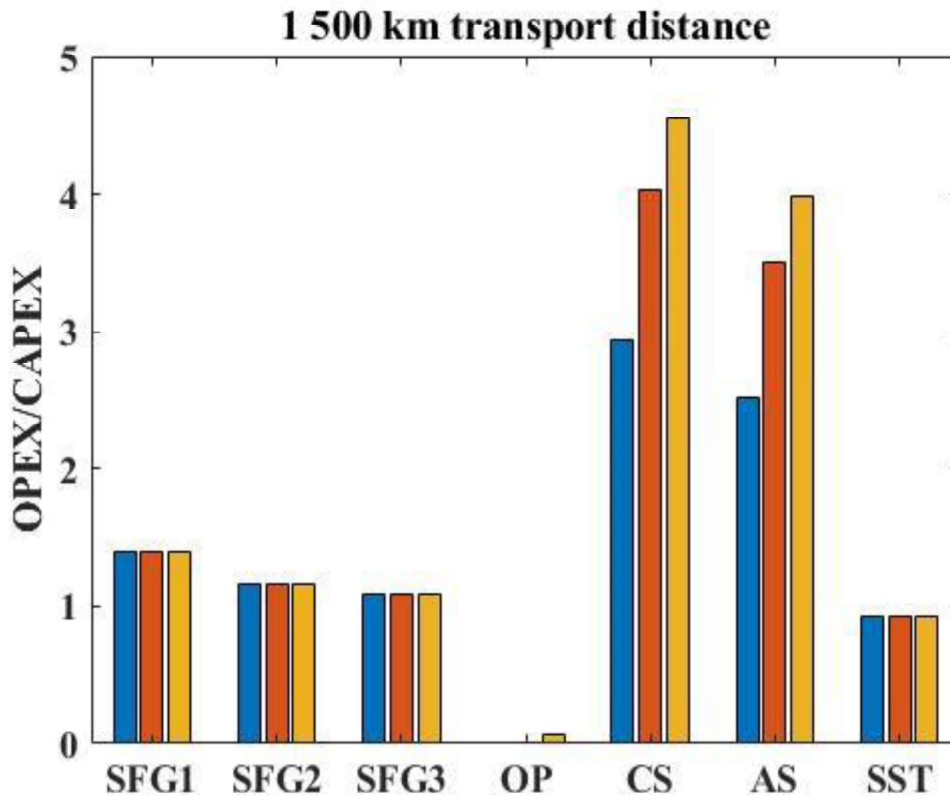
Figure 5.9 *CAPEX/OPEX ratios on different capacities for 1500 km distance.*

5.3. Economic Analysis

The cost of transporting CO2 is compared with the prices of various transportation methods, such as offshore pipelines, crew and autonomous tankers, the SFG and the SST. Generally, the lowest cost transportation method for short distances and high capacities are the offshore pipelines and SST. On the other hand, the tankers have the lowest cost of transporting CO_2 if the distances are long. The SFG is cost-effective for small volumes of CO_2 (0.5-1 mtpa) and short distances of 180-500 km. The cost per ton of CO_2 is presented in **Figure 5.10**, **Figure 5.11**, **Figure 5.12**, and **Figure 5.13**.
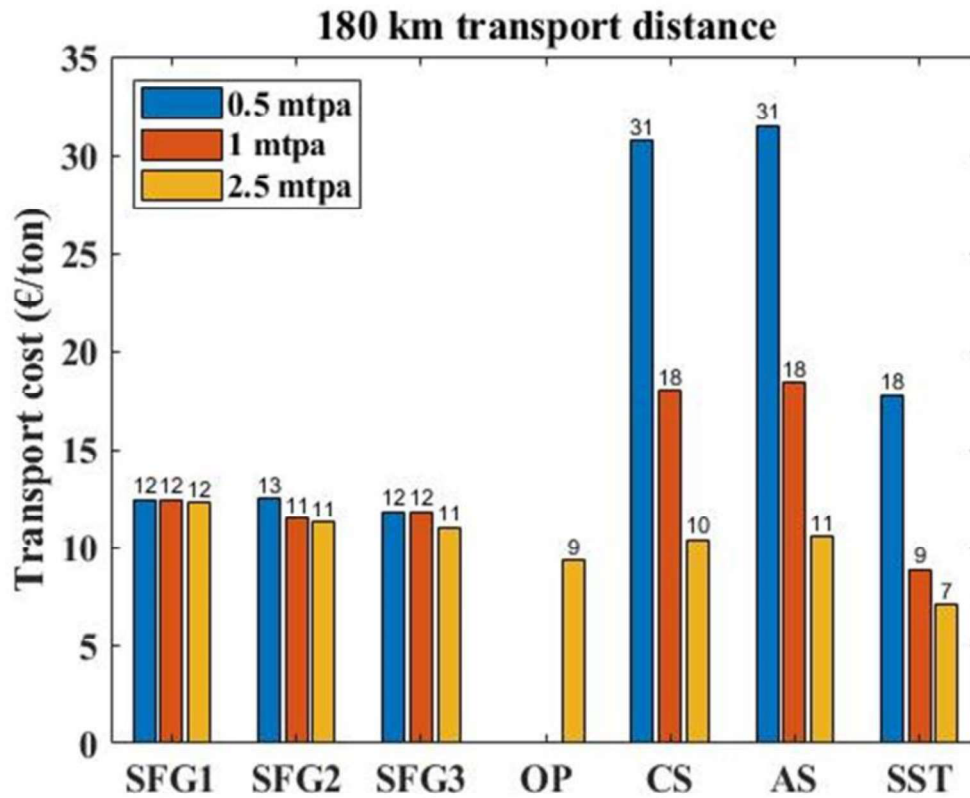
Figure 5.10 *Results for average cost per ton of CO₂ for 180 km transportation distance.*
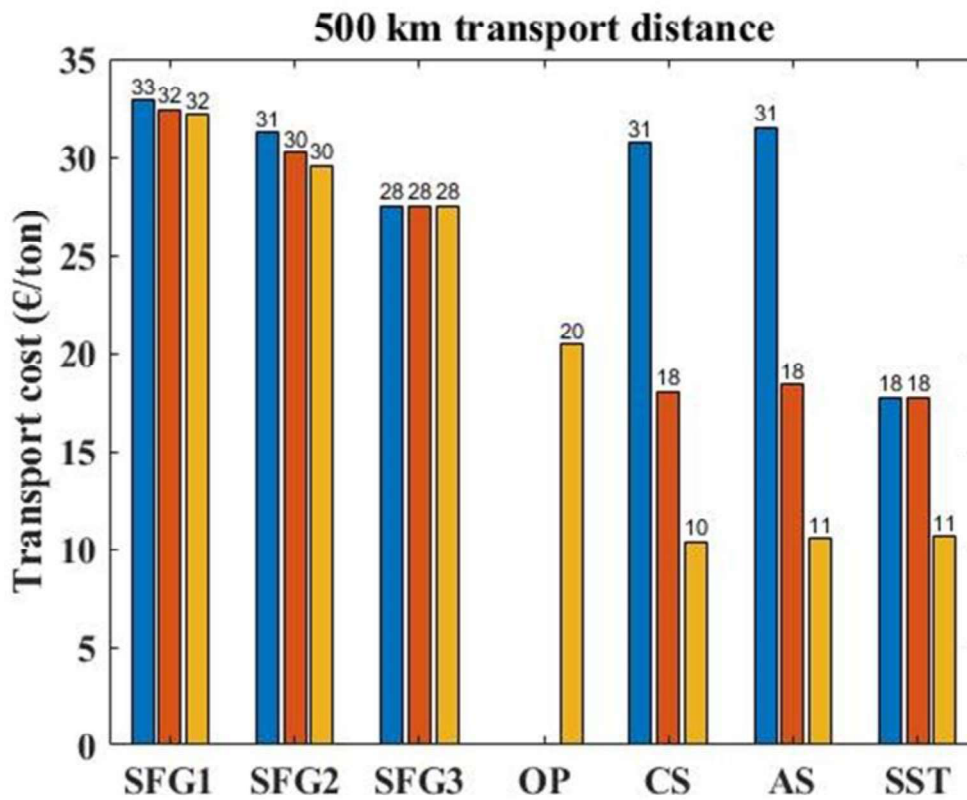
Figure 5.11 *Results for average cost per ton of CO₂ for 500 km transportation distance.*
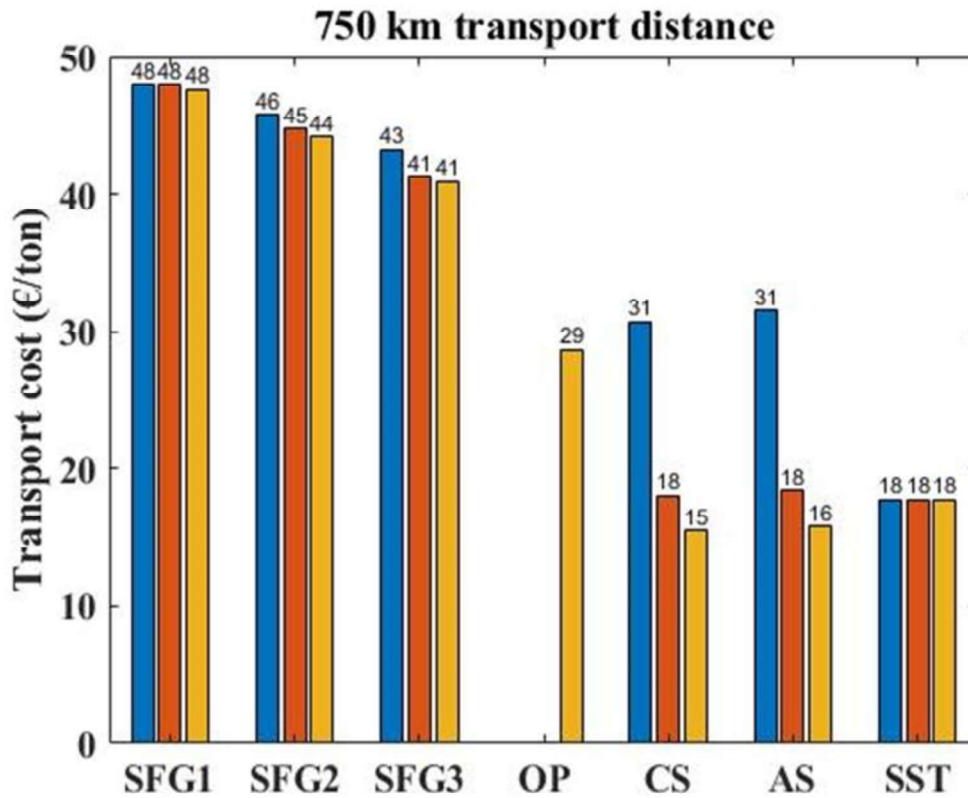
Figure 5.12 *Results for average cost per ton of CO₂ for 750 km transportation distance.*
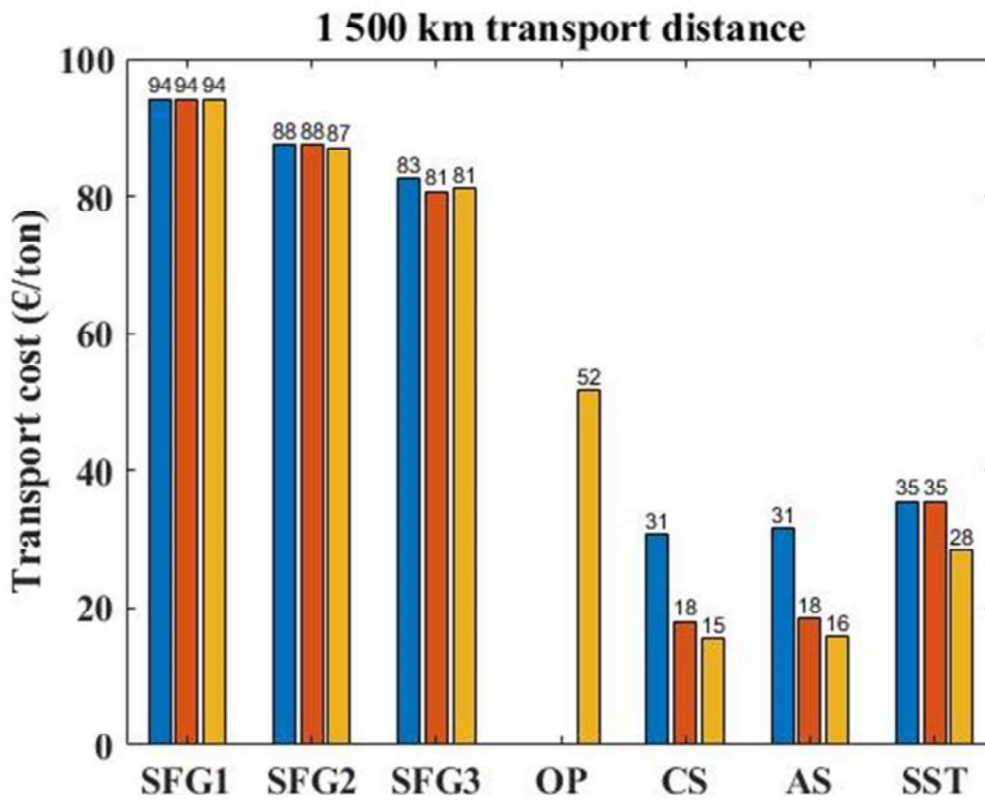
Figure 5.13 *Results for average cost per ton of CO₂ for 1500 km transportation distance.*

The results of the economic feasibility analysis with the lowest cost of transportation solutions are presented in **Table 5.1**. The results show that the SFG is the cheapest solution for transporting small amounts of CO_2 for small distances. It means that the most economically is to use SFG for distances lower than 500 km and transfer the CO_2 below 1 mtpa. The SFG has become a costly solution for the longer distances (more than 750 km) due to the high number of vessels required to perform the mission. The amount of submarines drastically increases with the number of kilometres the vessel needs to transport, automatically increasing the capital and operation expenditures.

The analysis shows that for longer distances (more than 750 km) is more economical to use the tanker ships, both crewed and autonomous. Also, if it is required to ship a large amount of CO_2, then the crew and autonomous tanker are the most cost-effective way to do this. The offshore pipelines become economic if the distance is small and a vast amount of CO_2 is needed to transport. Finally, based on the results in (Santoso, 2021), the SST is the most competitive solution for intermediate distances (500-750 km) and transporting a medium amount of CO_2 (1 mtpa).

Table 5.1 *Transport methods with the lowest costs for various distances and volumes.*

	180 km	**500 km**	**750 km**	**1500 km**
0.5 mtpa	SFG	SFG/SST	SST	CS/AS
1 mtpa	SFG/SST	SST	AS/CS/SST	CS/AS
2.5 mtpa	OP/SST	CS	CS	CS/AS

6. Conclusions and Recommendations

The performed study analyses the technical and economic feasibility of a conceptual Subsea Freight Glider. The first step of the performed analysis involves conducting a design analysis, while the second step includes performing an economic analysis. This technical study is based on the procedures provided in the DNV-RU-NAVAL-Pt4Ch1 standard, an ASME Boiler, and Pressure Vessel Code. Although the economic analysis is based on publicly open, the ZEP and MUNIN cost models are also used for the analysis.

The presented study shows that the SFG with a cargo capacity of 469 m^3, 1194 m^3, and 2430 m^3 meet the mission requirements. The scenario considered during the research involves the CO_2 transportation of 0.5, 1.0, and 2.5 million tons per year. The cost per ton of CO_2 is compared with the cost of transporting it on tanker ships or offshore pipelines. The study shows that the SFG can be economically feasible for short distances of up to 500 km and small volumes of CO_2 up to 1.0 mtpa. Due to the low CAPEX and OPEX, the SFG is a cheaper solution than a crewed and autonomous tanker. Moreover, with the low velocity of the SFG, and the low liquidation cost, the SFG can transport CO_2 in a saturated state, which significantly reduces the total price.

The technical and economic analysis of the SFG shows that the small underwater vehicle is technically feasible to perform the mission and economically profitable. However, there are still areas of work that need to be carried out in the future. In this work, the design by rules was applied, but there is a need to perform the design by analysis with finite element analysis. The performed design follows the DNV-RU-NAVAL-Pt4Ch1 standard that was initially created for military submarines. Due to high safety factors, the SFG became expensive. It is possible to decrease the CAPEX of SFG if the safety factor is reduced.

References

Ahmad, U. N., & Xing, Y. (2021). A 2D model for the study of equilibrium glide paths of UiS Subsea Freight-Glider. *IOP Conference Series: Materials Science and Engineering*, *1201*(1), 012022. https://doi.org/10.1088/1757-899X/1201/1/012022

Ahmad, U., Xing, Y., & Ma, Y. (2022). *UiS Subsea-Freight Glider: A Buoyancy-Driven Autonomous Glider*.

Bai, Y., & Bai, Q. (2018). Subsea engineering handbook. In *Subsea Engineering Handbook*. Elsevier. https://doi.org/10.1016/C2016-0-03767-1

Benjaminsen, C. (2019, October 7). *This is what you need to know about CCS – Carbon Capture and Storage - SINTEF*. https://www.sintef.no/en/latest-news/2019/this-is-what-you-need-to-know-about-ccs-carbon-capture-and-storage/

Berg, T. E. (2007). *Marine Operations Submarines, AUVs - UUVs and ROVs*. NTNU, Department of Marine Technology.

Cheeseman, I. C. (1976). Fluid-Dynamic Drag: Practical Information on Aerodynamic Drag and Hydrodynamic Resistance. In *The Aeronautical Journal* (Vol. 80, Issue 788). Cambridge University Press. https://doi.org/10.1017/S0001924000034187

DNV GL AS. (2018). *Rules for Classification: Naval vessels Part 4 Sub-surface ships Chapter 1 Submarines*. http://www.dnvgl.com,

Elsey, J. (2020, May 11). *How to Define & Measure Centrifugal Pump Efficiency: Part 1*. https://www.pumpsandsystems.com/how-define-measure-centrifugal-pump-efficiency-part-1

Equinor ASA. (2019). *Subsea Shuttle: the world's first drone to transport CO2*. https://www.equinor.com/en/magazine/here-are-six-of-the-coolest-offshore-robots.html

Equinor ASA. (2020, January 7). *Equinor aims to cut emissions in Norway towards near zero in 2050*. https://www.equinor.com/news/archive/2020-01-06-climate-ambitions-norway

Ersdal, G. (2001). *An overview of ocean currents with emphasis on currents on the Norwegian continental shelf*. https://www.semanticscholar.org/paper/An-overview-of-ocean-currents-with-emphasis-on-on-Ersdal/e90fcf6fcade300b540190ab57071f8961b125c9

Graver, J. G. (2005). *Underwater gliders: Dynamics, control and design*. Princeton University.

Gudmestad, O. T. (2015). *Marine technology and operations: theory & practice*. WIT Press. https://books.google.com/books/about/Marine_Technology_and_Operations.html?hl=pl&id=M8TqBgAAQBAJ

Hall, S. (2018). Rules of Thumb for Chemical Engineers. In *Rules of Thumb for Chemical Engineers*.

International Energy Agency. (2021). *Net Zero by 2050 - A Roadmap for the Global Energy Sector*. www.iea.org/t&c/

Kretschmann, L., Burmeister, H. C., & Jahn, C. (2017). Analyzing the economic benefit of unmanned autonomous ships: An exploratory cost-comparison between an autonomous and a conventional bulk carrier. *Research in Transportation Business & Management*, *25*, 76–86. https://doi.org/10.1016/J.RTBM.2017.06.002

Letcher, T. M. (2019). Why do we have global warming? In *Managing Global Warming: An Interface of Technology and Human Issues* (pp. 3–15). Academic Press. https://doi.org/10.1016/B978-0-12-814104-5.00001-6

Ma, Y., Xing, Y., Ong, M. C., & Hemmingsen, T. H. (2021). Baseline design of a subsea shuttle tanker system for liquid carbon dioxide transportation. *Ocean Engineering, 240*. https://doi.org/10.1016/J.OCEANENG.2021.109891

Metz, B., Davidson, O., de Coninck, H., Loos, M., & Meyer, L. (2005). *Carbon Dioxide Capture and Storage*.

MUNIN. (2015). *D9.3: Quantitative assessment*.

NASA Global Climate Change and Global Warming: Vital Signs of the Planet. (2008). *Global Climate Change: Evidence*. https://climate.nasa.gov/causes/

National Centers for Environmental Information (NCEI). (n.d.). *Greenland, Iceland and Norwegian Seas Regional Climatology*. Retrieved May 28, 2022, from https://www.ncei.noaa.gov/products/greenland-iceland-and-norwegian-seas-regional-climatology

Odland, J. (2018). *Offshore Field Development*.

Pollard, J. (2022). *Petronas, Shell Unit Tie Up to Explore Carbon Capture, Storage*. Asia Financial News. https://www.asiafinancial.com/petronas-shell-unit-tie-up-to-explore-carbon-capture-storage

Rackley, S. A. (2017). Carbon dioxide transportation. In *Carbon Capture and Storage*. Butterworth-Heinemann. https://doi.org/10.1016/B978-0-12-812041-5.00023-4

Ronca, D., & Mancimi, M. (2021). *How Carbon Capture Works | HowStuffWorks*. https://science.howstuffworks.com/environmental/green-science/carbon-capture.htm#pt3

Rudnick, D. L., Davis, R. E., Eriksen, C. C., Fratantoni, D. M., & Perry, M. J. (2004). Underwater Gliders for Ocean Research. *Marine Technology Society Journal*. https://www.academia.edu/17650844/Underwater_Gliders_for_Ocean_Research

Santoso, T. A. D. (2021). *Technical- and Economic-Feasibility Analysis of Subsea Shuttle Tanker*. University of Stavanger.

Scripps Institution of Oceanography at UC San Diego. (2022). *The Keeling Curve*. https://keelingcurve.ucsd.edu/

The American Society of Mechanical Engineers ASME. (2017). *ASME Boiler and Pressure Vessel Code An International Code R ules for Construction of Power Boilers SECTION I.*

Trading Economics. (2022). *Steel - 2022 Data - 2016-2021 Historical - 2023 Forecast* . https://tradingeconomics.com/commodity/steel

Tsang, N. W. H., Lam, K. Y., Qureshi, U. M., Ng, J. K. Y., Papavasileiou, I., & Han, S. (2018). Indoor activity tracking for elderly using intelligent sensors. *Intelligent Data Sensing and Processing for Health and Well-Being Applications*, 197–222. https://doi.org/10.1016/B978-0-12-812130-6.00011-1

UN FCCC. (2015). *Paris Agreement*.

United States Environmental Protection Agency US EPA. (2017). *Climate Impacts on Agriculture and Food Supply - Climate Change Impacts*. https://19january2017snapshot.epa.gov/climate-impacts/climate-impacts-agriculture-and-food-supply_.html#main-content

Wärtsilä. (2017). *WSD50 30K 30,000m3 LNG Carrier - Datasheet*.

Wigley, T. M. L. (1983). The pre-industrial carbon dioxide level. *Climatic Change 1983 5:4*, *5*(4), 315–320. https://doi.org/10.1007/BF02423528

Witkowski, A., Majkut, M., & Rulik, S. (2014). Analysis of pipeline transportation systems for carbon dioxide sequestration. *Archives of Thermodynamics*, *35*(1), 117–140. https://doi.org/10.2478/AOTER-2014-0008

Wood, & Stephen. (2009, January 1). Autonomous Underwater Gliders. *Underwater Vehicles*. https://doi.org/10.5772/6718

Xing, Y. (2021). A Conceptual Large Autonomous Subsea Freight-Glider for Liquid CO2 Transportation. *Proceedings of the International Conference on Offshore Mechanics and Arctic Engineering - OMAE*, *6*. https://doi.org/10.1115/OMAE2021-61924

Xing, Y., Ong, M. C., Hemmingsen, T., Ellingsen, K. E., & Reinås, L. (2021). Design considerations of a subsea shuttle tanker system for liquid carbon dioxide transportation. *Journal of Offshore Mechanics and Arctic Engineering*, *143*(4). https://doi.org/10.1115/1.4048926/1089683

Xing, Y., Santoso, T. A. D., & Ma, Y. (2021). Technical-Economic Feasibility Analysis of Subsea Shuttle Tanker. *Journal of Marine Science and Engineering 2022, Vol. 10, Page 20*, *10*(1). https://doi.org/10.3390/JMSE10010020

ZEP. (2011). *The Costs of CO2 Capture, Transport and Storage*. www.zeroemissionsplatform.eu/library/publication/168-zep-cost-report-storage.html

Appendix A

Appendix A provides the results of the technical feasibility analysis for the SFG 469 m³ (down-scale design) and the SFG 2430 m³ (up-scale design).

SFG 469 m³ (down-scale design)

External hull design

Table A.1 Calculation for the external hull of SFG baseline design.

Parameter	Symbol	Free flooding compartment			Flooded compartment	Units	Equation number (DNV GL RU Pt4C1 Appendix A)
		Nominal diving depth	Test diving depth	Collapse depth	Collapse		
Design pressure	p	20	25	40	20	[bar]	User input
Hull thickness	s	0.025	0.025	0.025	0.014	[m]	User input
Hull radius	R_m	2.00	2.00	2.00	2.00	[m]	User input
Frame web height	h_w	0.165	0.165	0.165	0.165	[m]	User input
Frame web thickness	s_w	0.003	0.003	0.003	0.003	[m]	User input
Flange width	b_f	0.08	0.08	0.08	0.08	[m]	User input
Flange thickness	s_f	0.03	0.03	0.03	0.03	[m]	User input
Frame spacing	L_f	1.0	1.0	1.0	1.5	[m]	User input
Frame cross-sectional area	A_f	0.0074	0.0074	0.0074	0.0074	[m²]	User input
Inner radius to the flange of the frame	R_f	1.78	1.78	1.78	1.78	[m]	User input
Youngs modulus	E	206	206	206	206	[GPa]	User input
Poisson Ratio	v	0.3	0.3	0.3	0.3	-	User input
Poisson ratio in elastic-plastic range	v_p	0.44	0.44	0.44	0.44	-	(A48)
Frame distance without thickness	L	0.97	0.97	0.97	1.47	[m]	(A9)
Effective length	L_{eff}	0.348	0.348	0.348	0.260	[m]	(A10)
Effective area	A_{eff}	0.0079	0.0079	0.0079	0.0079	[m²]	(A11)
The radial displacement in the middle between the frames	w_M	-0,0014	-0.00175	-0.00284	-0.00234	[m]	(A15)
The radial displacement at the frames	w_F	-0.00076	-0.00093	-0.00135	-0.000801	[m]	(A16)
The reference stress is the circumferential stress in the unstiffened cylindrical pressure hull	σ_0	160	200	320	286	[MPa]	(A13)
The equivalent stresses are composed of the single stresses in a longitudinal and circumferential direction in the middle between frames	$\sigma^m_{v,m}$	146	182	295	246	[MPa]	(A14)
The equivalent stresses are composed of the single stresses in a longitudinal and circumferential direction at the frames	$\sigma^m_{v,f}$	94	115	175	135	[MP]	(A14)
Average membrane stress in longitudinal direction	σ^m_x	80	100	160	143	[MPa]	(A17)
Membrane stress in circumferential the direction in the middle between the frames	$\sigma^m_{\varphi,M}$	168	211	340	284	[MPa]	(A18)
Membrane stress in circumferential direction at the frames	$\sigma^m_{\varphi,F}$	103	126	187	125	[MPa]	(A19)
Bending stresses in longitudinal direction in the middle between the frames	$\sigma^x_{\varphi,M}$	26	33	55	52	[MPa]	(A20)
Bending stresses in longitudinal direction at the frames	$\sigma^b_{x,F}$	105	135	244	291	[MPa]	(A21)
Bending stresses in circumferential the direction in the middle between the frames	$\sigma^b_{\varphi,M}$	8	10	16	15	[MPa]	(A22)
Bending stresses in circumferential direction at the frames	$\sigma^b_{\varphi,M}$	31	40	73	87	[MPa]	(A23)
Tangential module	E_t	206	206	206	206	[MPa]	(A38)
Secant module	E_s	204	204	204	204	[GPa]	(A39)
Elastic buckling pressure	p^{el}_{cr}	77	77	77	77	[GPa]	(A28)
Theoretical elastic-plastic buckling pressure	p^t_{cr}	76	76	76	76	[bar]	(A29)
Reduction factor	R	0.76	0.76	0.76	0.76	[bar]	(A43)

Table A.2 Stresses at nominal diving depth for SFG baseline design in the free-flooding compartment

Type of stresses	As the frame			In the middle of the field		
	Circumferential	Equivalent	Axial	Circumferential	Equivalent	Axial
Membrane stress	103 MPa	-	80 MPa	168 MPa	-	80 MPa
Membrane equivalent stress	-	146 MPa	-	-	93 MPa	-
Bending stress	31 MPa	-	105 MPa	8 MPa	-	26 MPa
Normal stress outside	134 MPa	-	185 MPa	176 MPa	-	106 MPa
Equivalent stress outside	-	165 MPa	-	-	153 MPa	-
Normal stress inside	134 MPa	-	185 MPa	176 MPa	-	106 MPa
Equivalent normal stress inside	-	165 MPa	-	-	153 MPa	-

Table A.3 Stresses at test diving depth for SFG baseline design in the free-flooding compartment.

Type of stresses	As the frame			In the middle of the field		
	Circumferential	Equivalent	Axial	Circumferential	Equivalent	Axial
Membrane stress	126 MPa	-	100 MPa	211 MPa	-	100 MPa
Membrane equivalent stress	-	182 MPa	-	-	115 MPa	-
Bending stress	41 MPa	-	135 MPa	10 MPa	-	33 MPa
Normal stress outside	167 MPa	-	235 MPa	220 MPa	-	133 MPa
Equivalent stress outside	-	210 MPa	-	-	192 MPa	-
Normal stress inside	167 MPa	-	235 MPa	220 MPa	-	133 MPa
Equivalent normal stress inside	-	210 MPa	-	-	192 MPa	-

Table A.4 Stresses at collapse diving depth for SFG baseline design in the free-flooding compartment.

Type of stresses	As the frame			In the middle of the field		
	Circumferential	Equivalent	Axial	Circumferential	Equivalent	Axial
Membrane stress	187 MPa	-	160 MPa	340 MPa	-	160 MPa
Membrane equivalent stress	-	295 MPa	-	-	175 MPa	-
Bending stress	73 MPa	-	244 MPa	17 MPa	-	55 MPa
Normal stress outside	260 MPa	-	404 MPa	357 MPa	-	215 MPa
Equivalent stress outside	-	354 MPa	-	-	311 MPa	-
Normal stress inside	260 MPa	-	404 MPa	357 MPa	-	215 MPa
Equivalent normal stress inside	-	354 MPa	-	-	311 MPa	-

Table A.5 Stresses at collapse diving depth for SFG baseline design in the flooded compartment.

Type of stresses	As the frame			In the middle of the field		
	Circumferential	Equivalent	Axial	Circumferential	Equivalent	Axial
Membrane stress	125 MPa	-	143 MPa	284 MPa	-	143 MPa
Membrane equivalent stress	-	246 MPa	-	-	135 MPa	-
Bending stress	87 MPa	-	291 MPa	2 MPa	-	5 MPa
Normal stress outside	213 MPa	-	434 MPa	285 MPa	-	148 MPa
Equivalent stress outside	-	376 MPa	-	-	274 MPa	-
Normal stress inside	213 MPa	-	434 MPa	285 MPa	-	148 MPa
Equivalent normal stress inside	-	376 MPa	-	-	274 MPa	-

Table A.6 *Permissible and equivalent stresses in the external hull of SFG baseline design.*

Case	Depth	Maximum equivalent stress	Permissible stress (DNVGL RU P4C1 Sec. 4.3)	Citation fulfilled?
Nominal diving depth	200 m	185 MPa	203 MPa	Yes
Testing diving depth	250 m	235 MPa	418 MPa	Yes
Collapse depth	400 m	404 MPa	460 MPa	Yes
Flooded compartment	-	434 MPa	460 MPa	Yes

Hydrostatic stability

Table A.7 *SFG Baseline design hydrostatic stability.*

Parameters	SFG 469 m³ (Half-scaled)			
	Submerged (CO₂ filled)	Submerged (SW filled)	Surfaced (CO₂ filled)	Surface (SW filled)
CoG(x,y,z)	[-0.58, 0.00, 0.33]	[-0.52, 0.00, 0.33]	[-0.52, 0.00, 0.33]	[-0.60, 0.00, 0.51]
CoB(x,y,z)	[-0.67, 0.00, 0.00]	[-0.67, 0.00, 0.00]	[-0.67, 0.00, 4.10]	[-0.67, 0.00, 3.50]
M(x,y,z)	[0.00, 0.00, 0.00]	[0.00, 0.00, 0.00]	[0.00, 0.00, 0.00]	[0.00, 0.00, 0.00]
BG	0.330	0.330	3.770	2.990
GM	0.330	0.330	0.330	0.510
Result	BG > 0.32 == OK	BG > 0.32 == OK	GM > 0.2 == OK	GM > 0.2 == OK

Weight estimation

Table A.8 *Weight distribution of SFG baseline design.*

Component	SFG 469 m³	
	Weight (tons)	Percentage
Machinery	9.610	2.00%
Permanent ballast	9.610	2.00%
Structure	187.999	39.12%
Mid-body seawater	69.051	14.37%
Compensation ballast	0.804	0.17%
Payload	200.082	41.64%
Trim tank	3.364	0.70%
Sum	**480.520**	**100%**

SFG 2430 m³ (double-scale design)

External hull design

Table A.9 *Calculation for the external hull of SFG baseline design.*

Parameter	Symbol	Free flooding compartment			Flooded compartment	Units	Equation number (DNV GL RU Pt4C1 Appendix A)
		Nominal diving depth	Test diving depth	Collapse depth	Collapse		
Design pressure	p	20	25	40	20	[bar]	User input
Hull thickness	s	0.036	0.036	0.036	0.026	[m]	User input
Hull radius	R_m	3.50	3.50	3.50	3.50	[m]	User input
Frame web height	h_w	0.165	0.165	0.165	0.165	[m]	User input
Frame web thickness	s_w	0.03	0.03	0.03	0.03	[m]	User input
Flange width	b_f	0.08	0.08	0.08	0.08	[m]	User input
Flange thickness	s_f	0.03	0.03	0.03	0.03	[m]	User input
Frame spacing	L_f	1.0	1.0	1.0	1.5	[m]	User input
Frame cross-sectional area	A_f	0.00735	0.00735	0.00735	0.00735	[m²]	User input
Inner radius to the flange of the frame	R_f	3.27	3.27	3.27	3.27	[m]	User input
Youngs modulus	E	206	206	206	206	[GPa]	User input
Poisson Ratio	v	0.3	0.3	0.3	0.3	-	User input
Poisson ratio in elastic-plastic range	v_p	0.44	0.44	0.44	0.44	-	(A48)
Frame distance without thickness	L	0.97	0.97	0.97	1.47	[m]	(A9)
Effective length	L_{eff}	0.552	0.552	0.552	0.469	[m]	(A10)
Effective area	A_{eff}	0.00768	0.00768	0.00768	0.00766	[m²]	(A11)
The radial displacement in the middle between the frames	w_M	-0.00249	-0.00312	-0.00503	-0.0042	[m]	(A15)
The radial displacement at the frames	w_F	-0.00285	-0.00362	-0.00590	-0.000873	[m]	(A16)
The reference stress is the circumferential stress in the unstiffened cylindrical pressure hull	σ_0	194	243	389	269	[MPa]	(A13)
The equivalent stresses are composed of the single stresses in a longitudinal and circumferential direction in the middle between frames	$\sigma^m_{v,m}$	153	191	307	249	[MPa]	(A14)
The equivalent stresses are composed of the single stresses in a longitudinal and circumferential direction at the frames	$\sigma^m_{v,f}$	170	216	352	119	[MP]	(A14)
Average membrane stress in longitudinal direction	σ^m_x	97	122	194	135	[MPa]	(A17)
Membrane stress in circumferential the direction in the middle between the frames	$\sigma^m_{\varphi,M}$	176	220	354	288	[MPa]	(A18)
Membrane stress in circumferential direction at the frames	$\sigma^m_{\varphi,F}$	197	249	406	91	[MPa]	(A19)
Bending stresses in longitudinal direction in the middle between the frames	$\sigma^x_{\varphi,M}$	57	74	131	24	[MPa]	(A20)
Bending stresses in longitudinal direction at the frames	$\sigma^b_{x,F}$	42	12	33	321	[MPa]	(A21)
Bending stresses in circumferential the direction in the middle between the frames	$\sigma^b_{\varphi,M}$	17	22	39	7	[MPa]	(A22)
Bending stresses in circumferential direction at the frames	$\sigma^b_{\varphi,M}$	1	4	1	96	[MPa]	(A23)
Tangential module	E_t	206	206	206	206	[MPa]	(A38)
Secant module	E_s	204	204	204	204	[GPa]	(A39)
Elastic buckling pressure	p^{el}_{cr}	99	99	99	23	[GPa]	(A28)
Theoretical elastic-plastic buckling pressure	p^i_{cr}	11	11	11	25	[bar]	(A29)
Reduction factor	R	0.76	0.76	0.76	0.76	[bar]	(A43)

Table A.10 *Stresses at nominal diving depth for SFG baseline design in the free-flooding compartment.*

Type of stresses	As the frame			In the middle of the field		
	Circumferential	Equivalent	Axial	Circumferential	Equivalent	Axial
Membrane stress	197 MPa	-	97 MPa	176 MPa	-	97 MPa
Membrane equivalent stress	-	153 MPa	-	-	170 MPa	-
Bending stress	1 MPa	-	4 MPa	17 MPa	-	57 MPa
Normal stress outside	198 MPa	-	102 MPa	193 MPa	-	154 MPa
Equivalent stress outside	-	171 MPa	-	-	177 MPa	-
Normal stress inside	198 MPa	-	102 MPa	193 MPa	-	154 MPa
Equivalent normal stress inside	-	171 MPa	-	-	177 MPa	-

Table A.11 *Stresses at test diving depth for SFG baseline design in the free-flooding compartment.*

Type of stresses	As the frame			In the middle of the field		
	Circumferential	Equivalent	Axial	Circumferential	Equivalent	Axial
Membrane stress	249 MPa	-	122 MPa	220 MPa	-	122 MPa
Membrane equivalent stress	-	191 MPa	-	-	216 MPa	-
Bending stress	4 MPa	-	12 MPa	22 MPa	-	74 MPa
Normal stress outside	253 MPa	-	134 MPa	242 MPa	-	196 MPa
Equivalent stress outside	-	219 MPa	-	-	223 MPa	-
Normal stress inside	253 MPa	-	134 MPa	242 MPa	-	196 MPa
Equivalent normal stress inside	-	219 MPa	-	-	223 MPa	-

Table A.12 *Stresses at collapse diving depth for SFG baseline design in the free-flooding compartment.*

Type of stresses	As the frame			In the middle of the field		
	Circumferential	Equivalent	Axial	Circumferential	Equivalent	Axial
Membrane stress	406 MPa	-	194 MPa	354 MPa	-	194 MPa
Membrane equivalent stress	-	307 MPa	-	-	352 MPa	-
Bending stress	10 MPa	-	33 MPa	39 MPa	-	131 MPa
Normal stress outside	416 MPa	-	228 MPa	393 MPa	-	325 MPa
Equivalent stress outside	-	361 MPa	-	-	364 MPa	-
Normal stress inside	416 MPa	-	228 MPa	393 MPa	-	325 MPa
Equivalent normal stress inside	-	361 MPa	-	-	364 MPa	-

Table A.13 *Stresses at collapse diving depth for SFG baseline design in the flooded compartment.*

Type of stresses	As the frame			In the middle of the field		
	Circumferential	Equivalent	Axial	Circumferential	Equivalent	Axial
Membrane stress	92 MPa	-	135 MPa	288 MPa	-	135 MPa
Membrane equivalent stress	-	249 MPa	-	-	119 MPa	-
Bending stress	96 MPa	-	321 MPa	7 MPa	-	23 MPa
Normal stress outside	188 MPa	-	455 MPa	295 MPa	-	158 MPa
Equivalent stress outside	-	396 MPa	-	-	256 MPa	-
Normal stress inside	188 MPa	-	455 MPa	295 MPa	-	158 MPa
Equivalent normal stress inside	-	396 MPa	-	-	256 MPa	-

Table A.14 Permissible and equivalent stresses in the external hull of SFG baseline design.

Case	Depth	Maximum equivalent stress	Permissible stress (DNVGL RU P4C1 Sec. 4.3)	Citation fulfilled?
Nominal diving depth	200 m	198 MPa	203 MPa	Yes
Testing diving depth	250 m	253 MPa	418 MPa	Yes
Collapse depth	400 m	416 MPa	460 MPa	Yes
Flooded compartment	-	456 MPa	460 MPa	Yes

Hydrostatic stability

Table A.15 SFG Baseline design hydrostatic stability

	SFG 2430 m^3 (Doubled-scaled)			
Parameters	Submerged (CO$_2$ filled)	Submerged (SW filled)	Surfaced (CO$_2$ filled)	Surface (SW filled)
CoG(x,y,z)	[-0.60, 0.00, 0.37]	[-0.56, 0.00, 0.39]	[-0.56, 0.00, 0.39]	[-0.65, 0.00, 0.39]
CoB(x,y,z)	[-1.00, 0.00, 0,00]	[-1.00, 0.00, 0.00]	[-1.00, 0.00, 5.10]	[-1.00, 0.00, 7.30]
M(x,y,z)	[0.00, 0.00, 0.00]	[0.00, 0.00, 0.00]	[0.00, 0.00, 0.00]	[0.00, 0.00, 0.00]
BG	0.372	0.388	4.712	6.13
GM	0.372	0.388	0.388	0.387
Result	BG > 0.35 == OK	BG > 0.35 == OK	GM >0.22 == OK	GM >0.22 == OK

Weight Estimation

Table A.16 Weight distribution of SFG baseline design.

Component	SFG 2430 m^3	
	Weight (tons)	Percentage
Machinery	49.798	2.00%
Permanent ballast	49.798	2.00%
Structure	962.768	38.67%
Mid-body seawater	277.306	11.14%
Compensation ballast	11.994	0.48%
Payload	1120.768	45.01%
Trim tank	17.429	0.70%
Sum	**2489.914**	**100%**

Appendix B

Appendix B contains all 'Cost per ton of CO_2' results. The outcomes are calculated based on the minimal and maximal price of the steel. Consequently, there are two 'Cost per ton of CO_2' prices, minimal and maximal.
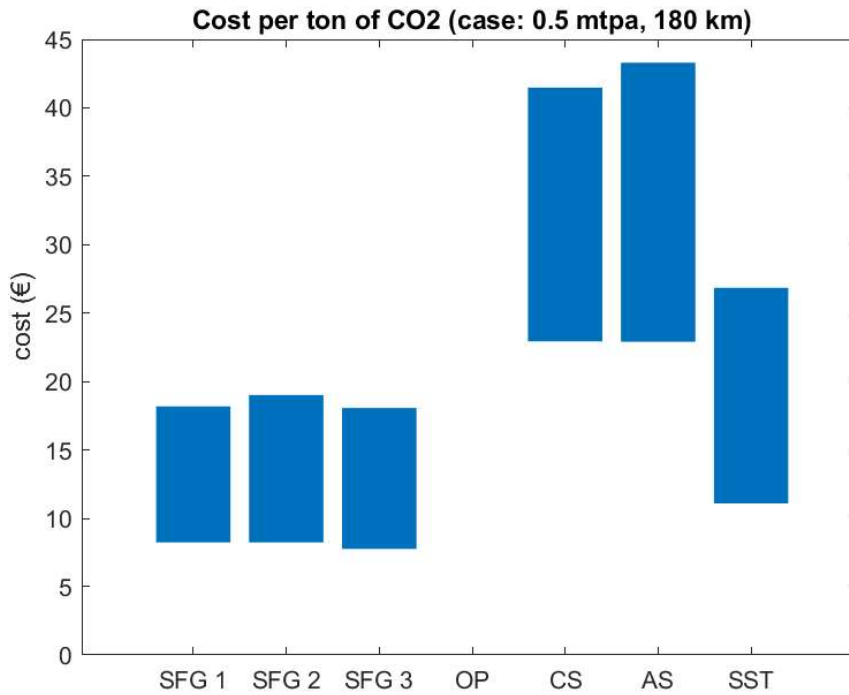
Figure B.1 *Cost per ton of CO_2 (case: 0.5 mtpa, 180 km).*
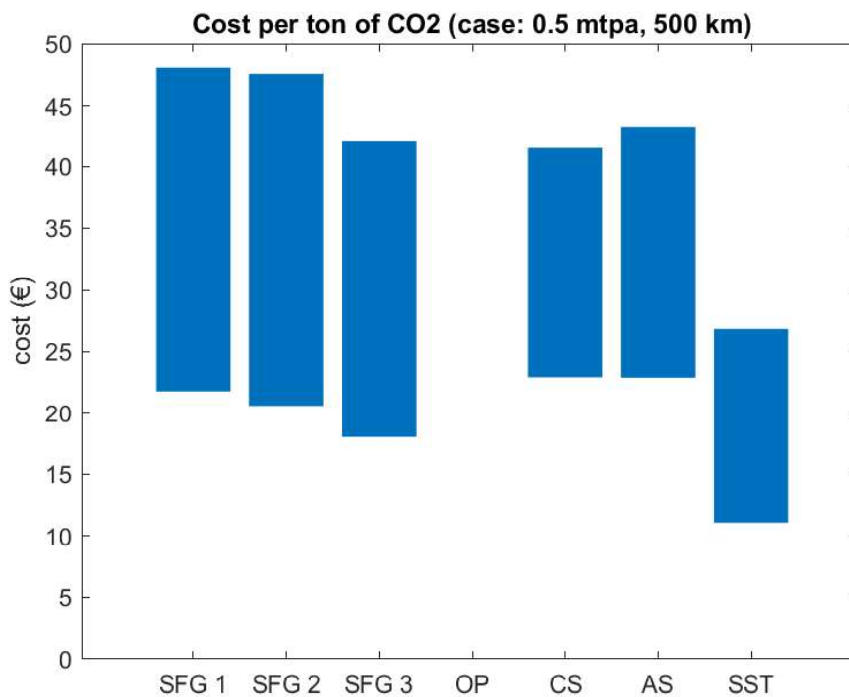
Figure B.2 *Cost per ton of CO_2 (case: 0.5 mtpa, 500 km).*
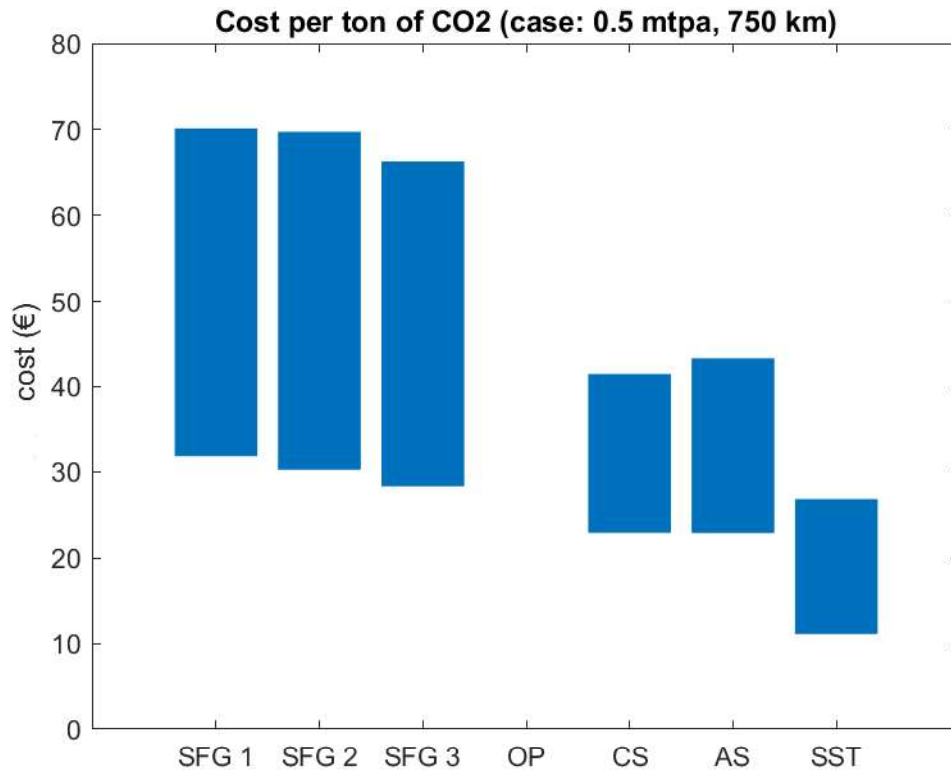
Figure B.3 *Cost per ton of CO$_2$ (case: 0.5 mtpa, 750 km).*
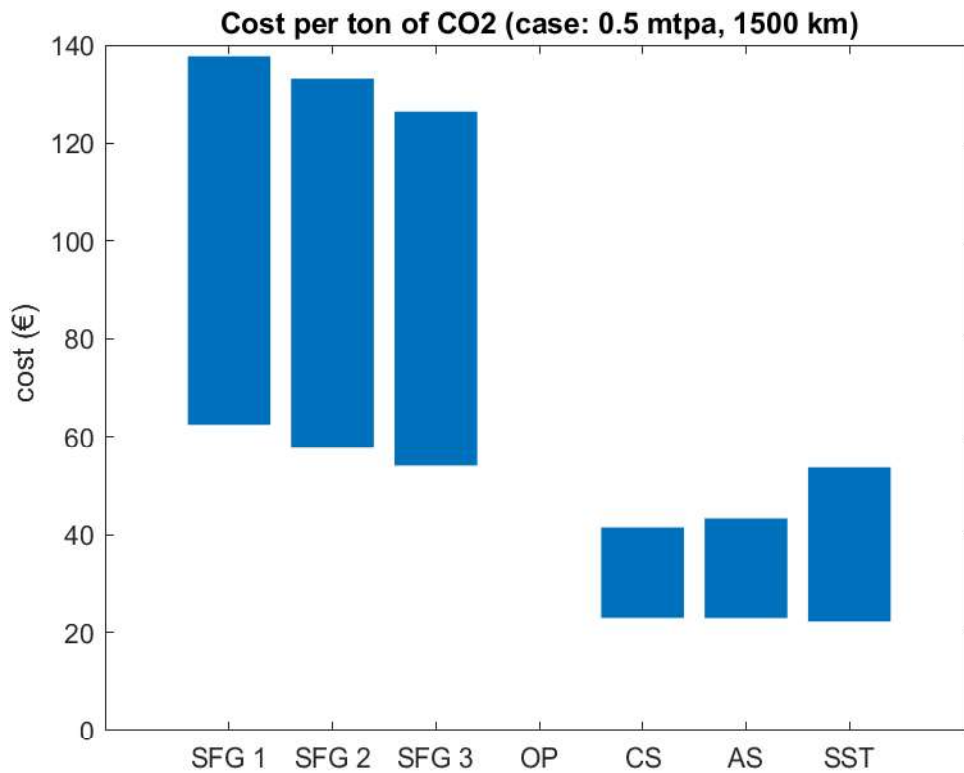
Figure B.4 *Cost per ton of CO$_2$ (case: 0.5 mtpa, 1500 km).*
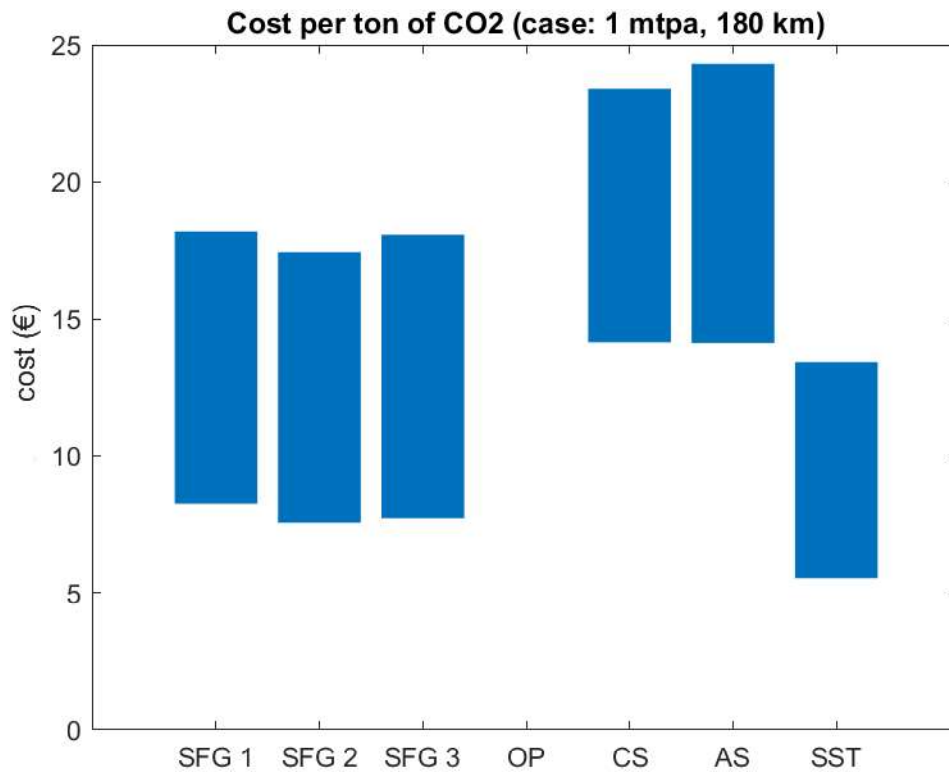
Figure B.5 *Cost per ton of CO₂ (case: 1 mtpa, 180 km).*
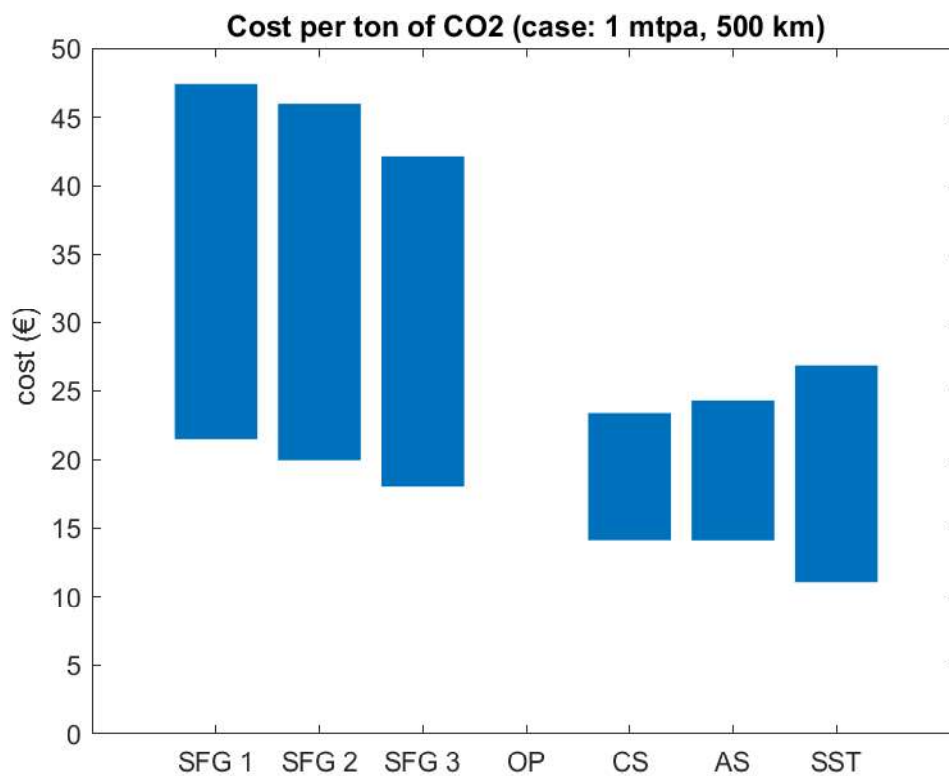
Figure B.6 *Cost per ton of CO₂ (case: 1 mtpa, 500 km).*
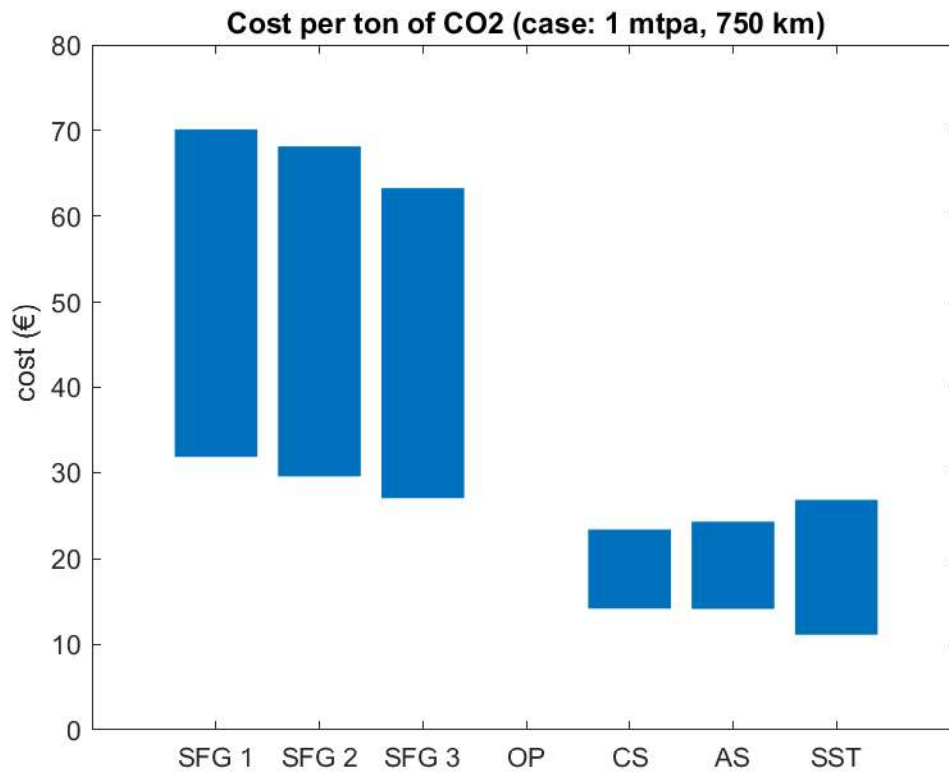
Figure B.7 *Cost per ton of CO₂ (case: 1 mtpa, 750 km).*
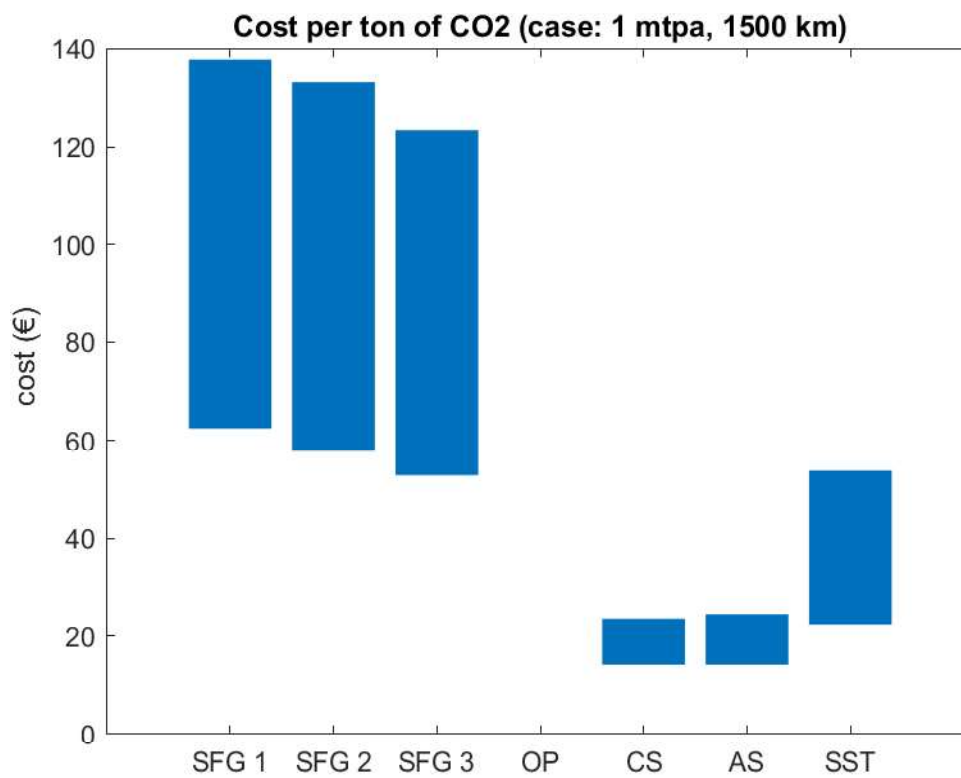
Figure B.8 *Cost per ton of CO₂ (case: 1 mtpa, 1500 km).*
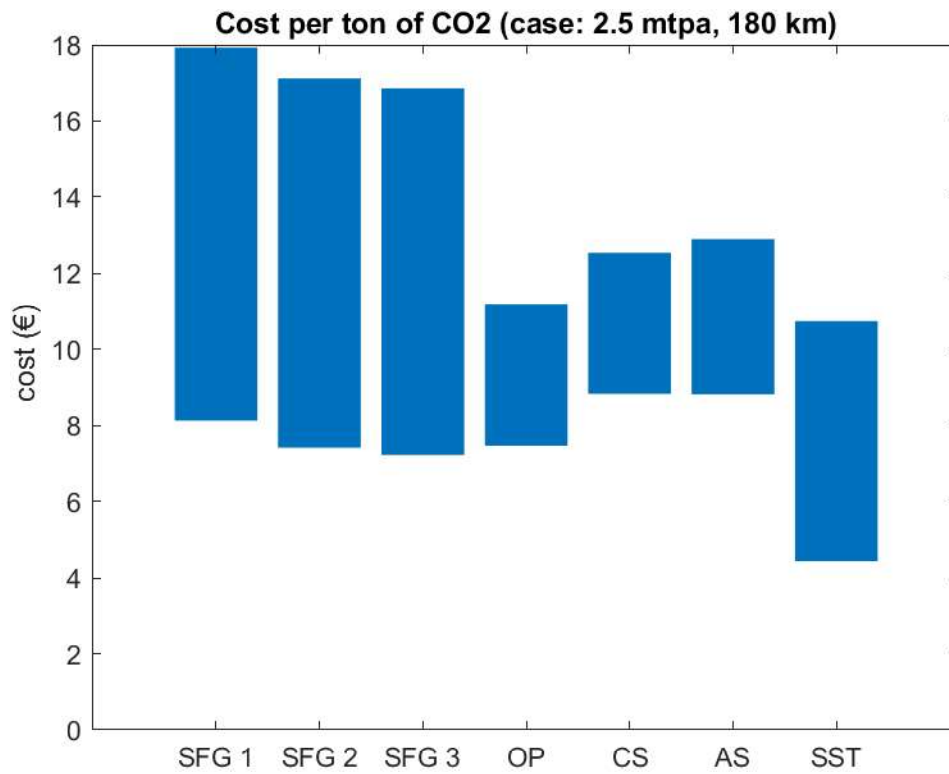
Figure B.9 *Cost per ton of CO₂ (case: 2.5 mtpa, 180 km).*
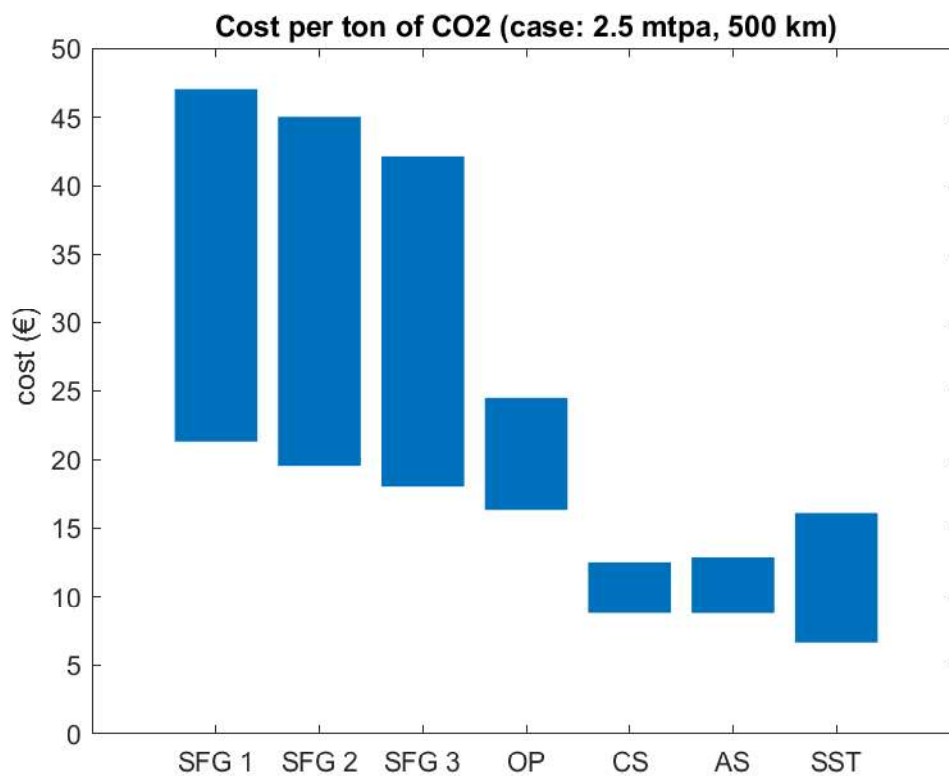
Figure B.10 *Cost per ton of CO₂ (case: 2.5 mtpa, 500 km).*
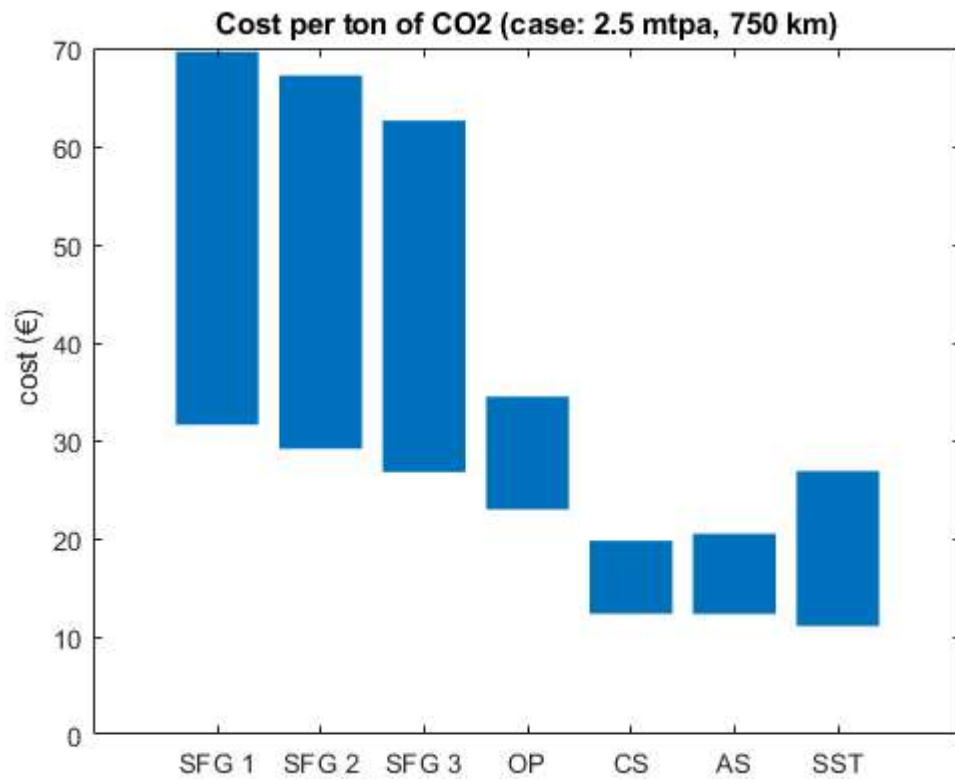
Figure B.11 Cost per ton of CO_2 (case: 2.5 mtpa, 750 km).
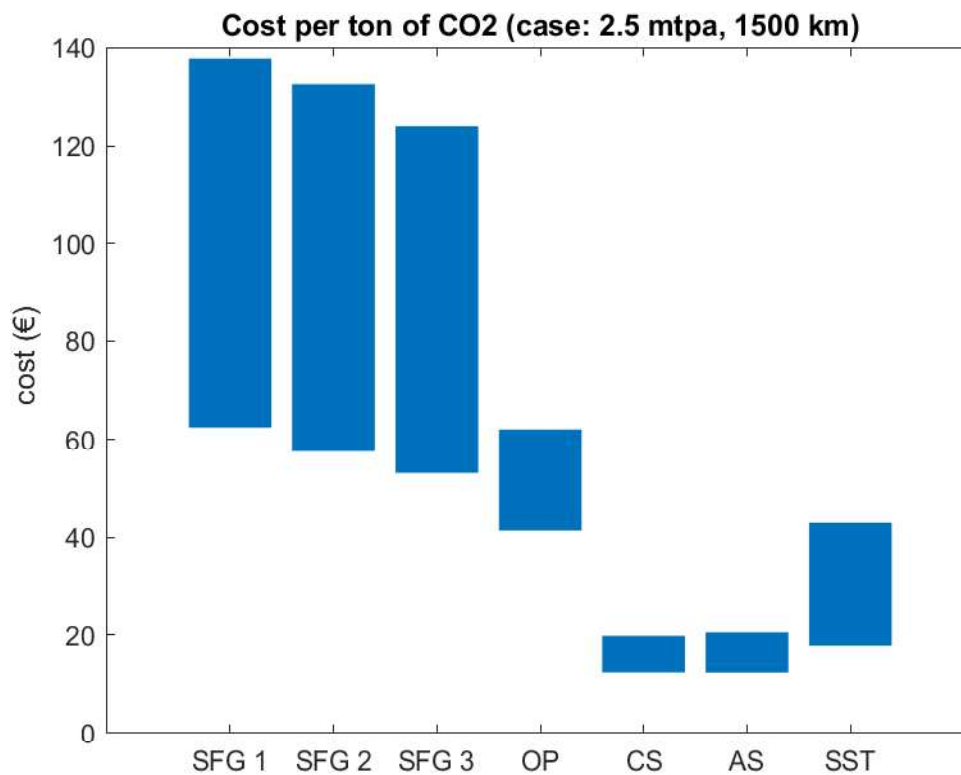
Figure B.12 Cost per ton of CO_2 (case: 2.5 mtpa, 1500 km).

Paper

This chapter contains the paper draft, which will be submitted to the scientific journal.

Technical and Economic Feasibility Analysis of a Conceptual Subsea Freight Glider for CO$_2$ Transportation

Pawel Klis[1], Yihan Xing[1,*] and Shuaishuai Wang[2]

[1] University of Stavanger, Norway

[2] Norwegian University of Science and Technology, Norway

[*] yihan.xing@uis.no

Abstract:

This study aims to analyse the technical and economic aspects of a novel Subsea Freight Glider (SFG). The SFG is an excellent replacement for tanker ships and submarine pipelines to transport liquefied CO$_2$. The main target of the SFG is to ship CO$_2$ from an offshore facility to an underwater well where the gas can be injected; as an advantage, the SFG vehicle may be used to transport all kinds of cargo. The SFG travels below the sea surface, making the vessel weather independent. The research is divided into two steps. Firstly, the technical feasibility is performed by designing a baseline design with a length of 56.5 m, a beam of 5.5 m, and a cargo volume of 1194 m^3. The SFG was developed using the DNVGL-RU-NAVAL-Pt4Ch1, initially created for military submarine design. Two additional half-scaled 469 m^3 and double-scaled 2430 m^3 models are created when the baseline design fulfils the technical requirements. Secondly, the economic analysis is carried out using freely accessible MUNIN D9.3 and ZEP reports. The economic feasibility analysis is illustrated through a case study with a CO$_2$ transport capacity of 0.5 to 2.5 mtpa (million tons per annum) and a transport length of 180 km to 1500 km. The prices of CO$_2$ per ton of the SFG, crew, and autonomous tanker and offshore pipelines are comprehensively compared. According to the results, the SFGs with capacities of 469 m^3, 1194 m^{3,} and 2430 m^3 are technically possible to manufacture. Moreover, the SFGs are competitive with smaller CO$_2$ capacities of 0.5 and 1 mtpa and distances of 180 and 500 km.

Keywords: subsea freight glider, subsea technology, economic analysis, cargo vessel, CO$_2$ transporting.

1. Introduction

1.1. General background

The Carbon Capture and Storage system (CCSs) requires transportation infrastructure development to enhance safety and economic efficiency [1]. The capture system should be interconnected with a storage system to complete the CO$_2$ transport operation. However, these systems are usually hundreds of kilometres apart. Additionally, carbon dioxide should be transported under appropriate pressure conditions, which depend on different transmission methods. The transport of CO$_2$ via the pipeline will take place at a different temperature and pressure condition compared to that by vessels.

Transporting CO2 by underwater pipelines is the most commonly used method. [2]. This is because by implementing this method, products can be transported continuously, which effectively enhances transportation efficiency. Additionally, pipelines can transport carbon dioxide in three states: liquid, gaseous and solid. They can also take shortcuts and be installed anywhere, including underwater or underground. Moreover, it is a closed type of transportation, which effectively avoids loss, and thus it is safe, reliable, and clean with no pollution. However, this solution has some limitations. Impurities like water or hydrogen sulfide in the CO_2 stream can cause corrosion in the pipelines. In the case of pipe cracks in a populated area, the unexpected release of carbon dioxide can lead to severe environmental and human threats. Furthermore, the installation and maintenance of a subsea system for transporting gases are very expensive. In addition. steel prices are increasing every year [3], which implies that the design and construction is a costly solution, often unprofitable in the case of small reservoirs.

Liquefied hydrocarbon gases are transported in very large LNG or LPG tanks. However, it was proven that these carries could also be used for CO_2 transportation. The largest LNG carriers have a capacity of 266,000 m^3, which means that they could carry 230,000 t of CO_2. The transport efficiency is maximised when the density of liquid CO_2 is as high as possible. The density increases sharply with the decreasing pressure in the triple point region, reaching 1200 kg/m^3 [4]; however, it is essential to avoid the formation of dry ice. The optimal conditions for transportation of the CO_2 are at a temperature of 218.15 K and a pressure of 7 bar.

Transporting CO_2 by vessel tanks allows carrying massive quantities of goods over long distances. Yet, sometimes it is impossible to perform a marine operation due to inclement weather conditions. Factors such as wind or rain may prevent or delay the performance of maritime operations.

Pipelines seem to be a perfect solution if continuous transport for a relatively short distance of CO_2 is needed. Vessel tanks should be utilised when the transportation distance is long. However, there is a gap between these two solutions. Currently, there is no transportation method that can transfer carbon dioxide for medium distances without continuous delivery. Pipelines and marine transportation leave a carbon footprint that negatively impacts the environment. Many countries and oil & gas companies have decided to reduce their absolute emissions to near zero by 2050 [5]. Therefore, looking for an alternative CO_2 transportation method is needed.

1.2. *Previous work*

In 2019, Equinor ASA proposed the concept of an underwater drone to transport CO_2 [6]. The Subsea shuttle is an autonomous 135-meter vehicle that could transport carbon dioxide back to the reservoirs, replacing the pipeline carrying CO_2. Even though the concept has been presented, there were very limited studies. Xing et al. [7] performed a detailed description of the baseline design and conducted a finite element analysis of ring-stiffened cylinders of the design. Santoso [8] presented and compared three different models of the Subsea Shuttle Tanker and proved that they are technically feasible. Also, an economic analysis was performed.

In the study of Xing et al. [9], a new type of underwater vehicle for CO_2 transportation was proposed. The concept is an autonomous Subsea Freight Glider, which is a novel cargo submarine equipped with large hydrodynamic wings that allow gliding underneath the sea surface. This solution covers the gap with the previous studies and enables transporting vast amounts of cargo autonomously over long distances. The gilder does not have a propeller, and the only driving force is buoyancy force. In the study of Ahmad [10], a control methodology was proposed based on feedback from the developed glider model and obtained the glide path.

These studies show that the concept of Subsea Freight Glider can compete with different methods of CO_2 transportation. However, performed analyses are insufficient, and some limitations exist. Previous studies concerned that large submarines that can transport an enormous amount of CO_2. On the other hand, there are some small offshore facilities close to land where CO_2 can be stored, and the conventional way of transporting CO_2 is too expensive. This paper presents the methodology of designing the small-size underwater gliding vehicle and compares it with traditional ways of CO_2 transportation. The research will cover the gap in shipping small amounts of carbon dioxide for small distances.
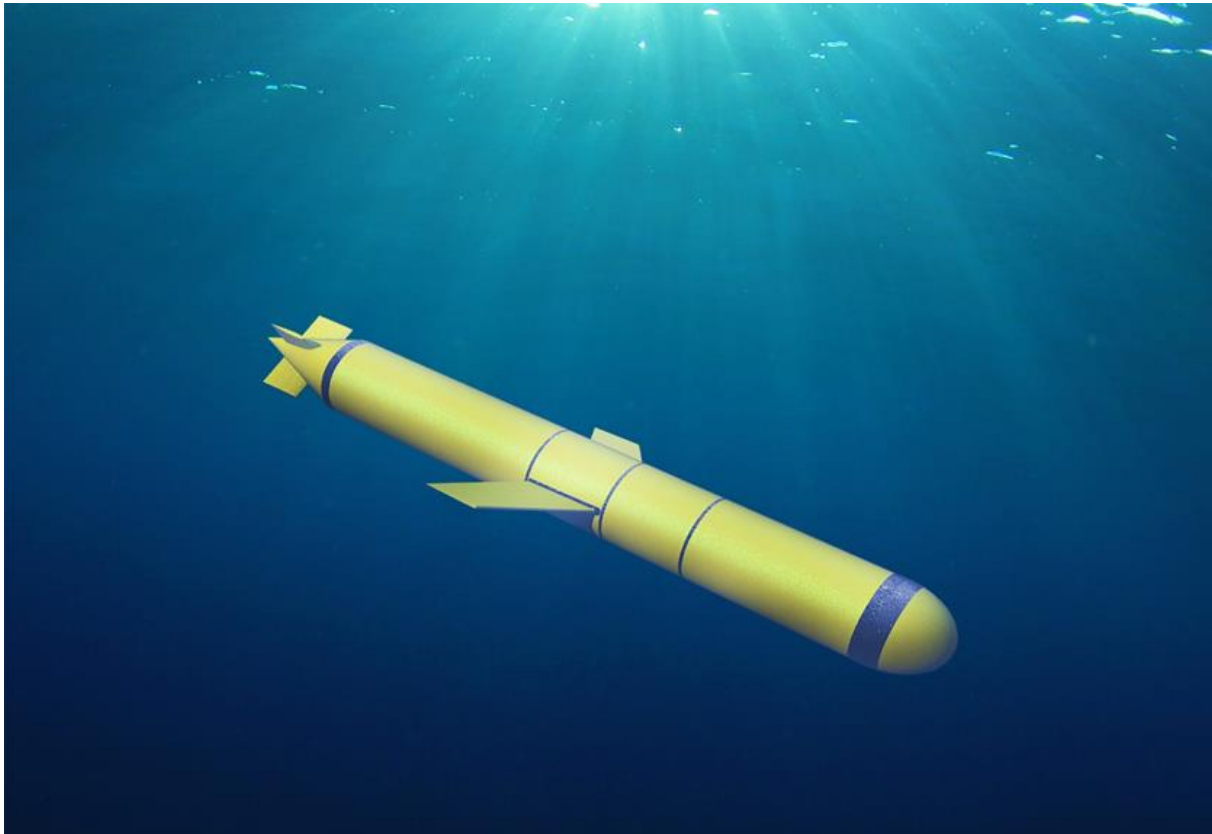
Figure 1 Design of Subsea Freight Glider.

2. Description of a novel Subsea Freight Glider

The baseline design of the Subsea Freight Glider is a 1224-ton underwater vehicle, which is specified with a beam of 5.5 m and a length of 56.5 m and can carry 1194 m^3 of CO_2. The distance that SFG can reach, with 1 m/s (2 knots), is 400 km.

It is possible to create models of different sizes based on the baseline design. In this paper, two more designs were performed:

- half scaled version of baseline SFG,
- doubled scaled version of baseline SFG.

The design methodology is displayed in Figure 2, and it is described as follows. The design starts by establishing the mission requirements (cargo capacity, operation range, operating depth, and environmental data) and detailed specifications of the SFG, such as demotions, speed, depth, or design loads. Then, the external hull design is performed, which

includes determining the stiffeners' dimension and pressure. Next, the internal hull arrangement is conducted, which includes the design of the main cargo, auxiliary cargo, compensation, trim, and buoyancy tanks. All structural calculations are based on DNVGL-RU-NAVAL-Pt4Ch1 [11] and American Society of Mechanical Engineers Boilers and Pressure Vessel Code ASME BPVC VIII-2 [12].

Furthermore, the wing is added, and the complete method of computing a reference area was introduced in the study of Ahmad and Xing [13]. Finally, a stability check is performed. If the vessel is unstable, dimension adjustments are needed. The design loop is iterative to satisfy all criteria. The power consumption is determined when the design is finished. A more detailed description of the design's steps can be found in the study of Ma et al. [14].
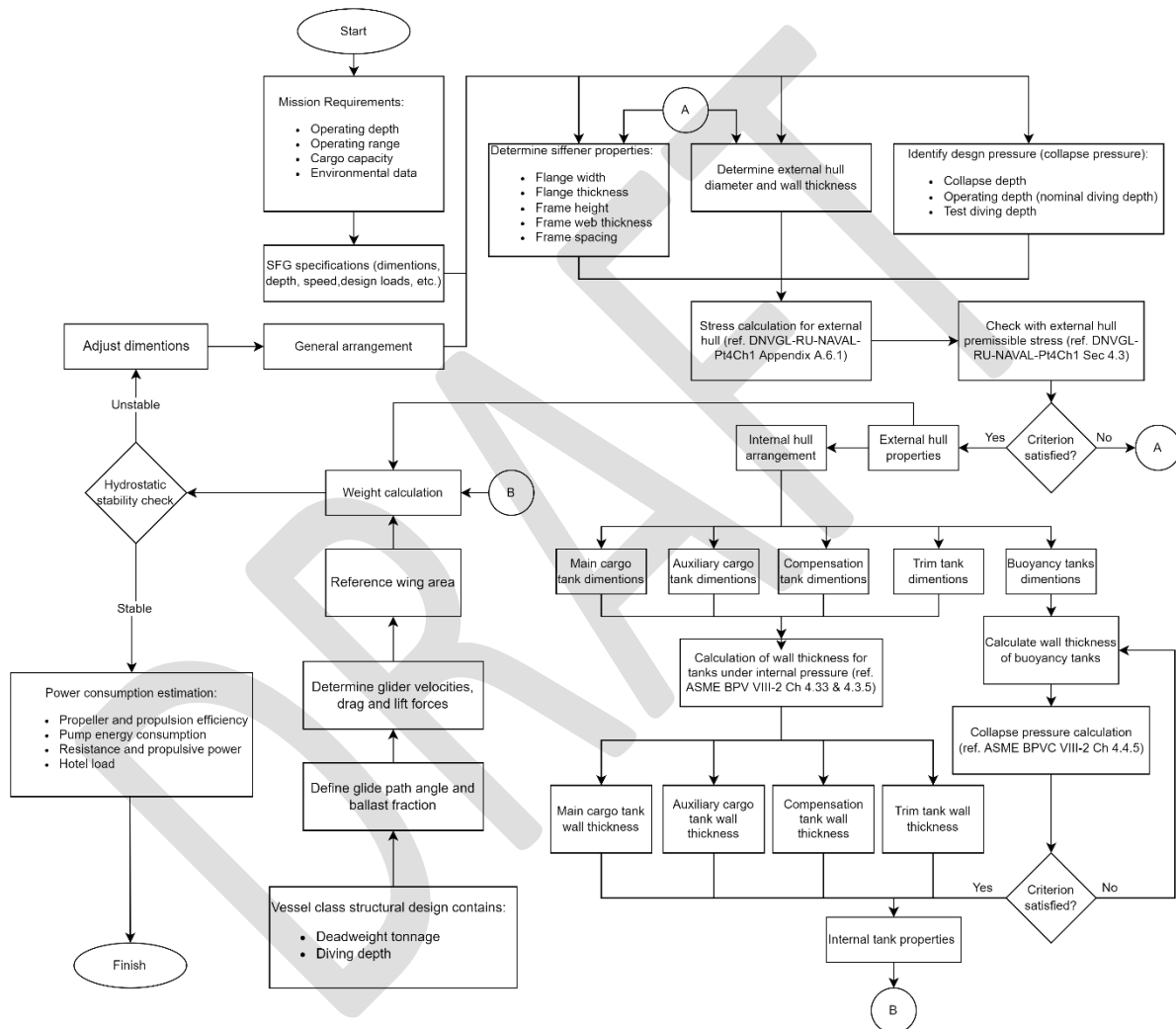
Figure 2 Flow chart of the SFG technical design.

One assumed condition is that the payload should be around 45% of the displacement. To reach this condition, a double-hull design with an active pressure compensating system should be used because it can limit the external pressure loads on the hull structure. Thus, it is not necessary to design the external hull for the depth that it operates.

2.1.   Mission Requirements and Subsea Freight Glider Specifications

The design process starts with establishing the requirement of the mission. Based on these data, it is necessary to determine SFG properties and specification that allows fulfilling the mission. This information gives the basis for the whole design process. Table 1 presents the baseline SFG operating parameters.

Table 1 Operating specifications.

Properties	Value	Units
Operating depth (nominal diving depth)	200	[m]
Collapse depth	400	[m]
Operating speed	2	[knots]
Cargo pressure	35 – 55	[bar]
Current speed	1	[m/s]
Cargo temperature	0 – 20	[ºC]
Maximum range	400	[km]

The SFG baseline has a cargo capacity of 1223 tons, which allows for 510 tons of CO_2 transportation. The half-scale and double SFG can carry approximately half and double payload of the baseline capacity, respectively.

To prevent a collision or any possible impacts from vessels or floating structures, a safety depth is defined as 40 m. Safety depth also reduces the dynamic loads on the SFG from waves, which, therefore, makes the submarine weather independent. Based on the recoverable depth, which refers to the limit of loss of control, the nominal diving depth is introduced. While carrying CO_2, the SFG has a nominal diving depth of 200 m. Collapse depth and test diving depth are defined in DNVGL-RU-NAVAL-Pt4CH1 [11]. According to the standard, the test diving depth is equal to 1.25 times the nominal diving depth, which is 250 m and the collapse depth is 2 times the nominal diving depth, which is 400 m. Depths of the CCS field in which the SFG transfers CO_2 are displayed in Figure 3.
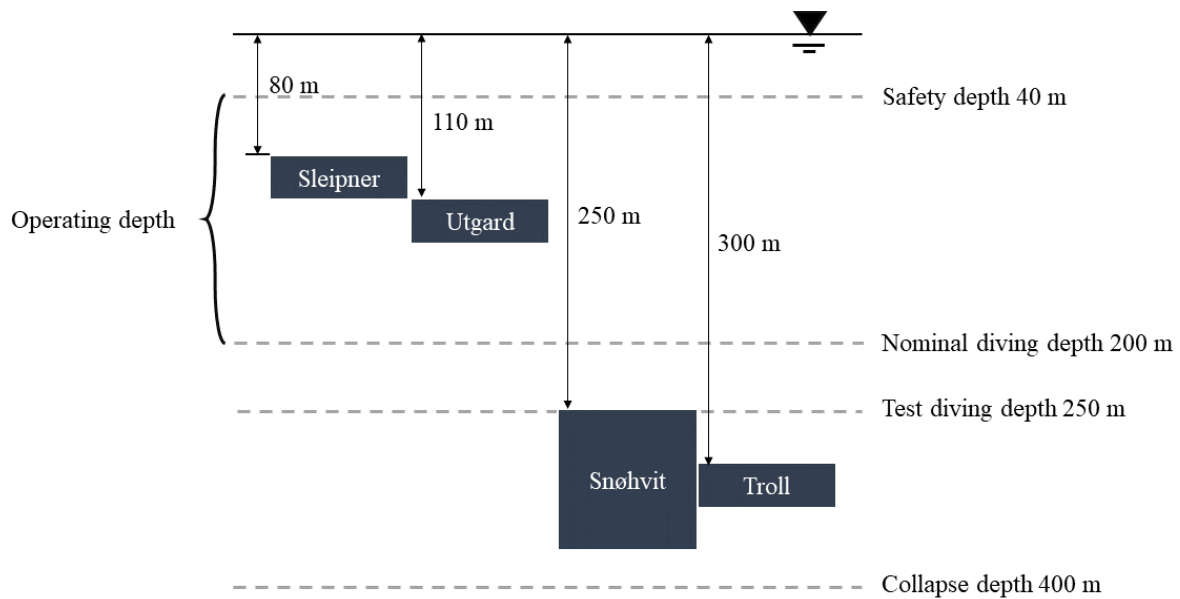
Figure 3 Working depth of Subsea Freight Glider.

The purpose of SFG is to transport CO_2 in the Norwegian Sea. In that region (0-10º E, 60-70º N), the range of temperature in seawater is in the range of 2-12ºC [15]. The SFG is designed to work in temperatures between 0 and 20 degrees Celsius. The design current's velocity is 1 m/s, which characterises the largest average current speed for the North Atlantic and Norwegian coastal areas. Nevertheless, the noted mean current velocity in the Norwegian Sea is about 0.2 m/s [16].

The baseline of SFG has a range of 400 km. This range allows transporting CO_2 back and forth between Snøhvit and Troll fields. Moreover, the SFG can travel one way between Sleipner and Utgard.

2.2. *Layout of SFG*

The general arrangement is shown in Figure 4. It displays both the external hull and the internal hull modules. The external hull of SFG has a torpedo shape to minimise drag resistance. The external hull consists of a hemispherical bow, a conical aft, and a cylindrical mid-body make up. In the baseline design, the mass of the aft and the bow modules is around 25% of the overall weight of the external hull. To avoid the collapse failure under pressure, a double hull structure is adopted for the cylindrically shaped mid-body. By implementing this solution, the external hull of the mid-body is not exposed to any differential loading, i.e., hydrostatic pressure. The cargo and buoyancy tanks are designed to resist collapse and burst pressure. The SFG is also equipped with four bulkheads that support internal cargo and buoyancy tanks and isolate the accessible flooding compartment from the flooded mid-body compartment.
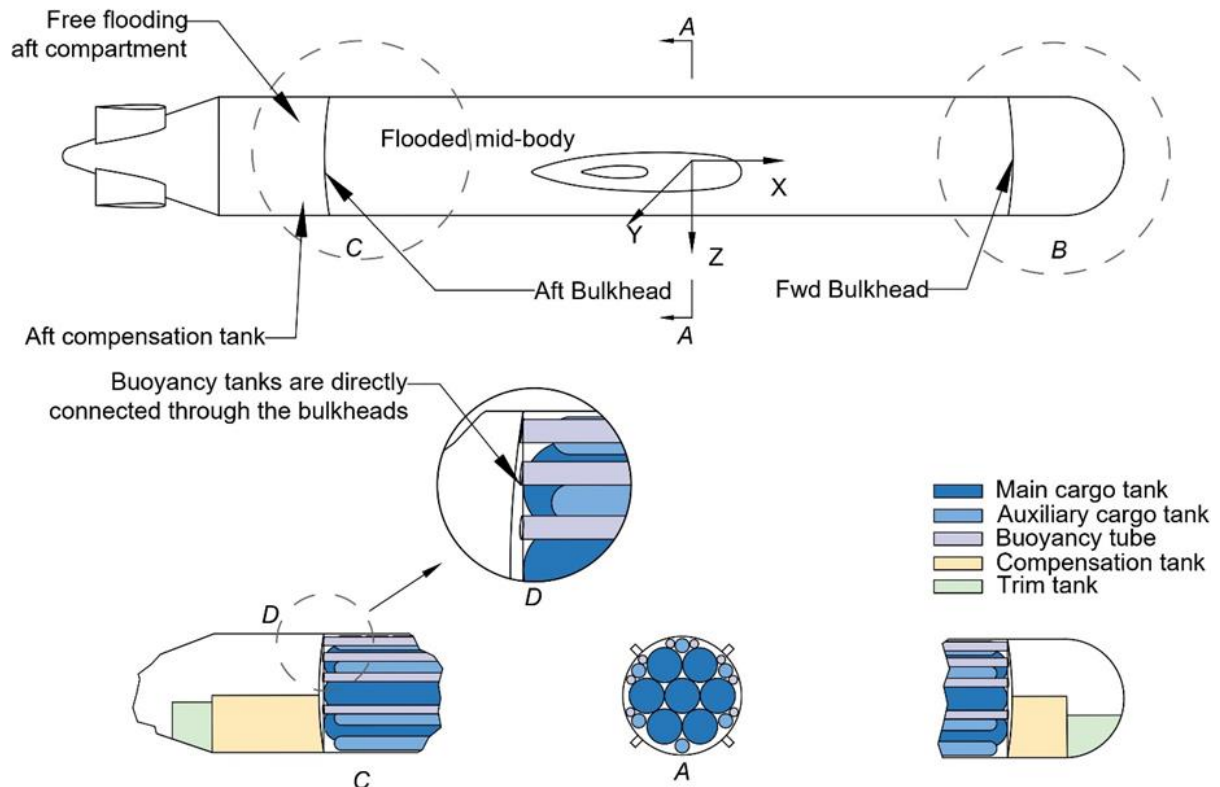
Figure 4 General arrangement of the SFG.

The external hull of SFG consists of free main different sections:

a) **a flooded mid-body compartment is** in the centre of the SFG. It is the largest part of the vessel, and it carries cargo tanks, buoyancy tanks, and piping;
b) **a free flooding bow compartment** which carries the front compensation tank, front trim tanks, radio, control station, sonar, and offloads pumps;
c) **a free flooding aft compartment** which carries sensitive equipment, i.e., battery, gearbox, motor, aft trim, compensation tank, and steering controls.

The internal compartment of SFG contains five different internal pressure modules, main cargo, auxiliary cargo, compensation, trim, and buoyancy tanks.

- **Cargo tank**: seven main and six auxiliary tanks are placed symmetrically in the SFG, as shown in Figure 4. The tanks have a rounded shape with hemispherical heads.
- **Buoyancy tanks**: to make the SFG neutrally buoyant, eight buoyancy tanks are distributed in the upper part of the mid-body to make the SFG neutrally buoyant. All tubes are the same volume, and they are attached to the front and back bulkhead.
- **Compensation tanks**: two compensation tanks give the weight and trimming moment to make the SFG neutral buoyancy under different hydrostatic loads. One of the compensation tanks is placed in the front of the vessel, and another one is in the back, as is presented in Figure 4.
- **Trim tanks**: there are two trim tanks inside the SFG. These tanks make the vessel neutrally trim by placing the centre of gravity below the centre of buoyancy. The trim tank is located in the front and back of the SFG. Both tanks are inaccessible flooding compartments. They do not interact with the open Sea, so they are free from external hydrostatic pressure and have to deal with the internal hydrostatic pressure.

2.3.   Structural design

2.3.1.   Materials

All types of materials for each compartment of the SFG and their mechanical properties are in Table 2. The selection is based on the international standard DNVGL-RU-NAVAL-Pt4CH1 [11].

Table 2 Materials selection SFG.

Properties	Material	Yield Strength	Tensile Strength
Bulkhead	VL D37	360 MPa	276 MPa
External hull – bow compartment	VL D47	460 MPa	550 MPa
External hull – aft compartment	VL D47	460 MPa	550 MPa
External hull – mid-body	VL D47	460 MPa	550 MPa
Internal hull – main cargo tank	SA-738 Grade B	414 MPa	550 MPa
Internal hull – compensation tank	SA-738 Grade B	414 MPa	586 MPa
Internal hull – auxiliary cargo tank	SA-738 Grade B	414 MPa	586 MPa
Internal hull – buoyancy tube	SA-738 Grade B	414 MPa	586 MPa
Internal hull – trim tank	SA-738 Grade B	414 MPa	586a

2.3.2.   External hull

The SFG is a torpedo-shaped vessel with a length-to-diameter ratio (a slenderness ratio) of 10:1. This design was chosen for the production simplicity of the vessel and for adjusting the structure's slenderness to get the largest cargo capacity with lowered drag resistance. The external hull of the SFG is reinforced by stiffeners, which prevents the external hull from having a buckling effect. The dimensions of the stiffener are in Table 3. The stiffeners are designed following the procedures provided in DNVGL-RU-NAVAL-Pt4CH1 [11].

Table 3 Stiffener dimensions.

Component	Symbol	Value	Units
Frame web thickness	s_w	30	[mm]
Frame web height	h_w	165	[mm]
Inner radius to the flange of the frame	R_f	2532	[mm]
Flange width	b_f	80	[mm]
Frame spacing	L_f	1000	[mm]
Flange thickness	s_f	30	[mm]
Frame cross-sectional area	A_f	73500	[mm^2]

The external hull compartments of the SFG are as follow:

- The acceptable stresses in the nominal diving depth are 203 MPa, in the test diving depth are 418 MPa and in the collapse depth are 460 MPa,
- Pressure hulls in the free-floating compartment are subjected to hydrostatic pressure. Stress at the collapse depth, nominal diving depth, and test diving depth for the fooded and free-flooding sections are computed and compared to the permissive stresses required in DNVGL Rules for Classification for Naval Vessels, specifically in Part 4 Sub-surface ship Chapter 1 Submarine (DNVGL-RU-NAVAL-Pt4Ch1) [11].
- The design of the flooded mid-body module uses the same procedure as for the free flooded compartments. Nonetheless, the flooded mid-body does not handle the hydrostatic pressure. Therefore, this section uses 20 bar (200 m) for collapse pressure to avoid mechanical failure in unintentional load cases.

The external hull of SFG is presented in

Table 4. Overall, the SFG mid-body of the external hull is the most massive part of the submarine and accounts for 44% of the total structural weight of the baseline SFG design.

Table 4 SFG Baseline design of the external hull.

Parameter		SFG 469 m³	SFG 1194 m³	SFG 2430 m³	Units
Free-floating bow compartment	Thickness	0.025	0.030	0.036	[m]
	Length	6.625	8.750	11.50	[m]
	Steel weight	21.899	43.877	87.510	[ton]
	Material	VL D47	VL D47	VL D47	
	Design collapse pressure	40	40	40	[bar]
Flooded mid-body	Thickness	0.009	0.013	0,026	[m]
	Length	25.00	33.75	42.00	[m]
	Steel weight	34.049	80.850	222.749	[ton]
	Material	VL D47	VL D47	VL D47	
	Design collapse pressure	20	20	20	[bar]
Free-floating aft compartment	Thickness	0.025	0.030	0.036	[m]
	Length	10.625	14.00	18.00	[m]
	Steel weight	27.412	54.581	105.942	[ton]
	Material	VL D47	VL D47	VL D47	
	Design collapse pressure	40	40	40	[bar]

2.3.3. Internal Hull Design

The design of the internal tanks is based on the ASME BPVC Chapter 4, Section VIII, Division 2 [12]. The internal tank is defined as follows:

- **Cargo tanks** that are used for the storage of CO_2 are subjected to internal and external hydrostatic pressure. The tanks are designed for burst pressure of 55 bar, which is the worst-case scenario if the SFG must emerge from the water. Due to external pressure being 0 bar gauge, the pressure difference equals 55 bar. A PCS (Pressure Compensation System) can be used to avoid failure caused by the collapse pressure. Detailed work on the PCS can be found in the studies of Ma et al. [14] and Xing et al. [17].
- **Buoyancy tubes** are designed to handle 20 bar of hydrostatic pressure. The pressure corresponds to the 200 m of nominal diving depth.
- **Compensation and trip tanks** are located in the free flooding section, and they do not have particular requirements to withstand external pressure. For this reason, they are called soft tanks. Accordingly, they only need to resist the internal pressure caused by the flooding of the mid-section in the SFG. The tanks can have various shapes to use the space as much as possible. However, the cylindrical shape is used for both compensation and trim tanks in the calculation.

The details of the SFG internal tanks design are displayed in Table 5.

Table 5 SFG Internal tank properties.

Parameter		SFG 469 m³	SFG 1194 m³	SFG 2430 m³	Units
Main Cargo Tank (Total No. = 7)	Diameter	1.20	1.62	2.20	[m]
	Length	25.00	33.75	42.00	[m]
	Thickness	0.014	0.018	0.025	[m]
	Hemisphere head wall thickness	0.007	0.009	0.012	[m]
	Steel weight	68.688	168.998		[ton]
	Total volume	190.376	468.395	1073.411	[m²]
	Allowable burst pressure	55.0	55.0	55.0	[bar]
	Material	SA-738 Grade B	SA-738 Grade B	SA-738 Grade B	
Auxiliary Cargo Tank (Total No. = 6)	Diameter	0.45	0.70	0.80	[m]
	Length	24.25	32.83	40.60	[m]
	Thickness	0.005	0.008	0.009	[m]
	Hemisphere head wall thickness	0.003	0.004	0.005	[m]
	Steel weight	8.153	26.670	43.115	[ton]
	Total volume	22,478	73.568	118.894	[m²]
	Allowable burst pressure	55.0	55.0	55.0	[bar]
	Material	SA-738 Grade B	SA-738 Grade B	SA-738 Grade B	

Compensation Tank (Total No. = 2)	Diameter	3.0	3.5	5.5	[m]
	Length	1.7	2.5	5.0	[m]
	Thickness	0.006	0.010	0.014	[m]
	Steel weight	20.224	72.063	96.214	[ton]
	Total volume	17.34	61.25	75	[m^2]
	Allowable burst pressure	8.0	8.0	8.0	[bar]
	Material	SA-738 Grade B	SA-738 Grade B	SA-738 Grade B	
Trim Tank (Total No. = 2)	Diameter	1.6	1.8	3.00	[m]
	Length	2.24	2.50	6.3	[m]
	Thickness	0.006	0.008	0.022	[m]
	Steel weight	12.479	14.702	78.728	[ton]
	Total volume	10.0	45.00	60.0	[m^2]
	Allowable burst pressure	10.0	10.0	10.0	[bar]
	Material	SA-738 Grade B	SA-738 Grade B	SA-738 Grade B	
Buoyancy Tube (Total No. = 8)	Diameter	0.30	0.35	0.40	[m]
	Length	24.1	32.5	40.2	[m]
	Thickness	0.003	0.004	0.005	[m]
	Hemisphere head wall thickness	0.002	0.002	0.002	[m]
	Steel weight	4.816	8.845	14.300	[ton]
	Total volume	13.572	24.910	40.279	[m^2]
	Allowable burst pressure	20.0	20.0	20.0	[bar]
	Material	SA-738 Grade B	SA-738 Grade B	SA-738 Grade B	

2.4. Wing design

The procedure of the design for the wings is illustrated in Figure 5. The nominal operating depth of the SFG defines the vessel class, which provides the foundations for selecting an actual angle of the glide path [18]. It is possible to compute SFG velocities, lift and yield drag forces based on the gliding angle. Next, the reference area of the hydrofoil and lift/drag ratio can be estimated. The parameters of the glider are shown in Figure 6, where *W* is the weight of the SFG; F_b is the buoyancy force [19].
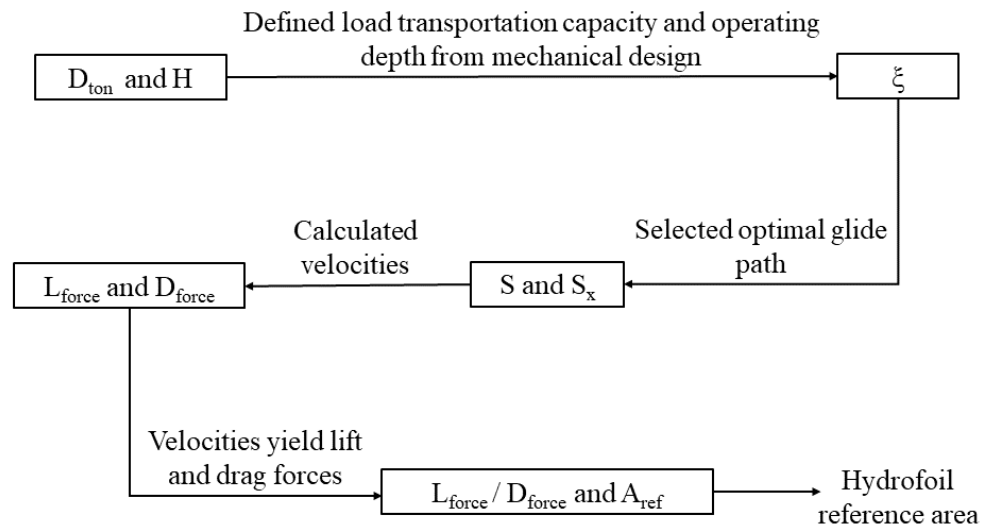
Figure 5 Global parameter of the SFG *(reproduced from Ahmad et al., [13])*.
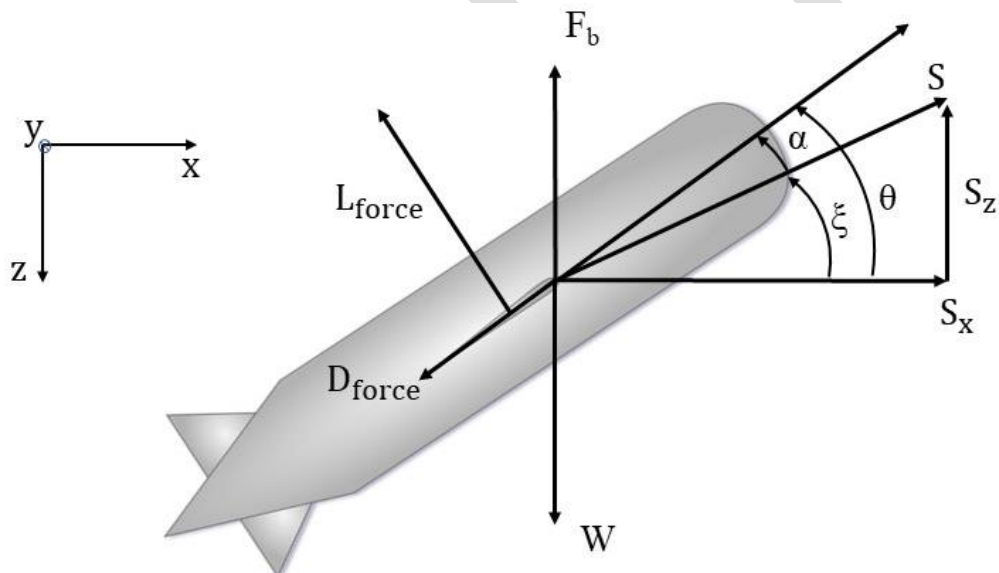
Figure 6 Scheme of SFG parameters.

2.5. *Weight Calculation*

The weight computation of SFG is performed when the structural design is finished. The following requirements are used for SFG:

- The machinery mass is 2% of displacement,
- The permanent ballast is 2% of displacement,
- The aimed payload is 40% of displacement,
- The trim ballast is 0.7% of displacement.

Table 6 presents the weight composition for the SFG design filled with CO_2.

Table 6 Weight compensation for individual SFG design (CO_2-filled condition).

Component	Weight (tons)					
	SFG 469 m³		**SFG 1194 m³**		**SFG 2430 m³**	
Machinery	9.610	2.00%	24.474	2.00%	49.798	2.00%
Permanent ballast	9.610	2.00%	24.274	2.00%	49.798	2.00%
Structure	187.999	39.12%	476.361	38.93%	962.768	38.67%
Mid-body seawater	69.051	14.37%	179.381	14.66%	277.306	11.14%
Compensation ballast	0.804	0.17%	0.999	0.08%	11.994	0.48%
Payload	200.082	41.64%	509.446	41.63%	1120.768	45.01%
Trim tank	3.364	0.70%	8.566	0.70%	17.429	0.70%
Sum	**480.520**	**100%**	**1223,700**	**100%**	**2489.914**	**100%**

2.6. *Hydrostatic Stability*

Once the structural design and weight estimation are completed, the hydrostatic stability is checked based on the requirements as specified in DNVGL-RU-NAVAL-Pt4Ch1 [11]. For the submarine with a displacement of 1000-2000 tons, the distance between the centre of gravity G and the centre of buoyancy B must be greater than 0.32. Moreover, the location of metacentric height GM must exceed 0.20 [20]. Four cases of hydrostatic stability are considered as follows:

a) **Submerged (CO_2 filled)**: seven main tanks and six auxiliary tanks are fully submerged with liquified CO_2. In this case, SFG is fully loaded.
b) **Surfaced (CO_2 filled)**: seven main tanks and six auxiliary tanks are fully submerged with liquified CO_2. In this case, SFG is floating on the surface of the Sea and ready to dive to the nominal operating depth.
c) **Submerged (seawater filled)**: seven main tanks and six auxiliary tanks are fully flooded with seawater. This case occurs after the SFG offloads the CO_2 at a well.
d) **Surfaced (seawater filled)**: five primary and three auxiliary submarine tanks at the bottom side are filled with seawater. This case occurs when the vessel starts or finishes its mission.

Table 7 Stability check of three different designs of SFG.

	SFG 469 m³ (Half-scaled)			
	Submerged (CO₂ filled)	**Submerged (SW filled)**	**Surfaced (CO₂ filled)**	**Surface (SW filled)**
CoG(x,y,z)	[-0.58, 0.00, 0.33]	[-0.52, 0.00, 0.33]	[-0.52, 0.00, 0.33]	[-0.60, 0.00, 0.51]
CoB(x,y,z)	[-0.67, 0.00, 0.00]	[-0.67, 0.00, 0.00]	[-0.67, 0.00, 4.10]	[-0.67, 0.00, 3.50]
M(x,y,z)	[0.00, 0.00, 0.00]	[0.00, 0.00, 0.00]	[0.00, 0.00, 0.00]	[0.00, 0.00, 0.00]
BG	0.330	0.330	3.770	2.990
GM	0.330	0.330	0.330	0.510
Result	BG > 0.32 == OK	BG > 0.32 == OK	GM > 0.2 == OK	GM > 0.2 == OK
	SFG 1194 m³ (Baseline Design)			
	Submerged (CO₂ filled)	**Surfaced (CO₂ filled)**	**Submerged (SW filled)**	**Surfaced (SW filled)**
CoG(x,y,z)	[-0.60, 0.00, 0.35]	[-0,54 0.00, 0.36]	[-0.70, 0.00, 0,37]	[-0.66, 0.00, 0.36]
CoB(x,y,z)	[-0.83, 0.00, 0.00]	[-0.84, 0.00, 0.00]	[-0.84, 0.00, 5.50]	[-0.84, 0.00, 4.20]
M(x,y,z)	[0.00, 0.00, 0.00]	[0.00, 0.00, 0.00]	[0.00, 0.00, 0.00]	[0.00, 0.00, 0.00]
BG	0.347	0.361	5.126	3.844
GM	0.347	0.361	0.374	0.356
Result	BG > 0.32 == OK	BG > 0.32 == OK	GM > 0.2 == OK	GM > 0.2 == OK
	SFG 2430 m³ (Doubled Scaled)			
	Submerged (CO₂ filled)	**Submerged (SW filled)**	**Surfaced (CO₂ filled)**	**Surface (SW filled)**
CoG(x,y,z)	[-0.60, 0.00, 0.37]	[-0.56, 0.00, 0.39]	[-0.56, 0.00, 0.39]	[-0.65, 0.00, 0.39]
CoB(x,y,z)	[-1.00, 0.00, 0,00]	[-1.00, 0.00, 0.00]	[-1.00, 0.00, 5.10]	[-1.00, 0.00, 7.30]
M(x,y,z)	[0.00, 0.00, 0.00]	[0.00, 0.00, 0.00]	[0.00, 0.00, 0.00]	[0.00, 0.00, 0.00]
BG	0.372	0.388	4.712	6.13
GM	0.372	0.388	0.388	0.387
Result	BG > 0.35 == OK	BG > 0.35 == OK	GM >0.22 == OK	GM >0.22 == OK

2.7. *Three SFG Schemes*

In Table 8, the critical parameters of the final design are displayed.

Table 8 Main parameters of final derived SFG design.

Parameter	Value		
	SFG 469 m^3	SFG 1194 m^3	SFG 2430 m^3
Lightweight [ton]	197.609	500.835	962.819
Lightweight [m^3]	192.789	488.619	939.336
Deadweight [ton]	282.911	722.866	1527.094
Deadweight [m^3]	276.011	705,235	1489.848
Length [m]	42.25	56.50	71.50
Beam [m]	4.00	5.50	7.00
Displacement [ton]	480.520	1223.701	2489.914
Displacement [m^3]	468.800	1193.854	2429.184
Total power consumption [kW]	6450	9545	14533
Power consumptions [kWh/day]	1381	2044	3112
Speed [knots]	2.00	2.00	2.00
Travel distance [km]	400.00	400.00	400.00

3. Methodology for the Economic Feasibility Analysis of the Novel SFG concept

The cost of a project for developing a subsea project is generally referred to as the CAPEX – capital expenditures and OPEX – operational expenditures. Capital expenditure is the total investment that is required to put a project into operation. It includes the initial design, engineering, and construction of the facility. The term OPEX refers to the expenses that a facility or component incurs during its operation. These expenses include labour, materials, and utilities. Aside from these, other costs such as testing and maintenance are also included in the OPEX [21].

The economic analysis was performed based on two publicly available cost models from MUNIN [22] and ZEP [23] reports. The MUNIN D9.3 [22] report presents a complete study of autonomous ship development, economic effects, security and safety effects, and relevant areas of law. In this paper, the data from the MUNIN report [22] related to autonomous ships are used for cost analysis of the economic impact assessment. The ZEP report [23] shows the analysis of CO_2 transportation on the deployment of Carbon Capture and Storage (CCS) and Carbon Capture and Utilisation (CCU). Data provided in the ZEP report [23] are given by members of maritime organisations, including stakeholders and essential players in marine transportation, such as Teekay Shipping, Open Grid Europe, and Gassco. The analysis is very detailed and covers all components. For instance, the cost of actual coating is specified and considered for the offshore pipeline. In the present work, the analysis uses cost models from the ZEP report [23] for cost estimation, including OPEX and CAPEX, ship capacities, electricity price, etc., for offshore pipelines.

The outline of the MUNIN D9.3 [22] and ZEP [23] reports is listed in Table 9.

Table 9 Cost models presented in MUNIN D9.3 and ZEP reports.

The cost model shown in MUNIN D9.3	The cost model presented in ZEP
Autonomous ship capital expenditure	Offshore pipelines' capital expenditure
Fuel price	Offshore pipeline operating expenditure
Ship fuel consumption	Electricity price
Discount rate	Discount rate
	Ship capacity
	Vessel loading and offloading durations
	Vessel transport velocity
	Ship capital expenditure
	Ship operating expenditure
	Transport distance cases
	Transport volume cases
	Liquefaction price
	Project lifetime

This paper considers transport distances of 180, 500, 750, and 1500 km with CO_2 shipping capacities of 0.5, 1, and 2.5 million tons per annum (mtpa). The CO_2 is carried from a capture plant at an ambient temperature and pressure of 110 bar. The following assumption of CO_2 transportation are used:

- SFG and ship transport offload straight to the well without the usage of intermediate buffer storage,
- in cases of large CO_2 volume or long distances, there is a need for more than one transportation vessel; for instance, in 180 km transport distance and 1 mtpa transport volume scenario, 6 SFG 2430 m^3 or 11 SFG 1194 m^3 are required,
- the cost of subsea well-head is not considered in the following study,
- the rate of currency exchange is 0.87 EUR/USD,
- the discount rate is 8%, and the project lifetime is 40 years.

3.1. SFG, Crewed and Autonomous Tanker Ship

The ship transporting CO_2 is equipped with semi-refrigerated Liquefied Petroleum Gas (LPG) tanks. The liquefied gas is transported at a temperature of -50ºC. During the transportation, the tanker ship requires refrigeration and liquefied gas, which is transported at 7-9 bar and close to -55ºC to avoid the risk of the formation of dry ice. While transporting, the temperature of CO_2 will increase, initiating a boil-off and rising internal pressure of the ship. Therefore, the pressure of cargo at the end of the loaded journey will typically be around 8-9 bar.

The properties of the tanker ship are displayed in Table 10.

Table 10 Properties of the autonomous and crewed ships.

Crew and Autonomous Tanker Ship Properties		
Liquefaction 2.5 mtpa	5.31	€/ton
Liquefaction 10 mtpa	5.09	€/ton
Loading/offloading time	12.00	hours
Speed	14.00	knots
Fuel consumption, ship 22,000 m^3	9.13	ton/day
Payload	80.00	%

The minimum number of SFG and tanker ships to fulfil the mission requirements is calculated using the following equation.

$$N = \text{roundup}\left(\frac{V_{CO_2}}{V_\vartheta \rho_{CO_2} \dfrac{365}{2L_t U_\vartheta + 2T_L}}\right)$$

where: N is a number of vessels; V_v is the total capacity for a vessel; U_v is the velocity of the vessel; T_L is the time of loading or offloading; ρ_{CO_2} is the CO_2 density; L_t is the distance of the transportation; V_{CO_2} is the total CO_2 capacity per annum.

Calculated parameters to find the number of SFG (baseline design – 1194 m^3) to complete the mission of transporting 2.5 mtpa of CO_2 for a distance of 180 km are displayed in **Error! Reference source not found.**.

Table 11 Required number of vessels SFG (baseline design).

Parameters	Value	Units
Total CO_2 capacity	2.5	[mtpa]
Transport distance	180	[km]
Loading and offloading time	4	[hours]
The velocity of the SFG	2	[knots]
Cargo volume	723	[m^3]
CO_2 density	940	[kg/m^3]
Number of required vessels	27	

The capital expenditure (CAPEX) is calculated based on the price per ton of structural steel weight. According to the ZEP report [23], the maximum and minimum cost for a ton of steel is calculated at 11,631-28,888 € per ton. As presented in Figure 11, it is assumed that a tanker ship has a CAPEX of 110% of the crew tanker ship. The vessels should be modern and equipped with submerged turret offloading buoy capabilities and dynamic positioning.

Table 12 CAPEX inputs for craw and autonomous tanker ship.

Inputs to CAPEX of Crew and Autonomous Tanker Ship		
Steel price (max) in ZEP report	28,888.50	€/ton
Steel price (min) in ZEP report	11,631.45	€/ton
Steel price (average) in the ZEP report	18,896.04	€/ton
Residual value	0	€
Autonomous ship price	110% crew ship price	

The CAPEX values of the SFGs and the tanker ships have been calculated using the following equation.

$$CAPEX = \text{Steel price} \cdot \text{Vessel structure volume}$$

The discount rate is estimated to be 8% and the lifetime to be 40 years. Based on these assumed parameters, the annuity is calculated using the following equation:

$$\text{Annuity} = \frac{CAPEX \times \text{discount rate}}{1 - (1 + \text{discount rate})^{-\text{lifetime}}}$$

The data used to calculate operating expenditure (OPEX) are displayed in Table 13. The tanker ship is powered by marine diesel oil or LNG. For both fuels, the price per ton is the same.

Table 13 OPEX inputs for SFG and crew and autonomous tanker ship.

Inputs to OPEX of Crew and Autonomous Tanker Ship		
Fuel price	573.33	€/ton
Electricity price	0.11	€/kWh
Crew Price	640,180.80	€/year – 20 crews
Maintenance	2	%

The OPEX values of SFGs and tanker ships are calculated using the following equations:

$$OPEX_{CS} = \text{Maintenance} + \text{Crew} + \text{Fuel} + \text{Liquefaction}$$

$$OPEX_{AS} = \text{Maintenance} + \text{Fuel} + \text{Liquefaction}$$

$$OPEX_{SFG/SST} = \text{Maintenace} + \text{Electricity}$$

Based on the data provided in the ZEP report [23], the crew tanker ship's capital expenditure is approximately 60-149 m€. Accordingly, the CAPEX for the autonomous tanker ship is about 66-164 m€.

3.2.   Offshore pipelines

Overall, offshore pipeline costs are controlled by CAPEX, and they are proportional to the pipe's length. In the design of offshore pipelines, the essential factors are pipeline diameter, wall thickness, transport capacity, outlet and inlet pressure, and steel quality. Also, factors like corrosion protection, design against trawling, installation method, dropped object protection, and bottom stability should be considered.

In this study, the manifold cost for the well and the drilling of the injection well are not considered. The capital expenditure is estimated based on the market price of steel, pipeline installation cost, trenching, and pipeline coating. CO_2 is sent through pipelines at 55-88 bar in the supercritical phase. In that case, the pressure boosters and the related costs are required, and they are contained in the calculation of CAPEX. Furthermore, the pressure of CO_2 in the pipeline is determined by the storage conditions. In this analysis, the cost of pre-transport CO_2 compression is included in the price of the capture facility.

In this study, the lowest volume case (1 mtpa of CO_2) for offshore pipelines is not considered. This is because offshore pipelines are too expensive due to their small transportation capacity, and it is not economical to use this method of transferring.

The components' properties and pricing for the offshore pipeline are displayed in Table 14 and Table 15.

Table 14 Properties of offshore pipelines.

Properties of the offshore pipelines		
Pressures	250	[bar]
Outlet pressure	60	[bar]
Inlet pressure	200	[bar]
Pipeline internal friction	50	
External coating	3	[mm]
Pipeline material	Carbon steel	
Concrete coating (pipeline above 16")	70 mm; 2600 kg/m^3	

Table 15 Pricing of offshore pipeline components.

Component Pricing of Offshore Pipelines		
Trenching cost	20-40	€/meter
Installation cost	200-300	€/meter
Pipeline OPEX for 2.5 mtpa	2.35	m€/year
Contingency	20%	
Steel price for pipeline 16"	160	€/meter
Steel price for pipeline 40'	700	€/meter
External coating for pipeline 16"	90	€/meter
External coating for pipeline 40"	200	€/meter

The CAPEX values for an offshore pipeline are shown in the ZEP [23] report. The maximum and minimum values are expected to be 120% and 80%, respectively.

The average OPEX values for an underwater pipeline are shown in the ZEP [23] report. The pipeline's CO2 volume is expected to be around 2.5 million tons per year. The minimum and maximum OPEX values are approximately 80% and 120%, respectively.

The offshore pipeline annuities are calculated based on the design definitions, and related costs are included in Table 14 and Table 15, respectively. A 2.5 transport capacity offshore pipeline will take the cost about 20.986-126.961 m€. All calculated data is displayed in Table *16*. All operational costs and aspects of maintenance are included in the OPEX. The operating expenditures OPEX are 2.35 m€/a.

Table 16 Offshore Pipelines Annuities.

CO_2 Volume	Offshore Pipeline Length			
	180 km	500 km	750 km	1 500 km
0.5 mtpa	-	-	-	-
1 mtpa	-	-	-	-
2.5 mtpa	20.986 m€	48.688 m€	69.412 m€	126.961 m€

4. Results and discussion

The technical and economic feasibility analysis results are discussed in this section. The analysis includes detailed technical-economic studies of modern transportation submarines, the SFG, used for CO_2 transport with comparisons, the crew, autonomous tanker ships, offshore pipelines, and SST.

4.1. Number of vessels

The minimum number of vessels required to perform the mission is illustrated in Figure **7**.

a)

b)

c)

d)
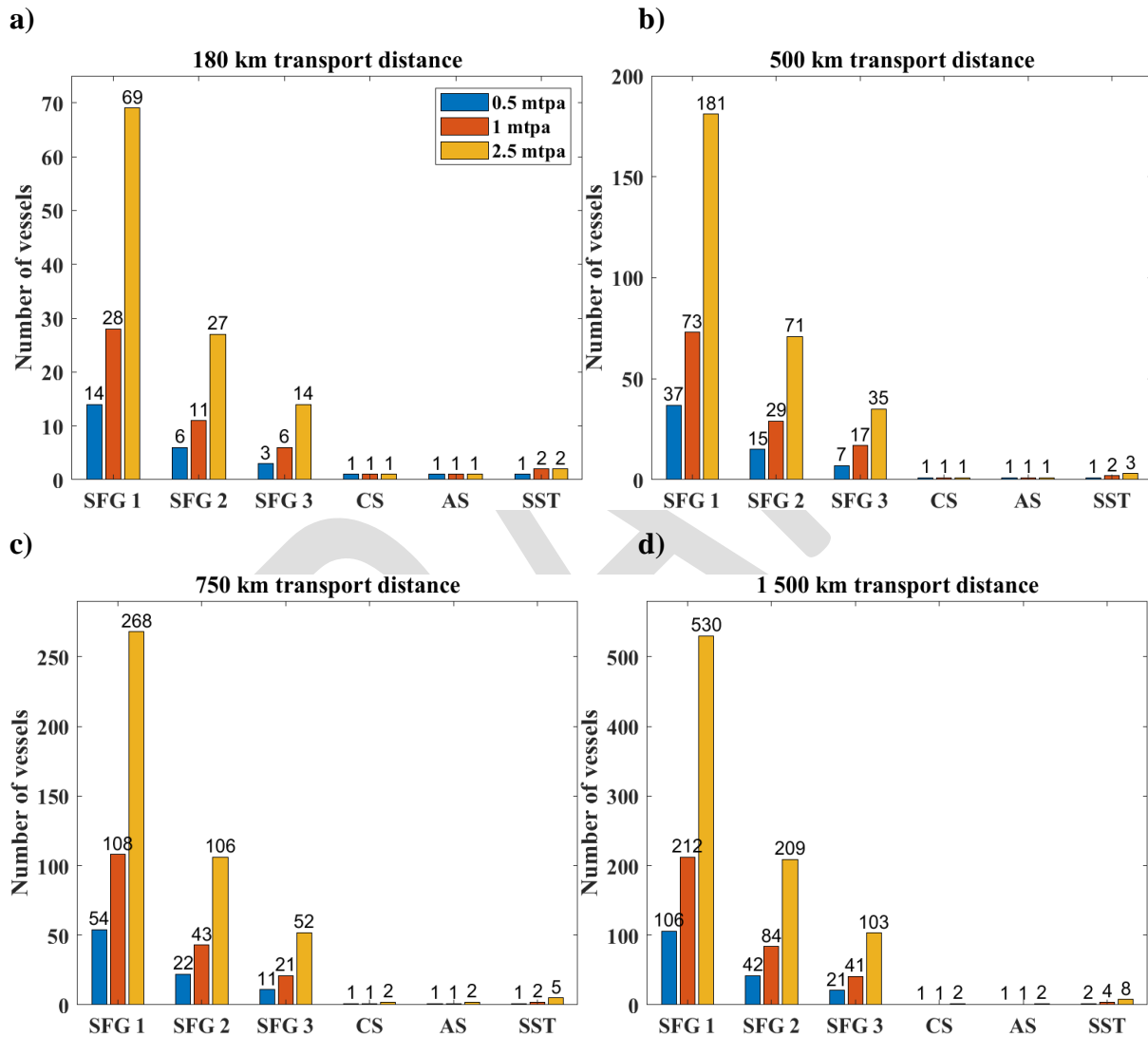
Figure 7 Minimum number of vessels to fulfill mission requirements. a) 180 km; b) 500 km; c) 750 km; d) 1500 km. SFG1: Subsea freight glider (469 m3); SFG2: Subsea freight glider (1194 m3); SFG3: Subsea freight glider (2430 m3); OP: Offshore pipeline; CS: Crew ship (22,000 m3); AS: Autonomous ship (22,000 m3); SST: Subsea shuttle tanker (10,569 m3).

4.2. CAPEX and OPEX results

The CAPEX results for all transportation methods are displayed in **Table** *8*. Overall, it is obviously seen that the SFG CAPEX increases significantly with the size. This implies that the SFG is not an economical solution if large transportation capacities are needed.

The SFG is designed based on DNV-RU-NAVAL-Pt4Ch1 [11], [24], which was initially created for military submarine design. Due to high safety requirements, the SFG has a very heavy structural weight, and that makes the CAPEX value significantly high. For a specific SFG, a potential solution to reduce the weight and CAPEX is to reduce the design safety factors that are suggested in the design code for general SFGs.
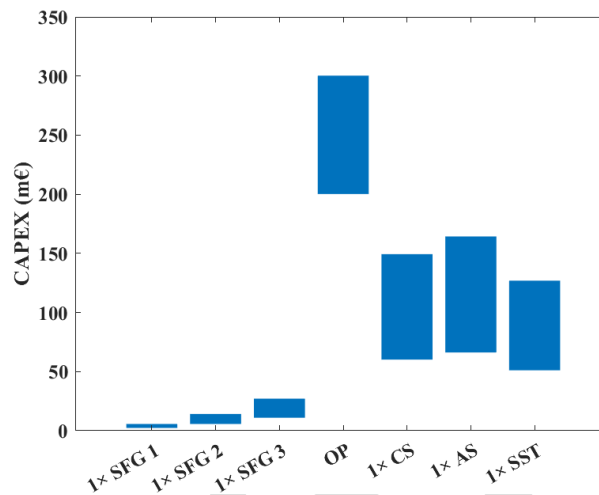
Figure 8 Capital expenditure estimation.

The OPEX/CAPEX ratios are displayed in Figure 9. It can be seen that OPEX dominates among the costs for crew and autonomous tanker ships. For these vessels, CAPEX/OPEX ratio is in the range of 2.59-7.28. On the other hand, the highest CAPEX and the lowest OPEX results are for offshore pipelines, and the OPEX/CAPEX ratio is 0.06-0.38. For the SFGs, the OPEX is comparable with CAPEX, and their CAPEX/OPEX is 1.07-1.39.

Figure 9 CAPEX/OPEX ratios on different transport distances and capacities. a) 180 km; b) 500 km; c) 750 km; d) 1500 km; SFG1: Subsea freight glider (469 m3); SFG2: Subsea freight glider (1194 m3); SFG3: Subsea freight glider (2430 m3); OP: Offshore pipeline; CS: Crew ship (22,000 m3); AS: Autonomous ship (22,000 m3); SST: Subsea shuttle tanker (10,569 m3)

4.3. Economic Analysis

Figure 10 displays the results of the average cost per ton of CO_2. Overall, the subsea shuttle tanker and offshore pipelines have the lowest cost for short distances with large capacities. In contrast, tanker ships (crew and autonomous) have the lowest price for longer distances. The SFG is economical for small CO_2 volumes of 0.5-1 mtpa and short distances, 180-500 km. It is noted that with increasing CO_2 volumes, the cost per ton of CO_2 decreases. This is because of the better economies of scale.

a)

b)

c)

d)
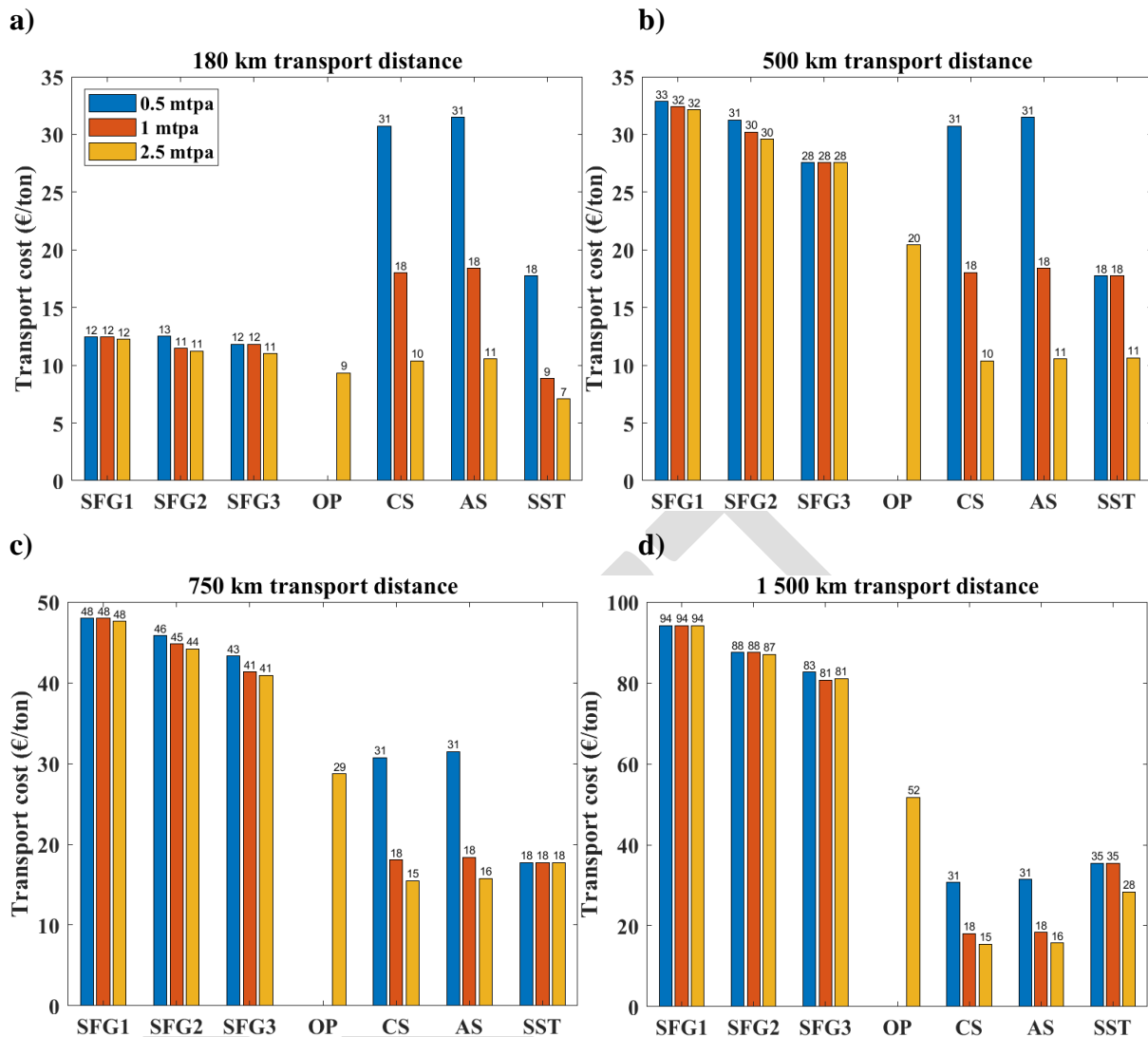
Figure 10 Results of average cost per ton of CO_2. **a)** 180 km; **b)** 500 km; **c)** 750 km; **d)** 1500 km. SFG1: Subsea freight glider (469 m^3); SFG2: Subsea freight glider (1194 m^3); SFG3: Subsea freight glider (2430 m^3); OP: Offshore pipeline; CS: Crew ship (22,000 m^3); AS: Autonomous ship (22,000 m^3); SST: Subsea shuttle tanker (10,569 m^3)
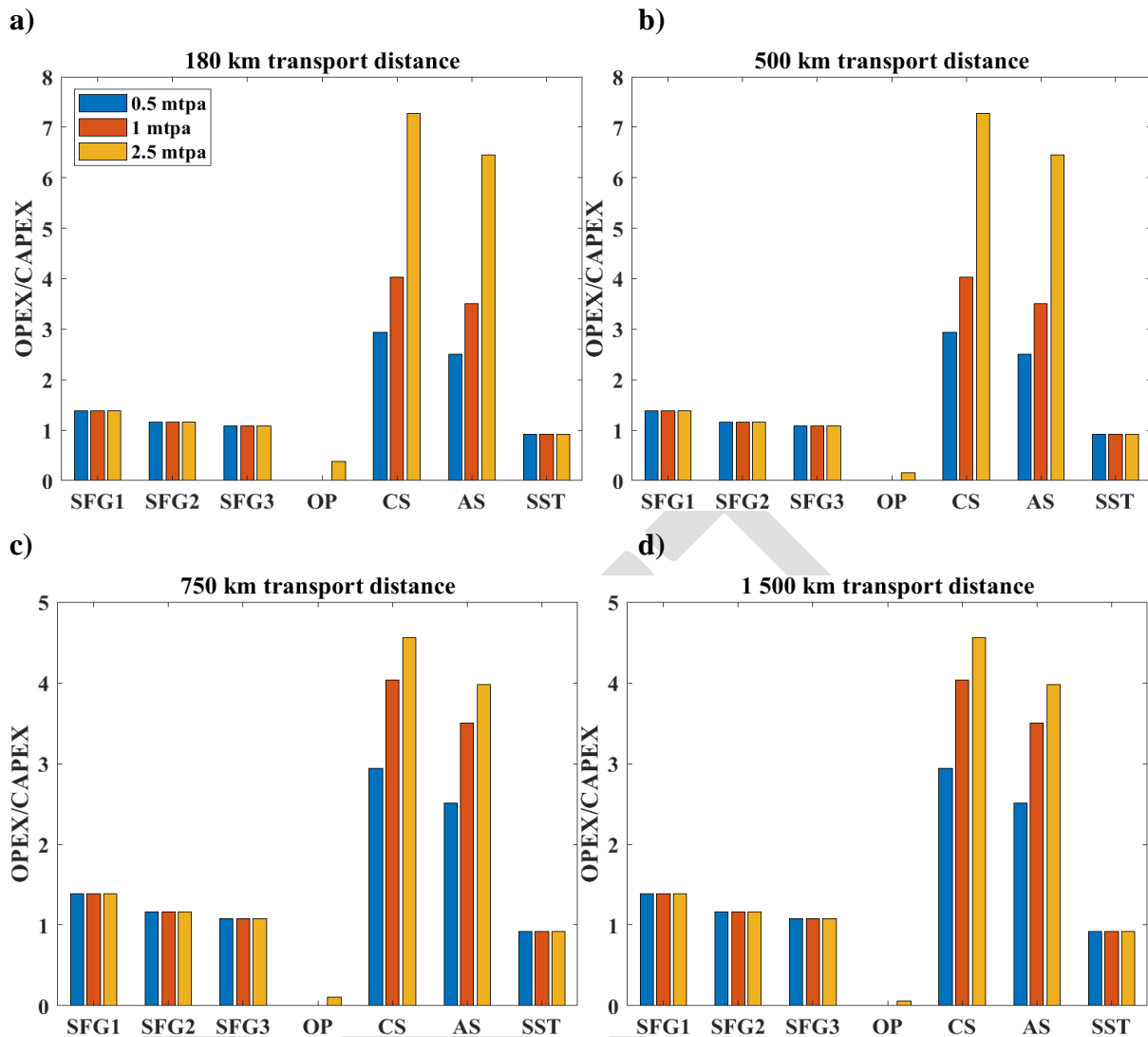
4.3.1. Short distances (<180 km)

For the small CO_2 capacity of 0.5-1 mtpa, the SFGs have the lowest cost. The major reason for the lowest price is the small number of vessels needed to complete the mission. In contrast, the crew tanker ship with the smallest capacity is oversized. As a result, the SFG has lower CAPEX and OPEX than other vessels.

The offshore pipelines are not considered in the 0.5 and 1 mtpa volume cases. Overall, offshore pipelines are not an economical solution for transferring a small volume of CO_2. They become the most profitable for large transport (10-20 mtpa) [25].

4.3.2. Intermediate and Long Distances (500-1500 km)

Due to travelling with low velocity, the SFG requires more vessels to meet the requirement of transporting CO_2 with larger than 1 mtpa capacity. This results in prominently higher capital expenditures and a significantly higher cost per ton of CO_2 than a crew or

autonomous tanker ship. For instance, if the amount of CO_2 is 2.5 mtpa and 1500 km, the SFG needs 103-530 ships. SFG CAPEX is 1827.33-1982.95 million euros, while it is 298.71 million euros for crew ships CAPEX. As a result, the average cost of SFG per ton of CO_2 is 82.93-94.13 million euros, while it is 15.47 million euros for crew ships. Nevertheless, SFG is economical for smaller CO_2 volumes (0.5 and 1 mtpa).

Table 16 presents the economic feasibility analysis results with the lowest costs.

Table 17 Transport methods with the lowest costs for various distances and volumes.

	180 km	**500 km**	**750 km**	**1500 km**
0.5 mtpa	SFG	SFG/SST	SST	CS/AS
1 mtpa	SFG/SST	SST	AS/CS/SST	CS/AS
2.5 mtpa	OP/SST	CS	CS	CS/AS

5. Conclusions and future work

This study deals with the technical-economic feasibility analysis for a novel Subsea Freight Glider, which consists of two steps. The first step lies in investigating the design limits of the SFG, while the second one focuses on performing an economic analysis. The SFG is designed based on the procedure provided in international standards of DNV-RU-NAVAL-Pt4Ch1 and ASME BPVC. The Marine Unmanned Navigation through Intelligence in Network (MUNIN D9.3) and Zero Emission Platform (ZEP) cost models are used for the economic analysis.

Presented research demonstrates that the SFGs with a cargo volume of 469 m3, 1194 m3, and 2430 m3 are able to fulfil the mission requirements. The scenarios considered for this study involve the transport of CO2 volumes of 0.5, 1.0 and 2.5 million tons per year with a distance of 180, 500, 750 and 1500 kilometres. The cost per ton of CO2 by SFGs is compared with the cost of transporting it on a tanker ship or offshore pipelines. The study indicates that the SFG is technically feasible for short distances of up to 500 kilometres and smaller CO_2 volumes of less than 1 million tons per year. The SFG is also a cheaper solution than crew and autonomous tanker ships due to its lower OPEX and CAPEX. Also, because of its slow-moving speed and the advantage of no liquefaction cost, the SFG can transport CO_2 in a saturated state, which significantly reduces the total price.

The performed technical-economic analysis of SFG shows that the small underwater vehicle is technically feasible and economically profitable to complete the mission. However, there is still work that can be done in the future. In this study, the design by rules method is applied. There is still a need to perform design by analysis with elastic stress and plastic analysis. In addition, This analysis includes only small size submarines. It is essential to carry out the economic study for the SFG with a drastically increased size.

Appendix A

External hull design calculation for baseline design SFG (1194 m³)

SFG's external hull design has been performed based on the computation method in DNV-RU-NAVAL-Pt4Ch1 [11], appendix A, section 6. Data used in calculations are shown in Table 18. All used symbols and numbers correspond to the guideline provided in the DNV standard. Stress values in the flooded mid-body external hull and free flooding compartments are presented in Table 22. The external hull in the free flooding compartment is subjected to hydrostatic pressures and examined against allowable stresses at the test diving depth, nominal

diving depth, and collapse depth. The stresses are checked with DNV-RU-NAVAL-Pt4Ch1 [11], chapter 4. The allowable values are given in Table 23.

Table 18 Calculation for the external hull of SFG baseline design.

Parameter	Symbol	Free Flooding Compartment			Flooded compartment	Units	Equation No. in DNVGL RU P4C1 Appendix A
Design Pressure Type		Nominal Diving Depth	Test Diving Depth	Collapse Depth	Collapse		
Design pressure	p	20	25	40	20	[bar]	User input
Hull thickness	s	0.03	0.03	0.03	0.013	[m]	User input
Hull radius	R_m	2.75	2.75	2.75	2.75	[m]	User input
Frame web height	h_w	0.165	0.165	0.165	0.165	[m]	User input
Frame web thickness	s_w	0.003	0.003	0.003	0.003	[m]	User input
Flange width	b_f	0.08	0.08	0.08	0.08	[m]	User input
Flange thickness	s_f	0.03	0.03	0.03	0.03	[m]	User input
Frame spacing	L_f	1.0	1.0	1.0	1.5	[m]	User input
Frame cross-sectional area	A_f	0.0074	0.0074	0.0074	0.0074	[m^2]	User input
Inner radius to the flange of the frame	R_f	2.53	2.53	2.53	2.53	[m]	User input
Youngs modulus	E	206	206	206	206	[GPa]	User input
Poisson Ratio	v	0.3	0.3	0.3	0.3	-	User input
Poisson ratio in elastic-plastic range	v_p	0.44	0.44	0.44	0.44	-	(A48)
Frame distance without thickness	L	0.97	0.97	0.97	0.97	[m]	(A9)
Effective length	L_{eff}	0.447	0.447	0.447	0.294	[m]	(A10)
Effective area	A_{eff}	0.0076	0.0076	0.0076	0.0077	[m^2]	(A11)
The radial displacement in the middle between the frames	w_M	-0.002	-0.0025	-0.0042	-0.0047	[m]	(A15)
The radial displacement at the frames	w_F	-0.0021	-0.0027	-0.0041	-0.0032	[m]	(A16)
The reference stress is the circumferential stress in the unstiffened cylindrical pressure hull	σ_0	183	229	367	423	[MPa]	(A13)
The equivalent stresses are composed of the single stresses in longitudinal and circumferential direction at the middle between frames	$\sigma^m_{v,m}$	156	196	318	360	[MPa]	(A14)
The equivalent stresses are composed of the single stresses in longitudinal and circumferential direction at the frames	$\sigma^m_{v,f}$	164	203	317	268	[MPa]	(A14)
Average membrane stress in longitudinal direction	σ^m_x	91	115	183	212	[MPa]	(A17)
Membrane stress in circumferential the direction in the middle between the frames	$\sigma^m_{\varphi, M}$	181	227	367	416	[MPa]	(A18)
Membrane stress in circumferential direction at the frames	$\sigma^m_{\varphi,F}$	189	235	366	301	[MPa]	(A19)
Bending stresses in longitudinal direction in the middle between the frames	$\sigma^x_{\varphi,M}$	52	67	117	27	[MPa]	(A20)

Bending stresses in longitudinal direction at the frames	$\sigma^b_{x,F}$	11	11	16	221	[MPa]	(A21)
Bending stresses in circumferential the direction in the middle between the frames	$\sigma^b_{\varphi,M}$	16	20	32	8	[MPa]	(A22)
Bending stresses in circumferential direction at the frames	$\sigma^b_{\varphi,M}$	3	3	5	66	[MPa]	(A23)
Tangential module	E_t	206	206	206	206	[MPa]	(A38)
Secant module	E_s	204	204	204	204	[GPa]	(A39)
Elastic buckling pressure	p^{el}_{cr}	82	82	82	62	[GPa]	(A28)
Theoretical elastic-plastic buckling pressure	p^i_{cr}	93	93	93	70	[bar]	(A29)
Reduction factor	R	0.75	0.75	0.75	0.75	[bar]	(A43)
Elastic-plastic buckling pressure	p'_{cr}	60	60	60	56	[bar]	(A45)

Table 19 Stresses at nominal diving depth for SFG baseline design in the free flooding compartment.

	At the Frame			In the middle of the Field		
Type of Stresses	Circum-feretial	Equivalent	Axial	Circum-ferential	Equivalent	Axial
Membrane stress	189 MPa	-	92 MPa	181 MPa	-	92 MPa
Membrane equivalent stress	-	156 MPa	-	-	164 MPa	-
Bending stress	3 MPa	-	11 MPa	16 MPa	-	52 MPa
Normal stress outside	192 MPa	-	102 MPa	196 MPa	-	144 MPa
Equivalent normal stress outside	-	166 MPa	-	-	176 MPa	-
Normal stress inside	192 MPa	-	102 MPa	196 MPa	-	144 MPa
Equivalent normal stress inside	-	166 MPa	-	-	176 MPa	-

Table 20 Stresses at test diving depth for SFG baseline design in the free flooding compartment.

	At the Frame			In the Middle of the Field		
Type of Stresses	Circum-feretial	Equivalent	Axial	Circum-fernetial	Equivalent	Axial
Membrane stress	235 MPa	-	115 MPa	227 MPa	-	115 MPa
Membrane equivalent stress	-	196 MPa	-	-	203 MPa	-
Bending stress	3 MPa	-	11 MPa	20 MPa	-	67 MPa
Normal stress outside	238 MPa	-	126 MPa	247 MPa	-	182 MPa
Equivalent normal stress outside	-	206 MPa	-	-	221 MPa	-
Normal stress inside	238 MPa	-	126 MPa	247 MPa	-	182 MPa
Equivalent normal stress inside	-	206 MPa	-	-	221 MPa	-

Table 21 Stresses at collapse diving depth for SFG baseline design in the free flooding compartment.

Type of Stresses	At the Frame			In the middle of the Field		
	Circum-feretial	Equivalent	Axial	Circum-fernetial	Equivalent	Axial
Membrane stress	366 MPa	-	183 MPa	367 MPa	-	183 MPa
Membrane equivalent stress	-	318 MPa	-	-	317 MPa	-
Bending stress	1 MPa	-	2 MPa	35 MPa	-	117 MPa
Normal stress outside	366 MPa	-	185 MPa	402 MPa	-	301 MPa
Equivalent normal stress outside	-	317 MPa	-	-	362 MPa	-
Normal stress inside	366 MPa	-	185 MPa	402 MPa	-	301 MPa
Equivalent normal stress inside	-	317 MPa	-	-	362 MPa	-

Table 22 Stresses at collapse diving depth for SFG baseline design in the flooded compartment.

Type of Stresses	At the Frame			In the middle of the Field		
	Circum-fernetial	Equivalent	Axial	Circum-fernetial	Equivalent	Axial
Membrane stress	301 MPa	-	212 MPa	416 MPa	-	212 MPa
Membrane equivalent stress	-	360 MPa	-	-	268 MPa	-
Bending stress	66 MPa	-	221 MPa	8 MPa	-	27 MPa
Normal stress outside	368 MPa	-	433 MPa	424 MPa	-	238 MPa
Equivalent normal stress outside	-	404 MPa	-	-	368 MPa	-
Normal stress inside	368 MPa	-	433 MPa	424 MPa	-	238 MPa
Equivalent normal stress inside	-	404 MPa	-	-	368 MPa	-

Table 23 Permissible and equivalent stresses in the external hull of SFG baseline design.

Case	Depth	Maximum Equivalent Stress	Permissible Stress (Ref. Sec. 4.3 in DNVGL RU P4C1)	Criterion fulfilled?
Nominal diving depth	200 m	196 MPa	203 MPa	Yes
Test diving depth	250 m	247 MPa	418 MPa	Yes
Collapse depth	400 m	402 MPa	460 MPa	Yes
Flooded Compartment	-	432 MPa	460 MPa	Yes

Internal tanks design calculation for baseline design SFG (1194 m^3)

The internal tanks' design of SFG has been calculated based on Chapter 4 of ASME BPVC Section VIII, Division 2 [12]. The main, auxiliary, trim, and compensation tanks are designed to resist burst pressure. The buoyancy tanks are designed to handle the collapse pressure.

All internal tanks except buoyancy tanks are designed to take burst pressure. The wall thickness of the hemispherical heads and cylindrical shells are determined in Chapter 4.3.3 and Chapter 4.3.5 in ASME VIII-2 [12]. The minimum thickness that a tank has to have to resist internal pressure is described by the following formula:

$$t_{shell} = \frac{D_t}{2}\left(\exp\left[\frac{p_i}{S_a \cdot E_w}\right] - 1\right)$$

Correspondingly, the minimum thickness that a hemisphere head has to have to resist internal pressure is described by the following formula:

$$t_{shell} = \frac{D_t}{2}\left(\exp\left[\frac{0.5 \cdot p_i}{S_a \cdot E_w}\right] - 1\right)$$

Where: t_{shell} is wall thickness; D_t is the diameter of the tank; p_i is a design pressure (it is assumed to be 55 bar for main, auxiliary, compensation, and trim tanks); S_a is the permissible material stress; E_w is an efficiency of the weld joint (it is assumed to be 1.0 for longitudinal and circumferential joints).

The buoyancy tubes are designed to handle the collapse pressure. The design description was found in ASME VIII-2 chapter 4.4.5. The properties of the buoyancy tanks are presented in Table 24.

Table 24 Calculation for the buoyancy tube of SFG baseline design.

Parameter	Symbol in ASME BPVC Sec. VIII Div. 2	Value	Equation Number in ASME BPVC Sec. VIII Div 2.
Outer diameter	D_0	0.346	User input
Thickness	t	0.004	User input
Unsupported length	L	1 m	User input
Minimum yield strength	S_y	414 MPa	User input
Young's modulus	E_y	200 GPa	User input
Design factor	FS	2	(4.4.1)
Predicted elastic bucking factor	F_{he}	71 MPa	(4.4.19)
Factor	M_x	45	(4.4.20)
Factor	C_h	0.01	(4.4.22)
Predicted buckling stress	F_{ic}	71 MPa	(4.4.27)
Allowable external pressure	P_a	8 bar	(4.4.28)

Computation of the reference area of the wing

The reference area of hydrofoils is 8 m^3. It was derived based on Graver's [26] and Ahmad et al. [13] studies. The following parameters are used in the computation of the area of the wing.

- **H** is nominal operating depth, and it is set to be 200 m.
- **BF** is ballast fraction, which is estimated to be 0.15%
- **D$_{ton}$** is the weight of the cargo.
- ξ is the gliding angle, which is 30º

The area of the hydrofoil is calculated using the following equations.

$$BF = \frac{m_o}{D_{ton} \cdot 1000}$$

where: m_o is the mass of the SFG;

$$S = \sqrt[2]{\left(\frac{m_o \cdot g \cdot \sin\xi}{\frac{1}{2} \cdot \rho_w \cdot C_{DVol} \cdot Vol^{\frac{2}{3}}}\right)}$$

Where: S is the glider velocity; ρ_w is the water density; g is the gravitational constant.

$$S_x = S \cdot \cos\xi$$

$$D_{force} = \frac{1}{2} \cdot S^2 \cdot \rho_w \cdot C_{DVol} \cdot V^{\frac{2}{3}}$$

where: C_{DVol} is the SFG volumetric drag coefficient; C_L is the SFG volumetric lift coefficient; V is the total SFG volume.

$$L_{force} = \frac{D_{force}}{\tan\xi}$$

where: L_{force} is the lift force and D_{force} is the drag force.

$$A_{reference} = \frac{L}{\frac{1}{2} \cdot S^2 \cdot \rho_w \cdot C_L}$$

Power Consumption Estimation

The total power consumption of a subsea freight glider that travels with a velocity of 2 knots and a range of 400 km with capacities of 469 m³, 1194 m³, and 2320 m³ is 6450 kW, 2044 kW, and 3112 kW, respectively. Based on the SFG resistance power in the direction of the water current, hotel load, pump energy, and consumption, the power consumption is estimated. Every factor is modified based on the requirements of the design. In Figure 11, the power consumption curves are displayed.
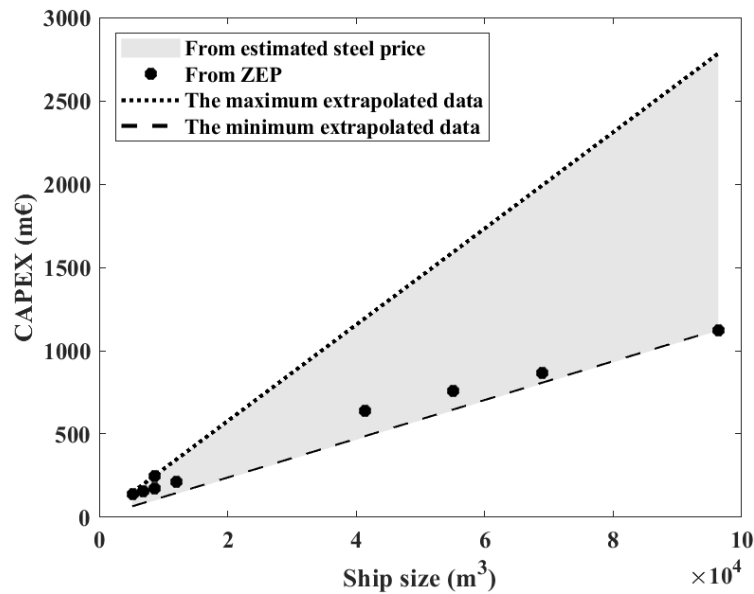
Figure 11 CAPEX of crew ship in comparison with ZEP report results

- The drag load is estimated analytically from Hoerner's scheme [27]. The resistance power on the skin friction is from the correlation line established at International Towing Tank Conference [28].
- The hotel load consumption is calculated based on the existing tanker ship, Wartsila [29], with about a 40% reduction since the SFG is autonomous and can be operated without a crew [30].
- The power of the pump is approximated based on the flow of the pump duration to load and unload the freight. It takes 4 hours to load and reload the cargo owing to the fact that the pumps give 3 bars of differential pressure. Every SFG design has different volumetric flow rates to guarantee the same loading and offloading intervals. The efficiency of the pumps is assumed to be not lower than 75% [31].

As a source of energy, the Li-ion battery is chosen for SFG. The batteries are dedicated to the baseline and half-scaled design of SFG weight 20 tons and using 10,000 kWh, while the 40-ton batteries with 20,000 kWh are used for double-scaled design.

Appendix B

The procedure and computations for the economic study for 180 km and 2,5 mtpu cases are presented in appendix B. It is the only CO_2 capacity scenario used by an offshore pipeline. The following abbreviations are used: SFG1: Subsea freight glider (469 m^3); SFG2: Subsea freight glider (1194 m^3); SFG3: Subsea freight glider (2430 m^3); OP: Offshore pipeline; CS: Crew ship (22,000 m^3); AS: Autonomous ship (22,000 m^3); SST: Subsea shuttle tanker (10,569 m^3).

Offshore pipelines – CAPEX

The CAPEX values for the offshore pipeline are listed in the ZEP report [23], annexe 3. The maximum and minimum CAPEX values are assumed to be 120% and 80% of the average values.

Table 25 Results for CAPEX calculations for average values; Scenario: 2.5 mtpa and 180 km.

	SFG	OP	CS	AS	Units
Autonomous ship factor	-	-	-	110%	-
Price per ton of vessel steel	18,896	18,896	18,896	18,896	[€/ton]
Structural volume	489	-	5170	5170	[ton]
CAPEX	255.61	250.25	97.69	107.46	[m€]
Annuity	21.44	20.99	8.19	9.01	[m€]

Offshore pipelines – OPEX

The OPEX values for the underwater pipeline are provided in the ZEP report [23]. The average OPEX for CO_2 volume of 2.5 mtpa and distance of 180 km is 2.35 m€. The maximum and minimum OPEX values are assumed to be 120% and 80% of the average value.

The OPEX computation for the average values for the baseline design of SFG, crew ship, autonomous ship, and offshore pipelines are displayed in Table 26.

Table 26 OPEX average value results.

	SFG	OP	CS	AS	Units
CAPEX	255.61	250.25	97.69	107.46	[m€]
Fuel price	-	-	573.33	573.33	[€/ton]
Fuel consumption	-	-	9.13	9.13	[ton/day]
Fuel cost	-	-	1.91	1.91	[m€/year]
Electricity price	-	-	-	0.11	[€/kWh]
Electricity consumption	-	-	-	2044	[kWh/day]
Electricity cost	-	-	-	0.24	[m€/year]
Liquification cost for 2.5 mtpa	-	-	13.28	13.28	[m€/year]
Crew cost	-	0.64	-	-	[m€/year]
Vessel maintenance cost	-	-	1.95	2.15	[m€/year]
Vessel maintenance	-	2%	2%	2%	
OPEX	7.33	2.35	17.78	17.33	[m€/year]

Cost of CO_2 per ton

The following equation was used to calculate the cost of CO_2 per ton:

$$CO_2 \, cost = \frac{Annuity + OPEX}{Total \, CO_2 \, per \, annual}$$

The example of CO_2 per ton calculations for the case of 2.5 mtpa and 180 km is displayed in Table 27.

Table 27 Competition of costs of the CO_2 ton for different vessels (180 km and 2.5 mtpa case).

	SFG	OP	CS	AS
OPEX	7.33 m€	2.35 m€	17.78 m€	17.33 m€
Annuity	21.44 m€	20.99 m€	8.19 m€	9.01 m€
Total CO_2 per annum	2.5	2.5	2.5	2.5
Cost of CO_2 per ton	11.51 m€	9.33 m€	10.39 m€	10.54 m€

Reference

[1] R. S. Middleton and J. M. Bielicki, "A comprehensive carbon capture and storage infrastructure model," *Energy Procedia*, vol. 1, no. 1, pp. 1611–1616, Feb. 2009, doi: 10.1016/J.EGYPRO.2009.01.211.

[2] Global CCS Institute, "The global status of CCS 2015: summary report," 2015.

[3] Trading Economics, "Steel - 2022 Data - 2016-2021 Historical - 2023 Forecast ," 2022. https://tradingeconomics.com/commodity/steel (accessed May 28, 2022).

[4] S. A. Rackley, *Carbon dioxide transportation*. Butterworth-Heinemann, 2017. doi: 10.1016/B978-0-12-812041-5.00023-4.

[5] Equinor ASA, "Equinor aims to cut emissions in Norway towards near zero in 2050," Jan. 07, 2020. https://www.equinor.com/news/archive/2020-01-06-climate-ambitions-norway (accessed May 28, 2022).

[6] Equinor ASA, "Subsea Shuttle: the world's first drone to transport CO2," 2020. https://www.equinor.com/en/magazine/here-are-six-of-the-coolest-offshore-robots.html (accessed May 07, 2022).

[7] Y. Xing, M. C. Ong, T. Hemmingsen, K. E. Ellingsen, and L. Reinås, "Design considerations of a subsea shuttle tanker system for liquid carbon dioxide transportation," *Journal of Offshore Mechanics and Arctic Engineering*, vol. 143, no. 4, Aug. 2021, doi: 10.1115/1.4048926/1089683.

[8] T. A. D. Santoso, "Technical- and Economic-Feasibility Analysis of Subsea Shuttle Tanker," University of Stavanger, Stavanger, 2021.

[9] Y. Xing, "A Conceptual Large Autonomous Subsea Freight-Glider for Liquid CO2 Transportation," in *Proceedings of the International Conference on Offshore Mechanics and Arctic Engineering - OMAE*, Oct. 2021, vol. 6. doi: 10.1115/OMAE2021-61924.

[10]   U. N. Ahmad and Y. Xing, "A 2D model for the study of equilibrium glide paths of UiS Subsea Freight-Glider," *IOP Conference Series: Materials Science and Engineering*, vol. 1201, no. 1, p. 012022, Nov. 2021, doi: 10.1088/1757-899X/1201/1/012022.

[11]   DNV GL AS, "Rules for Classification: Naval vessels Part 4 Sub-surface ships Chapter 1 Submarines," 2018. Accessed: May 28, 2022. [Online]. Available: http://www.dnvgl.com,

[12]   The American Society of Mechanical Engineers ASME, "ASME Boiler and Pressure Vessel Code An International Code R ules for Construction of Power Boilers SECTION I," 2017.

[13]   U. Ahmad, Y. Xing, and Y. Ma, "UiS Subsea-Freight Glider: A Buoyancy-Driven Autonomous Glider," 2022.

[14]   Y. Ma, Y. Xing, M. C. Ong, and T. H. Hemmingsen, "Baseline design of a subsea shuttle tanker system for liquid carbon dioxide transportation," *Ocean Engineering*, vol. 240, Nov. 2021, doi: 10.1016/J.OCEANENG.2021.109891.

[15]   National Centers for Environmental Information (NCEI), "Greenland, Iceland and Norwegian Seas Regional Climatology." https://www.ncei.noaa.gov/products/greenland-iceland-and-norwegian-seas-regional-climatology (accessed May 17, 2022).

[16]   G. Ersdal, "An overview of ocean currents with emphasis on currents on the Norwegian continental shelf ," 2001. Accessed: May 28, 2022. [Online]. Available: https://www.semanticscholar.org/paper/An-overview-of-ocean-currents-with-emphasis-on-on-Ersdal/e90fcf6fcade300b540190ab57071f8961b125c9

[17]   Y. Xing, T. A. D. Santoso, and Y. Ma, "Technical-Economic Feasibility Analysis of Subsea Shuttle Tanker," *Journal of Marine Science and Engineering 2022, Vol. 10, Page 20*, vol. 10, no. 1, Dec. 2021, doi: 10.3390/JMSE10010020.

[18]   D. L. Rudnick, R. E. Davis, C. C. Eriksen, D. M. Fratantoni, and M. J. Perry, "Underwater Gliders for Ocean Research," *Marine Technology Society Journal*, 2004, Accessed: May 28, 2022. [Online]. Available: https://www.academia.edu/17650844/Underwater_Gliders_for_Ocean_Research

[19]   Wood and Stephen, "Autonomous Underwater Gliders," Jan. 2009. doi: 10.5772/6718.

[20]   T. E. Berg, *Marine Operations Submarines, AUVs - UUVs and ROVs*. Trondheim: NTNU, Department of Marine Technology, 2007.

[21]   Y. Bai and Q. Bai, *Subsea engineering handbook*. Elsevier, 2018. doi: 10.1016/C2016-0-03767-1.

[22]   MUNIN, "D9.3: Quantitative assessment," 2015.

[23]   ZEP, "The Costs of CO2 Capture, Transport and Storage," 2011. Accessed: May 28, 2022. [Online]. Available: www.zeroemissionsplatform.eu/library/publication/168-zep-cost-report-storage.html

[24]   DNV GL AS, "Rules for Classification Naval vessels Part 4 Sub-surface ships Chapter 1 Submarines," 2018. Accessed: May 17, 2022. [Online]. Available: http://www.dnvgl.com,

[25]   J. Odland, "Offshore Field Development," 2018.

[26]   J. G. Graver, "Underwater gliders: Dynamics, control and design," Princeton University, 2005.

[27]   I. C. Cheeseman, *Fluid-Dynamic Drag: Practical Information on Aerodynamic Drag and Hydrodynamic Resistance*, vol. 80, no. 788. Cambridge University Press, 1976. doi: 10.1017/S0001924000034187.

[28]   ITTC, "Procedures and Guidelines Testing and Extrapolation Methods Resistance Uncertainty Analysis, Example for Resistance Test," 2002.

[29]   Wärtsilä, "WSD50 30K 30,000m3 LNG Carrier - Datasheet," 2017.

[30]   L. Kretschmann, H. C. Burmeister, and C. Jahn, "Analysing the economic benefit of unmanned autonomous ships: An exploratory cost-comparison between an autonomous and a conventional bulk carrier," *Research in Transportation Business & Management*, vol. 25, pp. 76–86, Dec. 2017, doi: 10.1016/J.RTBM.2017.06.002.

[31]   S. Hall, *Rules of Thumb for Chemical Engineers*. 2018.